66-5330

TURPIN, Jimmy Lee, 1937-
PREDICTION OF PRESSURE DROP FOR TWO-PHASE, TWO-COMPONENT CONCURRENT FLOW IN PACKED BEDS.

The University of Oklahoma, Ph.D., 1966
Engineering, chemical

University Microfilms, Inc., Ann Arbor, Michigan

THE UNIVERSITY OF OKLAHOMA

GRADUATE COLLEGE

PREDICTION OF PRESSURE DROP FOR TWO-PHASE, TWO-COMPONENT CONCURRENT FLOW IN PACKED BEDS

A DISSERTATION

SUBMITTED TO THE GRADUATE FACULTY

in partial fulfillment of the requirements for the

degree of

DOCTOR OF PHILOSOPHY

BY

JIMMY LEE TURPIN

Norman, Oklahoma

1966

PREDICTION OF PRESSURE DROP FOR TWO-PHASE, TWO-COMPONENT CONCURRENT FLOW IN PACKED BEDS

APPROVED BY

Chairman

DISSERTATION COMMITTEE

ABSTRACT

Two-phase, gas-liquid concurrent flow in packed beds has been investigated using an air-water system and 2-inch, 4-inch, and 6-inch diameter columns filled with tabular alumina packing. Total pressure drop, column operating pressure, and liquid saturation were measured as a function of gas flow rate, fluid temperatures, and flow direction at several constant liquid flow rates for each column.

Correlation of the frictional pressure loss for both upward and downward flow was achieved in terms of a defined two-phase friction factor and a second correlating parameter which is a function of the liquid Reynolds number, the gas Reynolds number, and the particle-to-column diameter ratio. The two-phase friction factor was found to be a function of the flow direction. A viscosity correction factor was required to extend the friction factor correlation to include liquid viscosities widely divergent from that of water.

The liquid saturation data for both upward and downward flow was correlated in terms of the ratio of mass flow rates of the respective phases. Calculation procedures were outlined for prediction of the total pressure drop for two-phase, gas-liquid concurrent flow in packed beds using the derived empirical correlations.

ACKNOWLEDGEMENTS

A complete listing of all persons to whom gratitude is due for their assistance during the course of the doctoral program is impossible. However, the author is particularly indebted to:

Dr. R. L. Huntington, chairman of the doctoral committee, whose sage advice and guidance overcame many crises, both small and large, and whose interest and enthusiasm provided incentive through the discouraging periods of the program.

Drs. C. P. Colver, M. L. McGuire, C. M. Sliepcevich, and C. E. Springer, committee members, for their suggestions and assistance.

Jersey Production Research Company for their fellowship support.

The American Gas Association for their fellowship support.

Aluminum Company of America for supplying the tabular alumina bed packing.

Reynolds Metals Company for their donation of needed supplies.

The Osage Computer Laboratory of the University of Oklahoma for the use of their facilities. A special thanks

goes to the personnel of the Osage Laboratory for their willingness to help overcome the many difficulties involved in the programming and execution of the programs.

Dick Hall for the use of his curve-fitting computer program which saved many hours of laborious work.

My wife, Joyce, first for her direct assistance in preparation of the dissertation and special problems, but most of all, for her patience, understanding and encouragement during the course of this work.

TABLE OF CONTENTS

TABLE OF CONTENTS (continued)

LIST OF TABLES

LIST OF ILLUSTRATIONS

LIST OF ILLUSTRATIONS (continued)

PREDICTION OF PRESSURE DROP FOR TWO-PHASE, TWO-COMPONENT CONCURRENT FLOW IN PACKED BEDS

CHAPTER I

INTRODUCTION

The general field of multi-phase flow has received much attention in recent years because of its widespread occurrence in engineering operations. It is encountered in such basic areas as distillation, evaporation, heat transfer, gas absorption, and other branches of the chemical processing industry. Reaction vessels utilizing multi-phase flow are assuming increasing importance, particularly for gas-liquid reactions. In addition to the chemical processing industry, applications of multi-phase flow are found in such diverse areas as conventional and nuclear powered propulsion systems, oil field drilling and production operations, plus varied applications in many other engineering operations. The most common type of multi-phase flow involves gas and liquid phases, and the term two-phase flow will be taken as the gas-liquid combination in this paper unless noted otherwise.

The complexity of two-phase flow has caused the theoretical understanding of this phenomenon to lag behind that of other general fields of flow theory (1). That it is

indeed a complex problem is illustrated by the fact that, in order to characterize a single two-phase flow, it is necessary to specify two flow rates, five fluid properties, a conduit diameter, a pipe orientation, and a flow regime (2). This complexity is compounded when the flow is through a packed bed because, in addition to the parameters describing the flow, the parameters describing the bed must also be considered.

Much effort has been expended for research on two-phase flow. By the end of 1964 there had been roughly 4500 published references, representing a cost of $22.5 million. It is estimated that there will be 750 new references in 1965 at a cost of $3,750,000 (54). Although this represents an impressive amount of empirical knowledge, the great majority of this work was concerned with concurrent two-phase flow in open tubes or with countercurrent two-phase flow in packed beds, with only a very minute portion of this research concerned with two-phase concurrent flow in packed beds.

The reason for the dearth of research on two-phase concurrent flow in packed beds was the apparent lack of a practical application for this work. However, it has been shown (3) that under certain conditions concurrent gas absorption is a more desirable operation than is gas absorption utilizing countercurrent flows. With countercurrent operation, the flow rates are limited by the flooding point of the column, while the only limit to flow rates in concurrent operation is the amount of power to be expended in forcing

the fluids through the column, thus providing a much more flexible design within which to optimize equipment and reduce costs (3).

Since the flow rates for concurrent flow are restricted only by the allowable pressure drop through the bed, rather than by a density difference, a very wide range of throughputs are possible (4) for much of which correlation and design information are unavailable. The few investigations published to date (5,6,7) have been largely empirical in nature and have drawn heavily from correlations for two-phase flow in conduits. Each of these investigators obtained data only for downward flow and, without experimental verification, postulated that the pressure drop for two-phase concurrent flow through packed beds was independent of pipe orientation.

There are several objectives of this investigation. First, it is desired to develop a mathematical model of two-phase concurrent flow through packed beds which will provide a basis for the correlation of experimental data. The second objective is to obtain experimental data for both upward and downward flow in order to either verify or dispute the assumption made by the previous investigators of the independence of pressure drop and flow orientation. The final objectives are to derive correlations and to present calculation procedures which will enable prediction of the pressure drop for two-phase concurrent flow for use in the design of packed columns and auxiliary equipment.

CHAPTER II

REVIEW OF THE LITERATURE

It is necessary that a review of the literature include publications from the areas of single-phase flow through packed beds and two-phase flow through conduits, because these areas provide the basis for investigation of two-phase concurrent flow in packed beds. In addition, many of the correlations, results, and experimental procedures of these areas are directly applicable to the field of interest.

Single-Phase Flow in Packed Beds

Zeisburg (8) was among the first to report data for flow through packed beds. His data were correlated according to:

$$\Delta P_f = \frac{f_1 L Q^2}{a^2} \qquad (1)$$

where f_1 was dependent upon the type of packing and the method of packing the column.

Probably the most significant of the early works was that of Blake (9) who by dimensional analysis derived the following correlating equation:

$$\frac{\Delta P_f D_p}{L V^2 \rho} = \varphi\left(\frac{D_p V \rho}{\mu}\right) \qquad (2)$$

where the group on the right is the Reynolds number and the group on the left is a friction factor. These correlating groups, or modifications of these groups, have been utilized by many subsequent investigators (10,11,12,13,14,15,16,17). Burke and Plummer (10) introduced a factor S to account for nonspherical packings and corrected the velocity to a true velocity by dividing by the porosity. Their data were then correlated according to:

$$\frac{\Delta P_f}{L} = C\left(\frac{\rho V^2 S}{\epsilon^3}\right) \tag{3}$$

where C is a function of a modified Reynolds number, $\mu S/V\rho$. These investigators also presented the concept of "state-of-flow" factor, n, for flow through packed beds, where n = 1.0 for completely laminar flow and n = 2.0 for completely turbulent flow and varies between these two values for intermediate flow types.

Furnas (18) accumulated the most comprehensive set of data of the early investigators and fitted it to the simple correlation:

$$\frac{\Delta P_f}{L} = AG^B \tag{4}$$

However, the "constants" A and B varied for each fluid and also with bed properties severely limiting the utility of this correlation.

A two-range correlation was proposed by Chilton and Colburn (19) with a different friction factor for the viscous and turbulent ranges plotted versus a modified Reynolds

number. An important conclusion drawn from this work was that the actual velocity of a fluid through a bed of packed particles was approximately five times greater than that predicted by use of bed porosity because of "dead-end" spaces.

Carman (11) obtained three important results in his work. First, it was verified that the dimensionless groups originally used by Blake provided a good correlation for beds of spherical particles over a very wide range of experimental data. Second, beginning with Poiseuille's Law,

$$V_s = \frac{D^2}{32\mu} \frac{\Delta P g_c}{L} \tag{5}$$

Kozeny's equation was derived:

$$V_s = \frac{\epsilon^3}{K\mu S^2} \frac{\Delta P g_c}{L} \left(\frac{L}{Le} \right)^2 \tag{6}$$

thus providing a theoretical basis for Blake's method of correlation. Third, he found that in the viscous range, the dependence of pressure drop on porosity would be given by:

$$\frac{\Delta P_f}{L} \propto \frac{(1 - \epsilon)^2}{\epsilon^3} \tag{7}$$

As correlating groups, Morcom (12) used the Reynolds number and the friction factor of Fanning's equation:

$$\frac{\Delta P_f g_c \rho D_p}{2LG^2}$$

The pressure drop per unit length was then expressed by:

$$\frac{\Delta P_f}{L} = \frac{\mu^2}{g_c \rho D_p^3} \varphi(N_{Re}) \tag{8}$$

where experimental determination of φ is required. The functional form was assumed to be:

$$\varphi(N_{Re}) = bN_{Re} + cN_{Re}^2$$

but the constants b and c were found to be dependent upon the bed.

Ergun and Orning (13,14) critically reviewed the works of previous investigators concerning the effect of porosity upon pressure loss. They concluded from these and from their own theoretical work that viscous energy loss is proportional to $(1 - \epsilon)^2/\epsilon^3$ and that kinetic energy loss is proportional to $(1 - \epsilon)/\epsilon^3$. A two-term equation was derived similar to that of Morcom but which included the effect of porosity on pressure drop:

$$\frac{\Delta P_f g_c}{L} = k_1 \frac{(1 - \epsilon)^2 \mu V_s}{\epsilon^3 D_p^2} + k_2 \frac{(1 - \epsilon) G V_s}{\epsilon^3 D_p} \qquad (9)$$

The constants k_1 and k_2 were evaluated experimentally and found to have values of 150 and 1.75, respectively.

Brownell et al (15,16,17) postulated a modified Reynolds number-friction factor relationship in which all pertinent variables were included in either one or the other of these groups. A Reynolds number function and a friction factor function were defined, respectively:

$$F_{N_{Re}} = K_4 \epsilon_{eff}^{-1/2}$$

$$F_f = K_5 \epsilon_{eff}^{-5/2}$$

where the K's are constants and ϵ_{eff} is the "effective" porosity, exclusive of dead voids, blind channels, and other such voids. Their general correlation was then a graphical relationship between the groups:

$$\frac{2g_c D_p \Delta P_f}{V^2 \rho L F_f} \text{ and } \frac{D_p G F_{N_{Re}}}{\mu}$$

A general correlation was obtained by Leva et al (20,21,22) from an analogy with flow of fluids through empty tubes:

$$\frac{\Delta P}{L} = \frac{k}{g_c}\left(\frac{D_p G}{\mu}\right)^n \left(\frac{\mu^2}{\rho}\right)\left(\frac{\lambda^{3-n}}{D_p^3}\right)\frac{(1-\epsilon)^{3-n}}{\epsilon^3} \qquad (10)$$

This general correlation is actually three correlations in one because of the inclusion of the state-of-flow factor, n. As noted above, n = 1.0 for completely laminar flow and n = 2.0 for completely turbulent flow, although Leva reports a value of 1.9 for his turbulent flow data. For the transition region, a correlation of n versus the modified Reynolds number, $D_p G/\mu$, is given in order that equation (10) may be applied for all flow rates.

Two-Phase Flow in Conduits

Lacking theoretical understanding of the complexities of two-phase flow, empirical correlations have been utilized for description of this phenomenon. More than twenty-two such correlations for prediction of pressure drops in two-phase flow have been published. Only very recently have

there been attempts to describe two-phase flow theoretically.

The first of these empirical correlations to appear was the classic work of Lockhart, Martinelli, and co-workers (23,24,25). They show the existence of four types of isothermal two-phase, two-component flow, depending upon whether each phase is flowing in a viscous or turbulent manner. A parameter, X, is defined for each of the four flow types in terms of the flow rate and fluid properties of the respective phases.

Correlations of X with a second parameter, Φ, are given where Φ is defined for the gas phase and the liquid phase, respectively, by:

$$\Phi_G^2 = \frac{(\Delta P/\Delta L)_{TP}}{(\Delta P/\Delta L)_G} \tag{11}$$

$$\Phi_L^2 = \frac{(\Delta P/\Delta L)_{TP}}{(\Delta P/\Delta L)_L} \tag{12}$$

and where $(\Delta P/\Delta L)_{TP}$ is the pressure drop observed for the simultaneous flow of liquid and gas in a pipe, $(\Delta P/\Delta L)_G$ is the pressure drop observed for the flow of the gas phase alone in the same pipe at identical conditions, and $(\Delta P/\Delta L)_L$ is the pressure drop for the flow of the liquid phase alone in the same pipe at identical conditions. In addition to being defined in terms of the flow rate and fluid properties of the respective phases, it is shown that X may also be defined by:

$$X^2 = \frac{(\Delta P/\Delta L)_L}{(\Delta P/\Delta L)_G} \tag{13}$$

and thus may be either calculated from an appropriate single-phase correlation or obtained from experimental observations.

The utility of X as a correlating variable is enhanced by the fact that the liquid saturation, R_L, is also a function of X alone and, moreover, it is represented by the same function for all four flow mechanisms. Such is not the case for pressure drop data as a different function of Φ with X is required for each of the four mechanisms. Thus, the major limitation of the Lockhart-Martinelli correlation is that precise criteria for determining exactly whether each phase is flowing in a viscous or turbulent manner, and hence which of the correlations of Φ with X to use, are not known.

In addition to the viscous-turbulent combinations of flow, there may be several flow patterns or regimes for each of the combinations, depending upon the liquid and gas flow rates. The various flow regimes have been described qualitatively by Alves (26), by Huntington and White (27), and by Galegar et al (28), with corresponding generalized graphical plots indicating location of the various regimes presented in (27) and by Baker (29).

The Lockhart-Martinelli correlation was shown (27) to be inadequate for larger diameter lines and also for certain of the flow regimes. This was verified by Brigham et al (30) who concluded that an all-inclusive correlation based on the usual Reynolds number criterion between laminar and turbulent flow should not be used, but rather that the various flow regimes should be treated separately.

Baker (29) sought to improve the Lockhart-Martinelli correlation and also to extend its use to include all flow regimes by defining the parameter Φ in terms of X for each flow regime. Chenoweth and Martin (31) presented an improved correlation for larger diameter pipes which was applicable to any two-phase mixture as long as the flow was turbulent in both phases. Their main contribution, however, was the presentation of a method for handling pipe fittings and presentation of considerable experimental data for fittings.

The Lockhart-Martinelli correlation was extended for use with rough pipes by Chisholm and Laird (32). They developed approximate correlations for the exponents of the Lockhart-Martinelli parameter, X, with a friction factor for rough tubes and a friction factor for smooth tubes.

A comprehensive review of the correlations of Baker (29), Chenoweth and Martin (31), Lockhart and Martinelli (23,24,25), and Bankoff (33), their applicability and their limitations, and their expected error for a wide range of system variables has been given by Dukler et al (34). An analytical treatment of two-phase flow is also developed forming a basis for comparison of these various empirical correlations. Much of the disagreement between the correlations is attributed to the failure to separate properly the frictional energy loss from the other sources of energy loss.

Dimensional analysis was utilized by Hoogendoorn (35) to determine the dimensionless groupings required to describe two-phase flow. He developed correlating groups for the plug,

slug, and froth flow regimes, other groups for the stratified and wave regimes, and still other groups for the mist regime. Hoogendoorn also employed an electrical capacitive method to measure liquid saturation, and a resulting correlation of liquid-saturation with the slip velocity was presented.

Liquid saturation data, obtained by the direct shut-in method and reported as in-place ratio versus flowing ratio, have been reported by Sobocinski and Huntington (36) for flow through horizontal piping and by Carter and Huntington (37) for vertical flow. Liquid saturation data for vertical flow were also presented by Hughmark and Pressburg (38), along with their resulting correlation which gave the volume fraction of liquid as a function of the system variables, grouped somewhat according to the Lockhart-Martinelli parameter, X. A later correlation by Hughmark (39) presented liquid saturation, in the form of a dimensionless flow parameter, as a function of the Reynolds number, the Froude number, and the entering liquid volume fraction. A comprehensive summary of the various methods of measuring liquid saturation, along with their respective advantages and limitations has been given by Gouse (40).

The theoretical description of two-phase flow in conduits has lagged far behind these reported empirical descriptions as only very recently have analytical attempts been published. Ros (41) wrote a momentum balance equation to separate the components of total pressure loss in oil well tubing but had to resort to dimensional analysis to complete

his work. Griffith and Wallis (42) concluded that no single mathematical model would fit all flow regimes and proceeded to an analysis of the slug flow regime in which they calculated the period and magnitude of pressure fluctuations in slug flow.

Other theoretical descriptions utilizing momentum and/or energy balances have been given by Hughmark and Pressburg (38), Levy (43), Vohr (44), and by Lamb and White (45). Govier and co-workers in a series of articles (46,47, 48,49,50,51,52,53) presented an analysis of two-phase flow supplemented by much experimental data for several different systems. An excellent comprehensive review of the various methods for description of two-phase flow in conduits has been published by Gouse (54).

Two-Phase Countercurrent Flow in Packed Beds

The literature of this area is of limited applicability to the problem of interest, because the great majority is concerned only with prediction of loading and flooding velocities in countercurrent operation. The desirability of concurrent flow, from the standpoint of tower pressure drop, was noted by Piret et al (57) in an early work in which they reported the pressure drop encountered in countercurrent flow to be almost double that encountered in concurrent flow of air-water mixtures.

Two-Phase Concurrent Flow in Packed Beds

Discounting the literature available for two-phase

flow in porous media, only four references were available pertaining to two-phase flow in packed beds, with three of these concerned with gas-liquid flow and the remaining one with two-phase flow of immiscible liquids. The first was that of Dodds et al (7), who presented pressure-drop data for two-phase vertically downward concurrent flow, but a general correlation was not attempted.

A much wider range of experimental variables was covered by Larkins (62), who studied the vertical downward flow of several gas-liquid systems through packed beds. Larkins utilized a combination of mathematical models in an attempt at a complete theoretical analysis but eventually resorted to empirical means to obtain a solution. He assumed the density change over a small distance was negligible, set the kinetic energy term to zero, and assumed that the frictional energy loss was independent of flow orientation. The mechanical energy balance was written for a single fluid and was extended to two-phase flow with the definition of a mean mixture density.

Further in this development it was postulated that each phase may be thought of as flowing in a bed restricted by the other phase. A single-phase Reynolds number and a two-phase friction factor were then defined, and a Lockhart-Martinelli type of analysis was used where the two-phase pressure drop is correlated with an appropriate single-phase pressure drop. A Martinelli-type "two-phase parameter" was then utilized for correlation of his data.

The data of Weekman and Myers (6) for downward concurrent flow are also correlated in terms of Lockhart-Martinelli two-phase parameters. In this work it is assumed that the packing supports essentially all of the liquid and hence that a static correction is not necessary for liquid loadings below 25,000 lbs/ft^2-hr. Thus, the total measured pressure drop is identical to the frictional pressure drop by this analysis.

Rigg (58) studied the vertical upward flow of several immiscible liquid systems. The mechanical energy balance was applied to each of the phases, and pseudo-homogeneous fluid properties were used to evaluate the frictional pressure drop. Single-phase packed bed correlations were used to obtain final results which were largely empirical.

CHAPTER III

THEORETICAL ANALYSIS

Upon examination of two-phase gas-liquid flow literature, the extremely large number of different analytical models is noted. However, it is possible to group this large number of variations under one or a combination of the following four general mathematical models (54):

1. Homogeneous Flow Model
2. Separated Flow Model
3. Friction Factor Model
4. Momentum Exchange Model

The homogeneous model is probably the simplest of the four models to use. It assumes that the two phases form a homogeneous mixture with no radial variation in mixture properties. The difficulty in using this method, however, lies in evaluation of the true mixture properties, e.g. mixture viscosity. Also, the homogeneous flow model will not adequately describe certain flow regimes such as annular flow or stratified flow.

The separated flow model assumes that each phase flows as a continuum, restricted in its flow area by the presence of the other phase. The use of this model usually involves

writing the mechanical energy balance for each phase separately and then combining the resulting equations in some manner. Assumptions are required about how the phases are separated or distributed.

The momentum exchange model is actually a separated flow model but it does not assume anything concerning how the phases are separated or distributed. Basic assumptions are that each phase satisfies the conservation of momentum separately and that the static pressures for each phase are equal and constant at every cross-section (54). However, even with this model, it becomes necessary to revert to the friction factor approach in order to evaluate the frictional pressure drop.

The friction factor model lends itself readily for use with experimental data by an extension of the definition of the friction factor for single-phase flow. Therefore, because it has been necessary to evaluate the frictional pressure drop by empirical means, the majority of investigators have utilized the friction factor model either by itself or in conjunction with one of the previous three models.

None of these models permits the ideal situation of a completely theoretical description of two-phase flow. Thus, while each possesses its inherent advantages, ultimately each must be supplemented by experimental data to obtain a complete solution.

Theoretical solutions were attempted by the writer

using each of the four mathematical models or combinations of these models. A solution was desired which would permit separation of the total pressure drop into its individual components of static, frictional, and acceleration pressure losses and isolation of each of these in a form to permit simple evaluation by integration and/or empirical means. The most satisfactory solution was produced from the separated flow model combined with momentum balances. The control surface for the momentum exchange model is shown in Figure 1 with the defined quantities.

Referring to Figure 1, the momentum balance for the gas phase is:

$$W_G V_G + PA_G g_c + g_c(P + dP/2)dA_G = g_c(P + dP)(A_G + dA_G) + g_c dF_{\tau G} + \rho_G g A_G \cos\theta\, dy + (W_G)(V_G + dV_G) \qquad (14)$$

The momentum balance for the liquid phase is:

$$W_L V_L + PA_L g_c = g_c(P + dP)(A_L - dA_L) + g_c(P + dP/2)(dA_L) + g_c dF_{\tau L} + \rho_L g A_L \cos\theta\, dy + W_L(V_L + dV_L) \qquad (15)$$

Multiplying, neglecting second order terms, and simplifying: for the gas phase:

$$W_G V_G + PA_G g_c + g_c P dA_G + g_c dA_G dP/2 = g_c PA_G + g_c P dA_G + g_c A_G dP + g_c dA_G dP + g_c dF_{\tau G} + \rho_G g_c A_G \cos\theta\, dy + W_G V_G + W_G dV_G \qquad (16)$$

$$g_c A_G dP + g_c dF_{\tau G} + \rho_G g A_G \cos\theta\, dy + W_G dV_G = 0 \qquad (17)$$

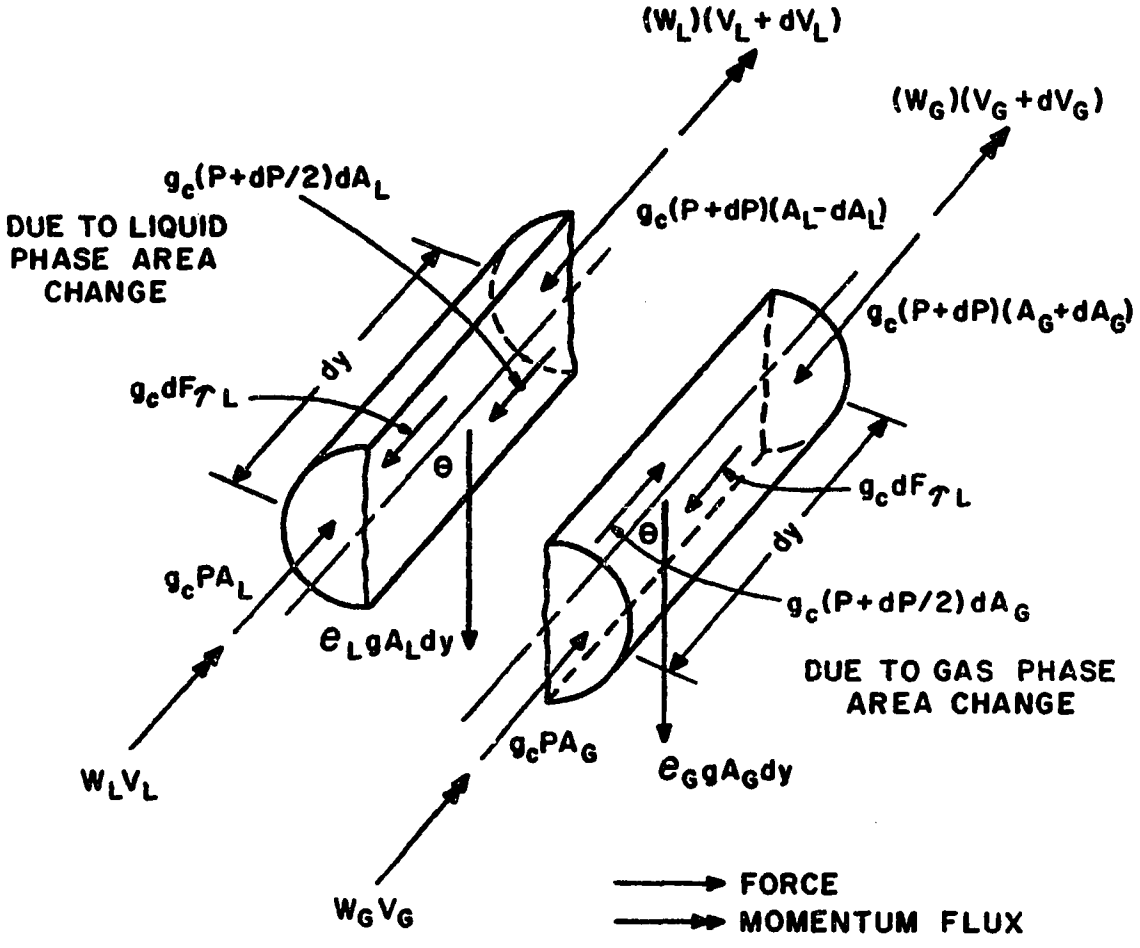

FIGURE 1. CONTROL SURFACE FOR THE MOMENTUM EXCHANGE MODEL

for the liquid phase:

$$W_L V_L + PA_L g_c = g_c PA_L + g_c A_L dP - g_c PdA_L - g_c dPdA_L + g_c PdA_L + g_c dA_L dP/2 + \rho_L g A_L \cos\theta\, dy + g_c dF_{\tau L} + W_L V_L + W_L dV_L \quad (18)$$

$$g_c A_L dP + g_c dF_{\tau L} + \rho_L g A_L \cos\theta\, dy + W_L dV_L = 0 \quad (19)$$

Adding (17) and (19):

$$g_c A_G dP + g_c A_L dP + g_c dF_{\tau G} + g_c dF_{\tau L} + \rho_G g A_G \cos\theta\, dy + \rho_L g A_L \cos\theta\, dy + W_G dV_G + W_L dV_L = 0 \quad (20)$$

$$(A_G + A_L)dP + dF_{\tau G} + dF_{\tau L} + (g/g_c)(\rho_G A_G + \rho_L A_L)\cos\theta\, dy + (W_G/g_c)dV_G + (W_L/g_c)dV_L = 0 \quad (21)$$

$$A = A_G + A_L \quad ; \quad g/g_c \cong 1 \quad (22)$$

Note that for horizontal flow, $\theta = 90°$, $\cos\theta = 0$, and the gravity term drops out. Using (22) in (21):

$$-dP = (dF_{\tau G} + dF_{\tau L})/A + (\rho_G A_G/A + \rho_L A_L/A)\cos\theta\, dy + [(W_G/g_c A)dV_G + (W_L/g_c A)dV_L] \quad (23)$$

However, equation (23) cannot be integrated as shown because ρ_G, A_G, and A_L are each functions of the distance through the packed bed, y, and assumptions must be made concerning the variation of these quantities with distance.

Assuming the gas behaves ideally and, for isothermal flow, the gas phase density is given by:

$$\rho_G = P(MW)/RT = C_1 P \tag{24}$$

Larkins (62) reported an almost linear variation of pressure with distance through the packed bed. Therefore, it is assumed that:

$$P = P_1 + ky \tag{25}$$

and using (25) in (24):

$$\rho_G = C_1(P_1 + ky) = C_2 + C_3 y \tag{26}$$

A relationship for A_L (and hence A_G) is now required. Hughmark and Pressburg (38) achieved satisfactory results for two-phase flow through an open pipe by assuming a linear dependence of A_G on y and, in the absence of data for packed beds, this relationship will be assumed:

$$\overline{A}_L = (A_{L_1} + A_{L_2})/2 \tag{27}$$

$$\overline{A}_G = (A_{G_1} + A_{G_2})/2 \tag{28}$$

Replacing the individual friction losses of the gas phase and the liquid phase by a combined friction loss for the two-phase flow as given by:

$$\Delta P_{TPf} = \int (dF_{TG} + dF_{TL})/A \tag{29}$$

Using (26), (27), (28) and (29) and taking $y_1 = 0$ and $y_2 = L$, equation (23) integrates to:

$$-(P_2 - P_1) = \Delta P_{TPf} + (\cos\theta/A)(C_2\overline{A}_G L + \rho_L \overline{A}_L L + C_3 \overline{A}_G L^2/2) + (W_G/g_c A)(V_{G_2} - V_{G_1}) + (W_L/g_c A)(V_{L_2} - V_{L_1}) \tag{30}$$

which is equivalent to:

$$-\Delta P_{total} = \Delta P_{friction} + \Delta P_{static} + \Delta P_{acceleration} \qquad (31)$$

However, in order to be able to use equation (30), the two-phase frictional pressure drop, ΔP_{TPf}, and the quantity $\overline{A}_L$ (and thus $\overline{A}_G$) must be evaluated. Lacking theoretical means, evaluation must be done experimentally, followed by correlation of each of the respective quantities in terms of known system variables. These empirical correlations used in conjunction with equation (30) then permit calculation of the total pressure drop for two-phase concurrent flow for use in the design of packed columns and auxiliary equipment.

CHAPTER IV

EXPERIMENTAL PROGRAM

General Considerations

The major objectives of this investigation were to develop a mathematical model of two-phase flow through packed beds which isolated the frictional pressure drop in a form that would permit easy and accurate empirical evaluation, followed by the actual experimental determination of this quantity and subsequent correlation of it with the independent system variables. Other objectives were to check experimentally the assumption made by Larkins (62) that the frictional pressure drop is independent of flow orientation and also to determine the effect of column-to-packing diameter ratio upon the frictional pressure drop in order that the results might be of more general applicability.

Noting the general objectives as outlined above, an overall experimental program was formulated, the fluid system and the bed packing material were chosen, and the equipment which is described in the next section was selected and assembled. In general terms, the overall experimental program consisted of obtaining sufficient data to establish suitable correlations for the prediction of frictional

pressure drop in terms of the independent system variables for both upward and downward vertical two-phase flow in a packed bed of any given particle-to-column diameter ratio. Specifically, this required measurement of column pressures and pressure drops, fluid temperatures, and liquid saturations over a range of liquid and gas flow rates for several different packing diameter and column diameter combinations.

Compromising between maximum column size to be employed and cost of the columns, columns of 2-inch, 4-inch, and 6-inch diameters were selected for investigation. A fluid system was desired which would be cheap, safe, readily attainable, easy to work with, and whose physical properties were available or could be easily and accurately calculated. The air-water system was selected as the one best fitting these conditions. The desired properties of the packing material were identical to those of the fluids, and tabular alumina was selected as most closely fitting those requirements.

Description of Experimental Apparatus

The equipment used in this investigation consisted of 2-inch, 4-inch, and 6-inch diameter, 84-inch long packed columns and the related components and piping required to establish and measure flow rates, pressures, temperatures, and liquid saturations. A schematic diagram of the experimental apparatus is shown in Figure 2 with a photograph of the packed columns plus a portion of the related equipment included as Figure 3.

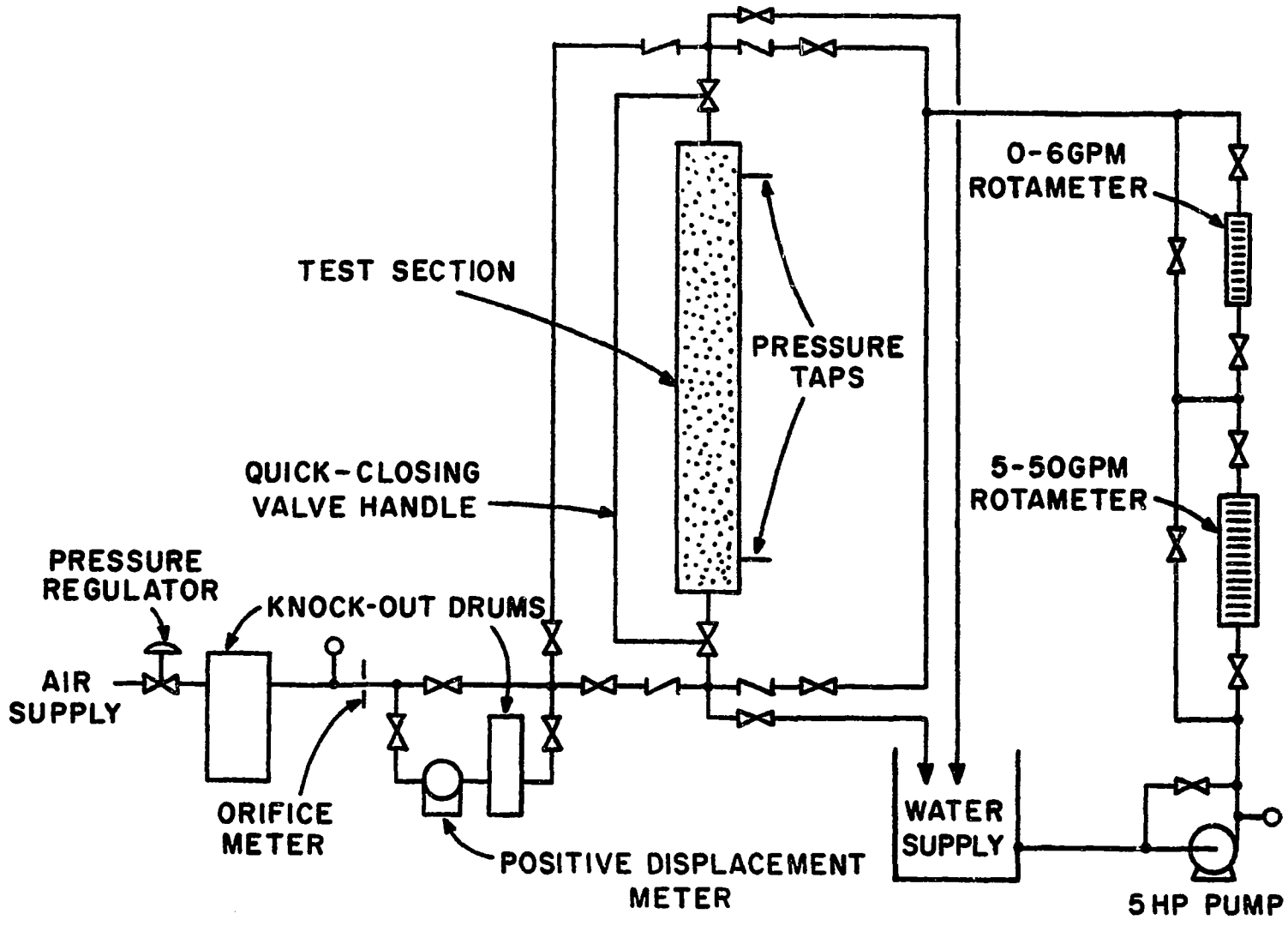

FIGURE 2. SCHEMATIC DIAGRAM OF EXPERIMENTAL APPARATUS

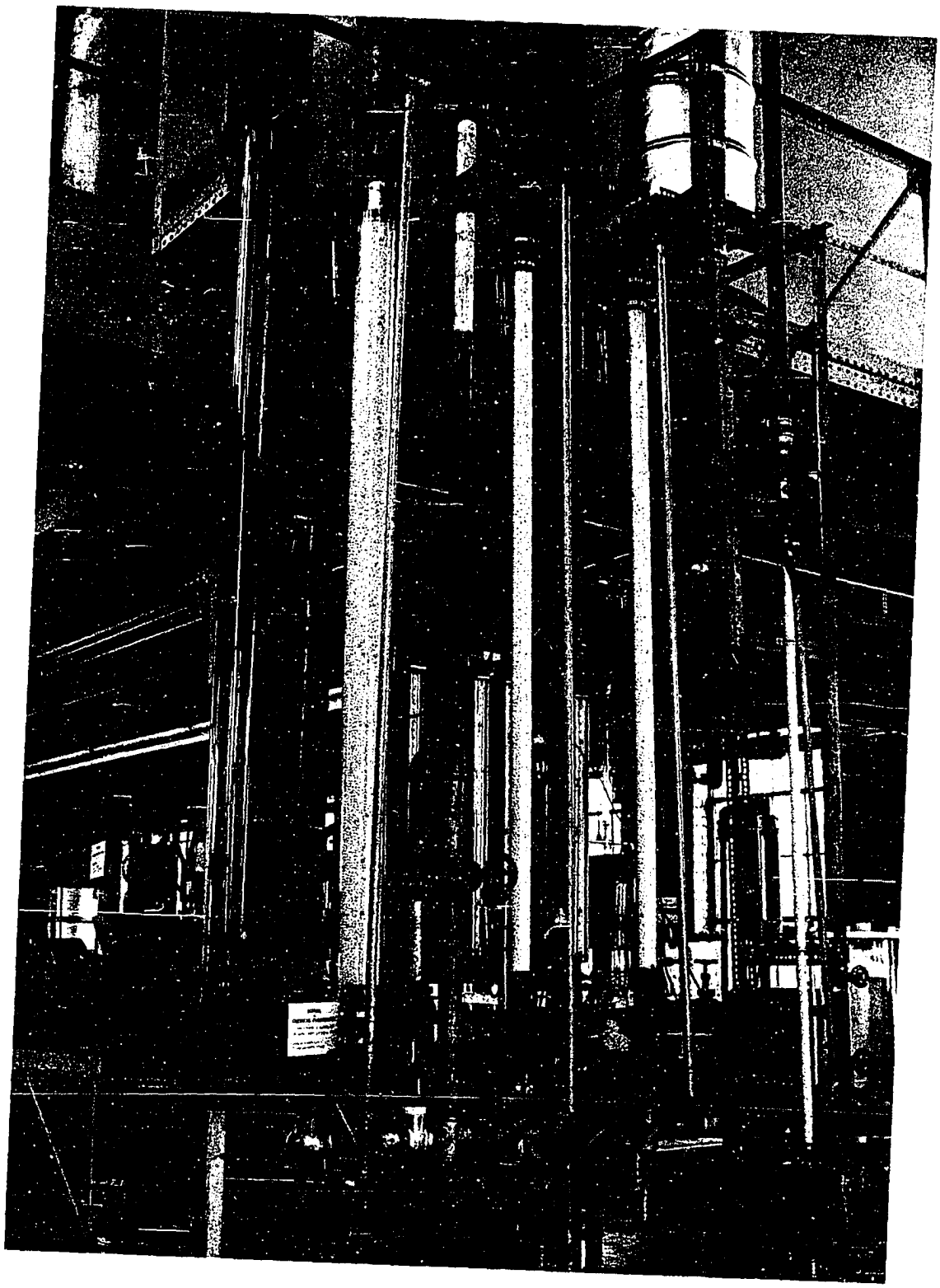

Figure 3. PHOTOGRAPH OF THE EXPERIMENTAL APPARATUS

Figure 4 shows the construction of the test section with the various dimensions of each of the respective columns given in Table I. The columns themselves were of transparent

TABLE I

TEST SECTION DIMENSIONS

Dimension	2" Column	4" Column	6" Column
Inside dia., in.	2.125	4.125	6.000
Total tube length, in.	84.0	84.0	84.0
Cross-sectional area, in^2	3.46	13.39	28.25
Distance between taps, in.	72.0	72.0	72.0
Distance - tap to column end, in.	6.0	6.0	6.0
Unpacked tube volume, in^3	291.0	1124.0	2380.0
*Packed volume of lower valve, in^3	23.8	34.8	33.6
*Packed volume of upper valve, in^3	27.2	45.7	33.6

*Includes packed volume of the two connecting pipe nipples between the column and the quick-closing valve.

Busada 210 butyrate plastic tubing. Two 2-inch columns were available and were piped so that both upflow and downflow data could be taken simultaneously. In order to conserve packing material, only one 4-inch and one 6-inch column were utilized, thus requiring two individual determinations to obtain both the upflow and the downflow data for given flow rates.

Quick-closing valves were attached at the top and

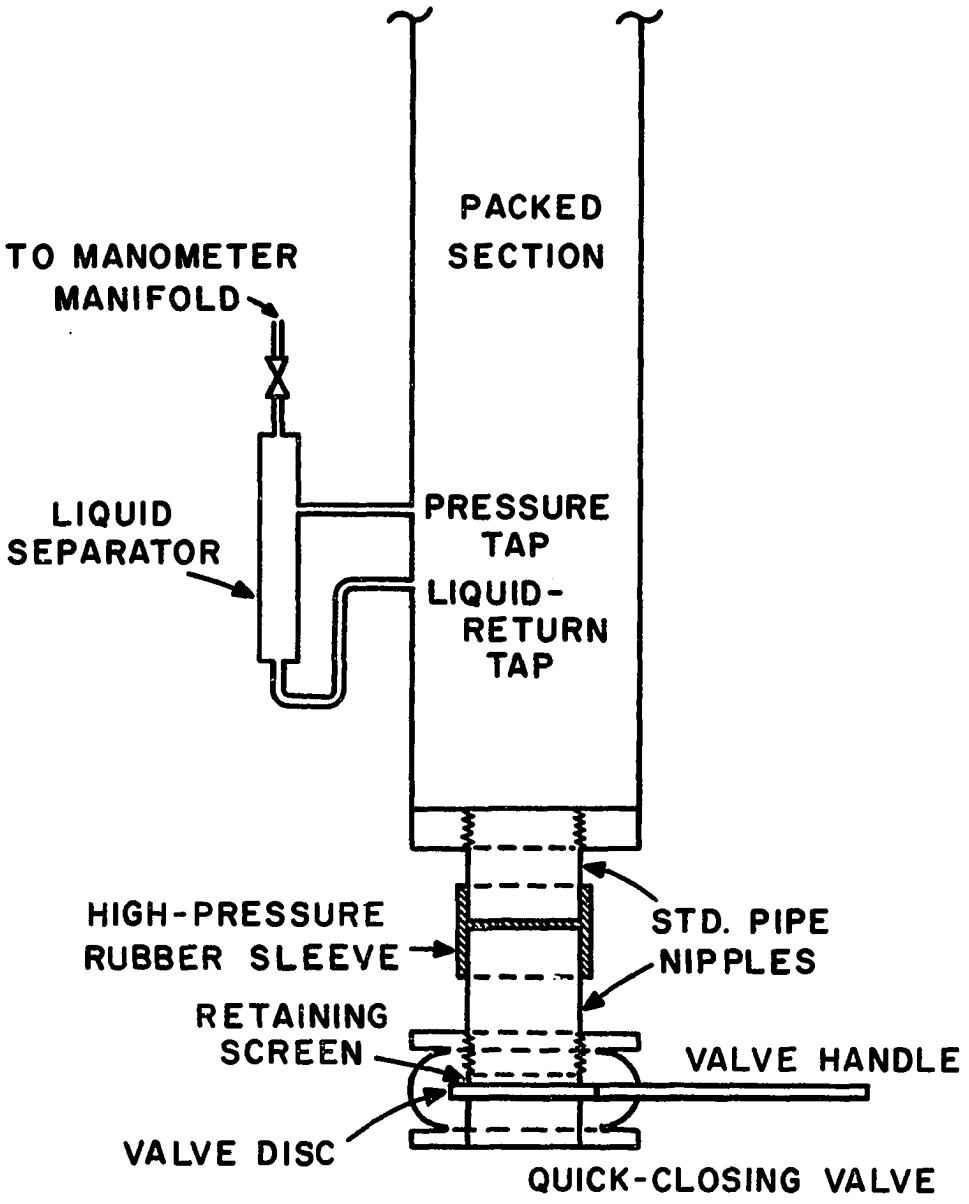

FIGURE 4. TEST SECTION. DETAILS OF CONSTRUCTION

bottom of each of the columns by means of high-pressure rubber hose and hose clamps, and their respective handles were joined rigidly by a metal rod. This provided for simultaneous closing of the valves and thus enabled determination of the liquid saturation. A retaining screen was attached inside each valve immediately adjacent to the valve seat and the valves themselves were packed with the tabular alumina.

Pressure taps were drilled at a distance of 6-inches from both top and bottom of each of the columns and a second hole was drilled 2 inches below each respective pressure tap. These were fitted with separators which returned the liquid to the column through the lower tap and thus maintained the manometer leads in a single-phase gas condition.

Liquid was supplied to the column by an Ingersoll-Rand centrifugal pump with a 15-gpm capacity at 30 psi head, powered by a 5-hp, 3450-rpm General Electric motor. The liquid was recirculated through the system from a 55-gallon storage tank. Two rotameters located in a series and/or parallel arrangement provided for metering of the liquid flow. The low flow range was metered by a 0-6 gpm, Fischer-Porter rotameter calibrated in 0.06-gpm increments while a 5-50 gpm Fischer-Porter rotameter equipped with a flow recorder calibrated in 1/2-gpm increments provided for metering of the higher flows. Thermometers were available for measuring the liquid temperature at the entrance and exit of the column.

The gas phase flow was obtained from the Oklahoma University Physical Plant air supply. A knock-out drum was

in the inlet line for removal of water from the air stream. The inlet line was also equipped with a pressure regulator and, located in parallel, a 1/8-inch needle valve, a 1/2-inch globe valve, and a 2-inch globe valve which provided for accurate flow control at all flow rates.

Two meters were utilized for determination of the air flow rates. Low flows were metered by a positive displacement type 80-B meter manufactured by American Meter Company, Inc., which had a capacity of 2500 cubic feet per hour at two inches of water differential pressure. A second knock-out drum was downstream from this meter to prevent back-up of water into the meter should a leak develop in a downstream check valve where the two phases were combined.

The measurement of intermediate and high air flows was by an Emco type 38 orifice meter using standard sharp-edged plates in a 2-inch standard steel pipe. Plates of 0.25-, 0.375-, 0.500-, 0.688-, and 0.750-inch diameters were used in order to obtain a suitable differential pressure across the orifice plate. The meter was also equipped with a 20-inch manometer and a 0-45 psi gage for determination of the metering pressure, and a thermometer was located immediately upstream for determination of the metering temperature.

The liquid and gas flows were brought together in a 2-inch tee, and the combined flows were then passed through a stainless steel wire mesh filter to distribute the phases equally across the column diameter. All two-phase flow piping was 2-inch standard steel, as was the single-phase gas

piping except for the connections to the positive displacement meter which were 1/2-inch standard steel. The single-phase liquid system was constructed of 1-inch standard steel pipe and fittings.

A schematic diagram of the system for measuring pressures and pressure drops is given in Figure 5. Two such systems were available. In addition to the separators attached directly to the column, a surge pot was available on each lead line from the column to damp pressure fluctuations. The ratio of the pot diameter to the line diameter was 16 to 1 and the pots were packed with stainless steel wire mesh to further aid in reducing the fluctuations. Four 30-inch and one 50-inch mercury manometers were used for the lower pressure determinations, with 0-45 psi and 0-60 psi gages available in each line for use when the range of the manometers was exceeded. The complete manifold was constructed of 1/8-inch copper tubing and fittings.

Preliminary Procedures

Prior to calibration of the apparatus and the actual taking of experimental data, it was necessary to perform certain preliminary procedures. These included establishing the fluid and packing properties, packing the column, and determining the properties of the packed bed.

The fluid properties were obtained from literature values and by direct calculation. The water viscosity as a function of temperature is given in Figure A-1 of Appendix A

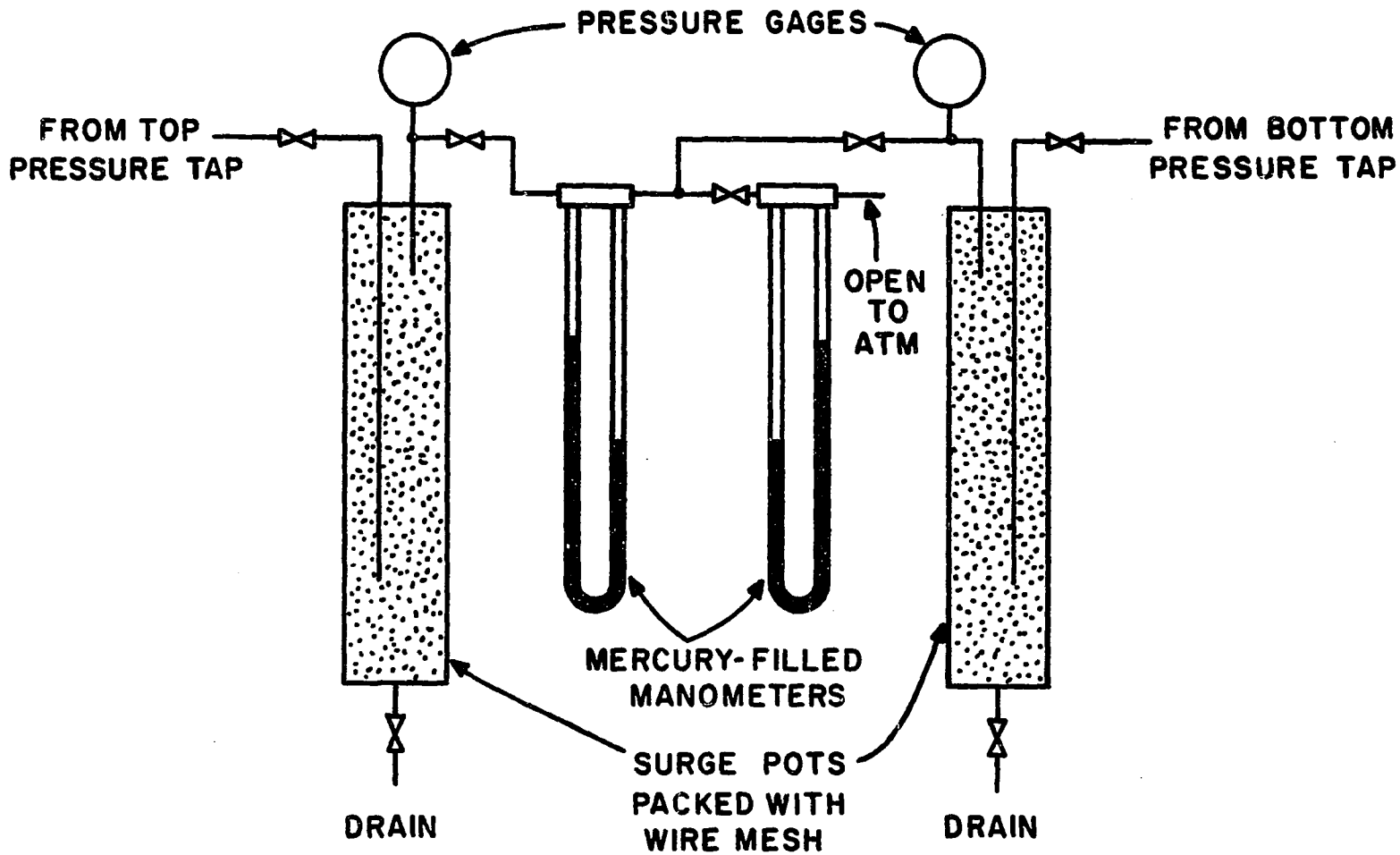

FIGURE 5. DIAGRAM OF PRESSURE MANIFOLD SYSTEM

with the data for this figure being taken from the Chemical Rubber Handbook (60). Data for the viscosity of air as a function of temperature are presented in Figure A-2 and were obtained from the International Critical Tables (61). Calculations revealed that the effect of pressure on viscosity was negligible for the range of pressures employed in this investigation. The air density was calculated from the ideal gas equation while the water density was assumed to be constant for the temperature range involved. A maximum error of 0.5% was introduced by this assumption.

Properties of the packing material which were determined for individual particles were the particle diameter and density. Several measurements were required because of the nonuniformity of the particles with respect to both size and shape. For each of the nominal packing sizes employed, 50 particles were selected at random from the packing material. The diameter of each of these was taken in three directions by means of a micrometer, and the particle diameter for each particle was recorded as the average of the three determinations. An arithmetic mean of the averaged diameters of the 50 particles was then taken as the particle diameter for each of the respective packing sizes. The volume of the 50 particles was determined by water displacement and the average particle diameter was calculated assuming perfect spheres of identical size. The two values of particle diameter agreed within 0.8% of each other.

Prior to this volume determination by water

displacement, the 50 particles were weighed and the density was calculated from these measurements of weight and volume. The value of the density obtained in this manner differed by less than 0.25% from the density value reported by the manufacturer. This grain density was utilized subsequently as one method for calculation of the bed porosity. These individual particle properties are presented in Table II along with the composite bed properties for each of the packed beds.

After determination of individual properties, the columns were packed using procedures reported in the literature (58,62) which were designed to obtain reproducible bed properties. The lower valve of the column was closed and the column was partially filled with a known quantity of water. A given volume of packing material was weighed and dumped into the column while tapping the sides of the column with a rubber hammer to ensure complete settling of the particles. The liquid level was noted and recorded after the addition of the given quantity of packing material.

This procedure was repeated several times, with occasional addition of a known volume of water to keep the water level always above the packing level, until the column was completely filled with packing to within 1/2 inch of the top valve seat. Upon completion of the packing operation, a retaining screen was fitted into the top valve to prevent carry-over of the packing material.

The overflow water from the final packing addition was measured so that the total quantities of both water and

packing material contained between the quick-closing valves were known. Values of bed porosity were calculated for each of the individual additions of packing material, and these were compared to the porosity calculated from the total quantities of water and packing material in the column and the known column volume. These quantities were all within 1% of each other. Values of porosity were also calculated using the total weight of the tabular alumina added to the column in conjunction with the particle density determined previously. Porosity values obtained using the grain density were higher than the measured porosities by 3.35%, 10.42%, and 1.15% for the 2-inch, 4-inch, and 6-inch columns, respectively.

Following the packing operation and the subsequent determination of their respective porosities, the columns were in a suitable condition for determination of the permanent liquid holdup, i.e., the amount of water retained by the packing upon draining the column. The total volume of water contained within each packed column was known from the previous operation. This water was drained from the column into graduated cylinders and the permanent holdup was obtained by difference. It was found that more than 99% of the total volume recovered from a 4-hour drainage period was obtained during the first 10 minutes, and thus a 10-minute drainage period was considered sufficient.

Air was then passed through the column for several hours to remove the remaining water and to completely dry the

packing. A second determination of permanent liquid holdup was made by completely filling the column with a measured volume of water, followed by drainage and measurement of the liquid recovered. The values of permanent liquid holdup were within 3% of each other for each of the columns. Average values for the permanent liquid holdup for each of the columns are presented in Table II along with the other bed and particle properties.

TABLE II

PACKING AND BED PROPERTIES

Property	Column Size		
	2"	4"	6"
Particle dia., cm	8.27	7.64	7.64
Particle dia., ft	0.02715	0.02505	0.02505
Particle density (measured), g/cc	3.79	3.81	3.81
Particle density (manufacturer), g/cc	3.80	3.80	3.80
Porosity (measured), %	35.8	37.4	34.9
Porosity (grain density), %	37.0	41.3	35.3
% Difference (based on measurement)	3.35	10.42	1.15
Permanent liquid holdup, %	9.16	4.18	11.02

Calibration of Equipment

Several of the components of the experimental apparatus required calibration prior to the taking of data. Both the low range and the high range rotameters were calibrated

by direct weighing using a stop watch. A sufficient quantity of water was collected at each flow rate over a sufficiently long time period to reduce the errors due to weighing and reading the stop watch to less than 0.5%. A calibration curve for each rotameter is presented in Appendix B.

The gas flow meters were calibrated versus each other. A given flow of air was established through the meters in series. The orifice differential was recorded along with the metering temperature and pressure and the flow rate was calculated using the standard orifice equation. At this same flow rate, the time required for a given volume of air to pass through the positive displacement meter was recorded. Making temperature and pressure corrections, the flow rate was calculated and compared to that calculated from the orifice meter measurements. The average difference between the two meters was 2.7% with the maximum difference of 5.5% occurring near the maximum capacity of the positive displacement meter.

The usual procedure concerning the gas flow meters during each series of experimental determinations was to use the positive displacement meter for the low flow rates, the orifice meter for high flow rates, and both meters in series for a few intermediate flow rates. This permitted a frequent check of the meters during the entire course of the experimental work. It was found that for flows not near the maximum capacity of the positive displacement meter, the usual difference between the two meters was approximately 2%.

Pressure gages used in the experimental work were

calibrated using a dead weight tester at the University of Oklahoma Research Institute. All gages were within the accuracy with which they could be read. Thermometers were checked at the ice point and at the boiling point of pure water.

Operating Procedures

General details of the experimental investigation are included in this section followed by the specific operating procedures which were employed. Following the lead of previous investigators in this field, data were taken for a range of gas flow rates for each of several constant liquid flow rates. Four liquid rates were selected arbitrarily for each column with the maximum rate determined by the maximum pump capacity and the remaining rates distributed over the capacity range of the pump. The gas flow rate was varied at approximately equal increments from almost zero to the maximum rate as determined by the maximum allowable column operating pressure. Identical flow rates were used for both the upward and downward flow studies.

Prior to making two-phase determinations, single-phase data were taken for each fluid over a range of flows for use in single-phase correlations as a check of the operating procedures. For these determinations, the flow rate of the air was established, the system was allowed to reach a steady-state as evidenced by constant pressures, and measurements were made of pressures, temperatures, and the

flow rate. This procedure was repeated for single-phase liquid flow.

For the two-phase determinations, the desired liquid flow rate was obtained and the gas flow was established immediately to prevent the separators and the manometer lines from becoming filled with liquid. Adjustments were then made to obtain the approximate desired gas flow rate, followed by final adjustments to both the liquid and gas streams to obtain the exact desired rates. These final adjustments were necessary because a change in the flow rate of one stream produced a somewhat smaller change in the rate of the other stream.

Time was allowed for the system to reach steady-state, as evidenced by constant column pressures, before readings were taken. Upon reaching a steady-state condition, the following data were recorded: The flow rate of each stream, the temperature of each stream, the column pressure and pressure drop, plus a note concerning the observed flow pattern in the packed bed.

Procedures were then initiated to determine the liquid saturation. The quick-closing valves were shut simultaneously by means of the common valve handle. The pump by-pass was opened and the air supply valve was closed. After waiting ten minutes for the liquid to drain down, a measurement was made of the height of the liquid above the bottom of the column. The column pressure after shut-in was also recorded.

These procedures were repeated for all determinations for both upward and downward flow in all three columns.

After completion of the experimental determinations, motion pictures were made of representative flow patterns in each packed bed at normal speed (24 frames per second), and at 500 frames per second or 5% of normal speed when shown on the screen.

CHAPTER V

EXPERIMENTAL RESULTS

Calculated results obtained from the preceding experimental program are presented in this section along with a qualitative description of the various flow patterns observed. Correlation of these calculated results is reserved for the subsequent chapter. The raw data as obtained from the experimental program are included in tabulated form as Appendix D.

Pressure drop data as a function of the gas mass flow rate at constant liquid rates for both upward and downward vertical flow are presented graphically in Figures 6-17. These reported are total pressure drops which include the static head. From each of these graphs it is seen that although the pressure drop for downflow is less at low gas rates, it eventually becomes greater than that for upflow at higher gas rates. It is noted that the upflow curve approaches zero gas rate at a pressure drop below the static head for single-phase liquid. This indicates that the pressure gradient must drop sharply from the single-phase liquid gradient with the introduction of only a very small gas flow. This "dip" in the pressure drop curve has been observed for two-phase, gas-liquid flow in open conduits but at gas rates

substantially higher than those observed here. Such behavior is only postulated for downflow because a negative gradient would have to occur to obtain the "dip" in the curve. Several of the downflow curves presented do appear to be approaching negative pressure drops rapidly at very low gas rates.

Figures 18-20 give representative liquid saturation data for each of the three columns reported as in-place ratio of liquid-to-gas versus flowing ratio of liquid-to-gas. From these figures it is seen that slip velocity ratios in the packed beds were in the range of 10 to 35.

Three distinct flow patterns were observed experimentally. These were termed bubble flow, slug flow, and spray flow and the relative location of each of these flow regimes in terms of the mass velocities of the respective phases is given in Figure 21. In order to visualize each of these flow patterns, a given liquid rate will be discussed as the gas rate is varied from zero to its maximum value. With single-phase liquid flow established in the column, the bubble flow regime is encountered with the introduction of very low gas flows. This regime is characterized by bubbles of gas flowing unbroken in the liquid-continuous phase at slightly higher velocities than the liquid phase. As expected, the higher the given liquid rate, the wider is the range of gas flows which will produce bubble flow.

As the gas rate is increased further at the given liquid rate, a nonhomogeneous flow regime termed slug flow is encountered. This regime is characterized by alternate

portions of more dense and less dense mixtures of the two phases passing through the column. At the onset of slugging, a portion of the mixture with a density approaching that of the liquid collects at the entrance to the column and is swept through the column by an alternate portion of the mixture with a density approaching that of the gas phase. As the slugs first occurred, they appeared to be 4-6 inches thick separated by approximately 12 inches of the lighter phase, which propelled them through the packed bed at a velocity of approximately 6 feet per second. At low liquid rates there were roughly 30 slugs per minute increasing to nearly twice that figure at higher flows. As the gas flow was increased further for the given liquid rate, the frequency of the slugs increased, and the difference in density between the alternate slugs of fluid became progressively less.

With further increases in gas flow rate the density difference between the alternate slugs disappeared entirely, producing the third flow pattern, spray flow. This is a gas-continuous flow regime with the liquid being carried through the column suspended as a heavy mist in the gas stream. At this point the packing surfaces were covered by a rather thick layer of liquid which became progressively thinner with increasing gas rate. At the upper limiting gas rates, for the lower liquid rates, this liquid layer on the packing became very thin and essentially all the liquid was transported in the gas stream as a very fine mist.

It should be noted that the lines drawn on Figure 21

to separate the three flow regimes are actually transition regions rather than points of abrupt change from one flow type to another. Either of the flow patterns may be encountered in the vicinity of this separating line which was drawn to locate only qualitatively the various flow regimes. Figure 21 is applicable for both upward and downward flow with the only differences being that slugging is initiated at slightly lower gas velocities and persists to slightly higher gas velocities for upward flow at a given liquid rate.

An indication of the flow type for each experimental point is included in Figures 7-17. It is noted that there is no abrupt change of pressure drop with gas mass flow rate for any of the transitions from one flow type to another. There are also no abrupt changes noted in the liquid saturation data with the observed flow pattern. This suggests that the correlation of the data should be possible, independent of the flow pattern.

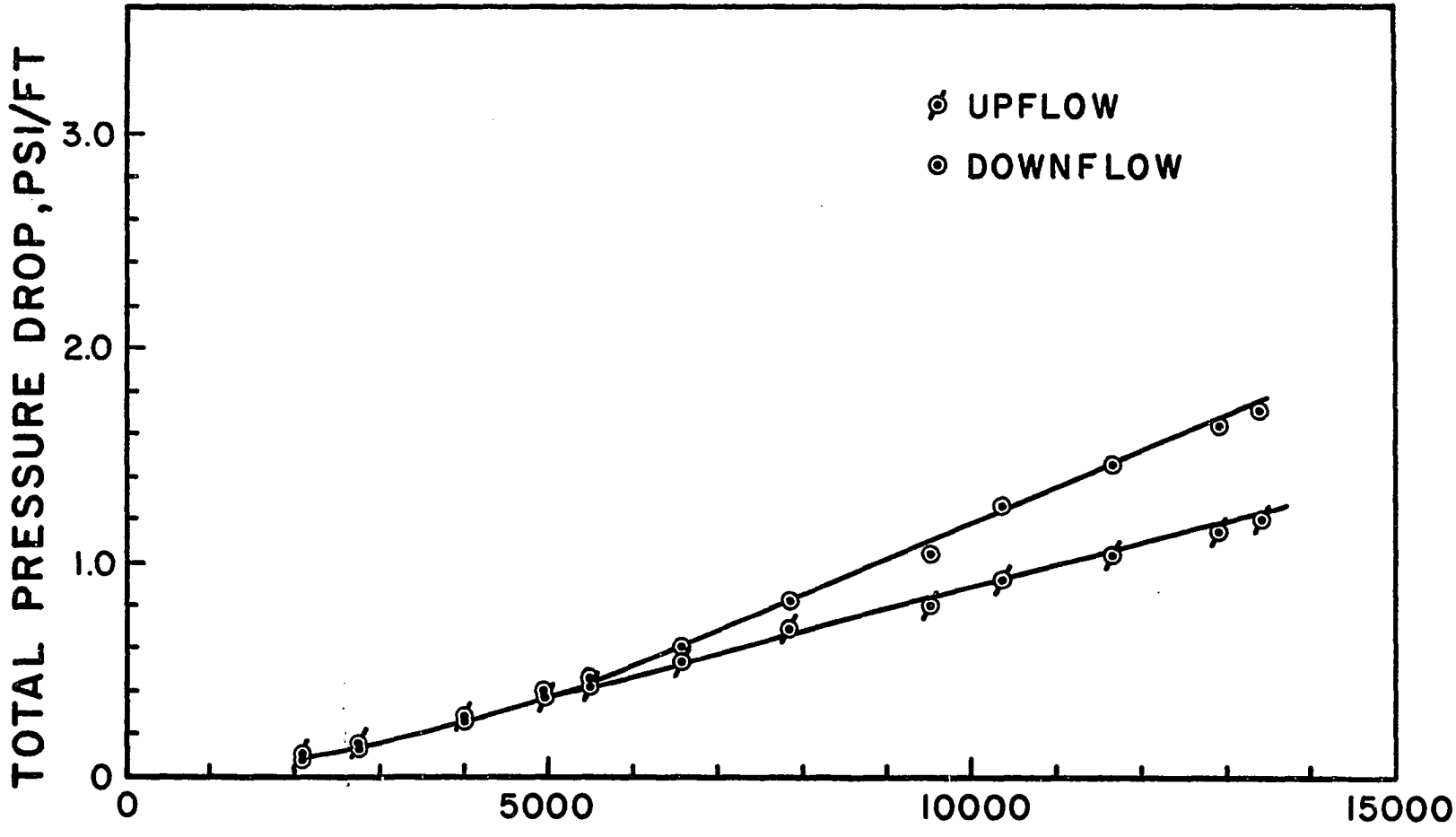

FIGURE 6. TOTAL PRESSURE DROP : 2 INCH DIA. COLUMN
WATER RATE = ZERO

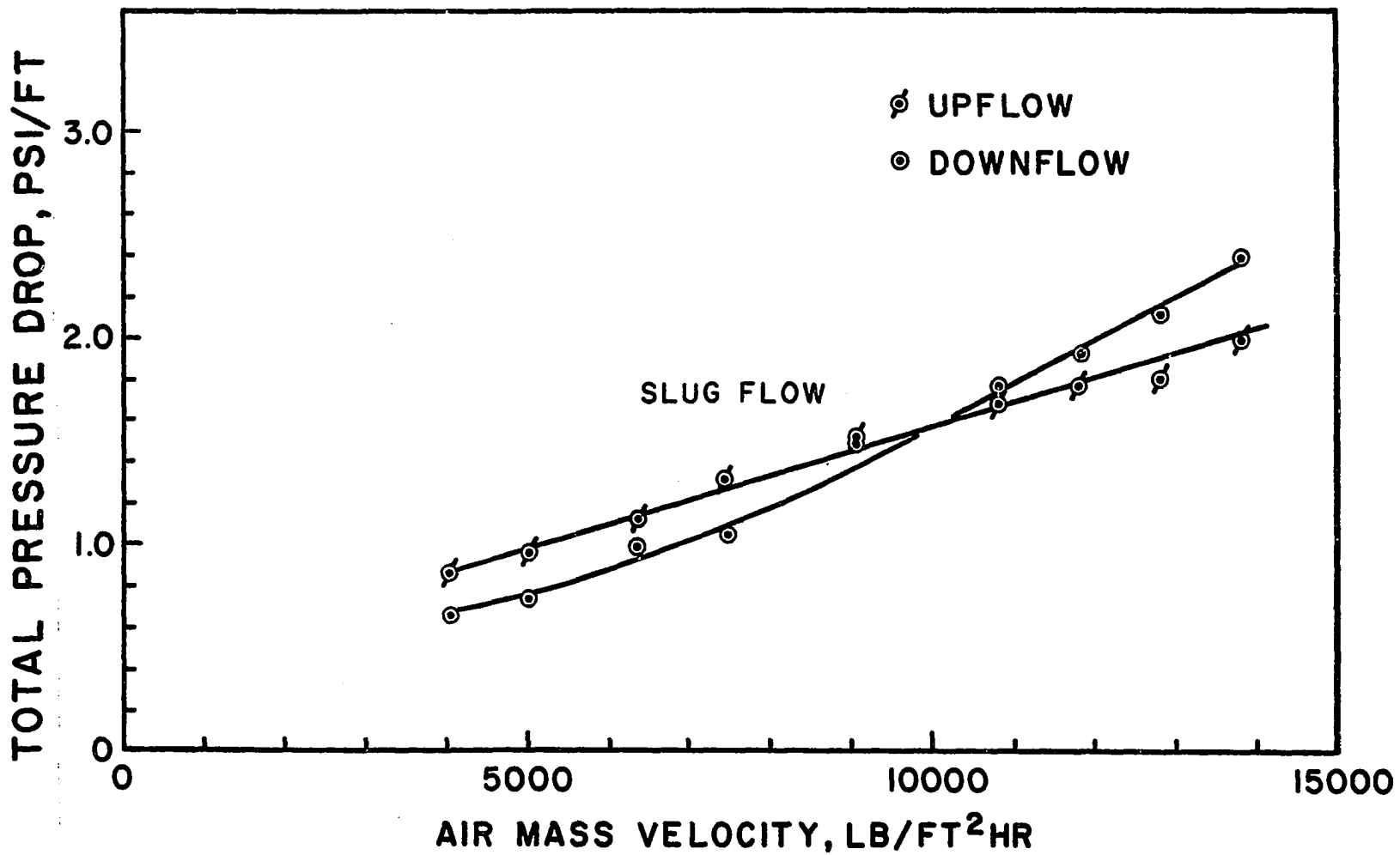

FIGURE 7. TOTAL PRESSURE DROP: 2 INCH DIA. COLUMN
WATER RATE = 13620 LB/FT²HR

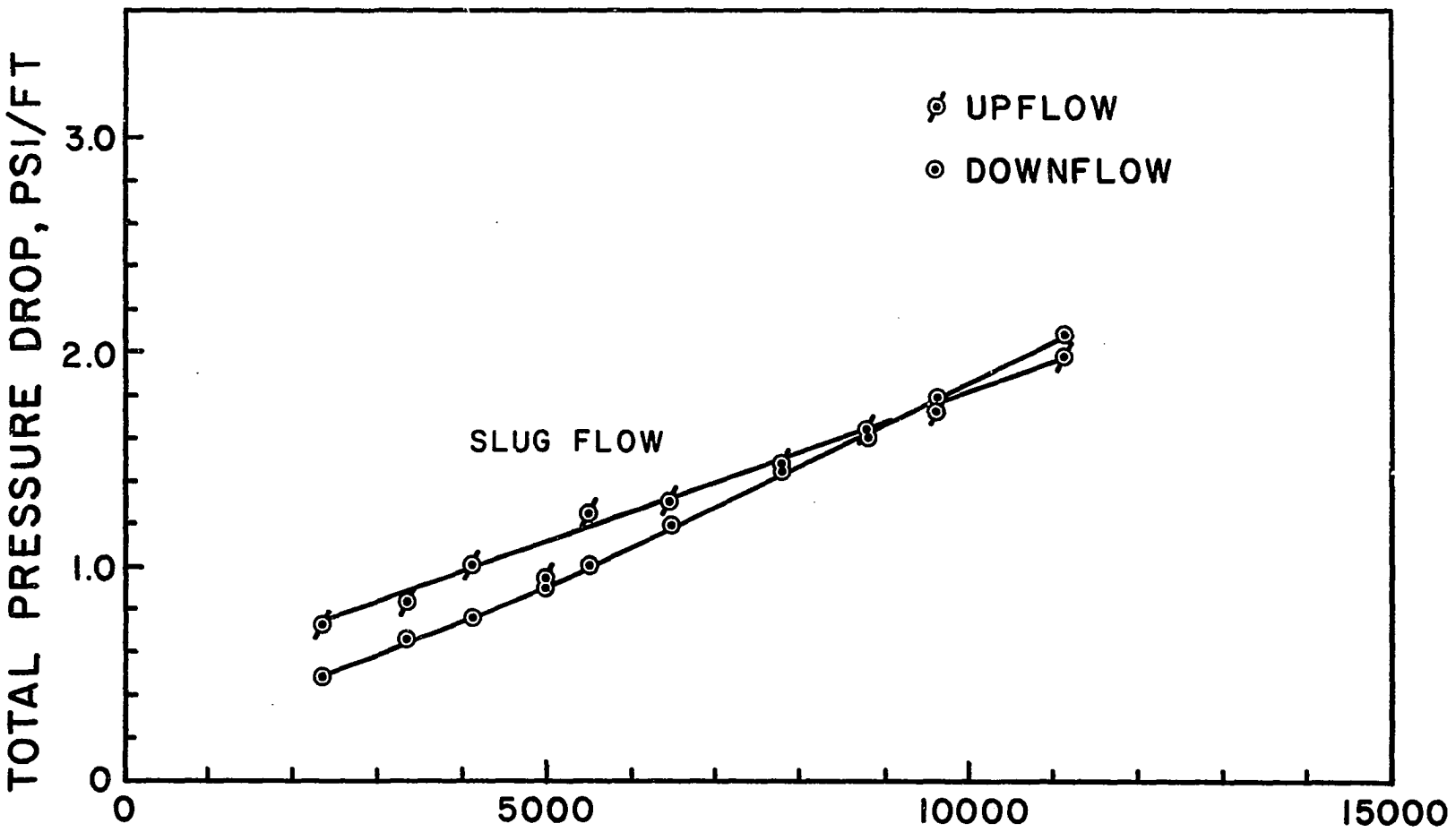

FIGURE 8. TOTAL PRESSURE DROP: 2 INCH DIA. COLUMN
WATER RATE = 30,100 LB/FT²HR

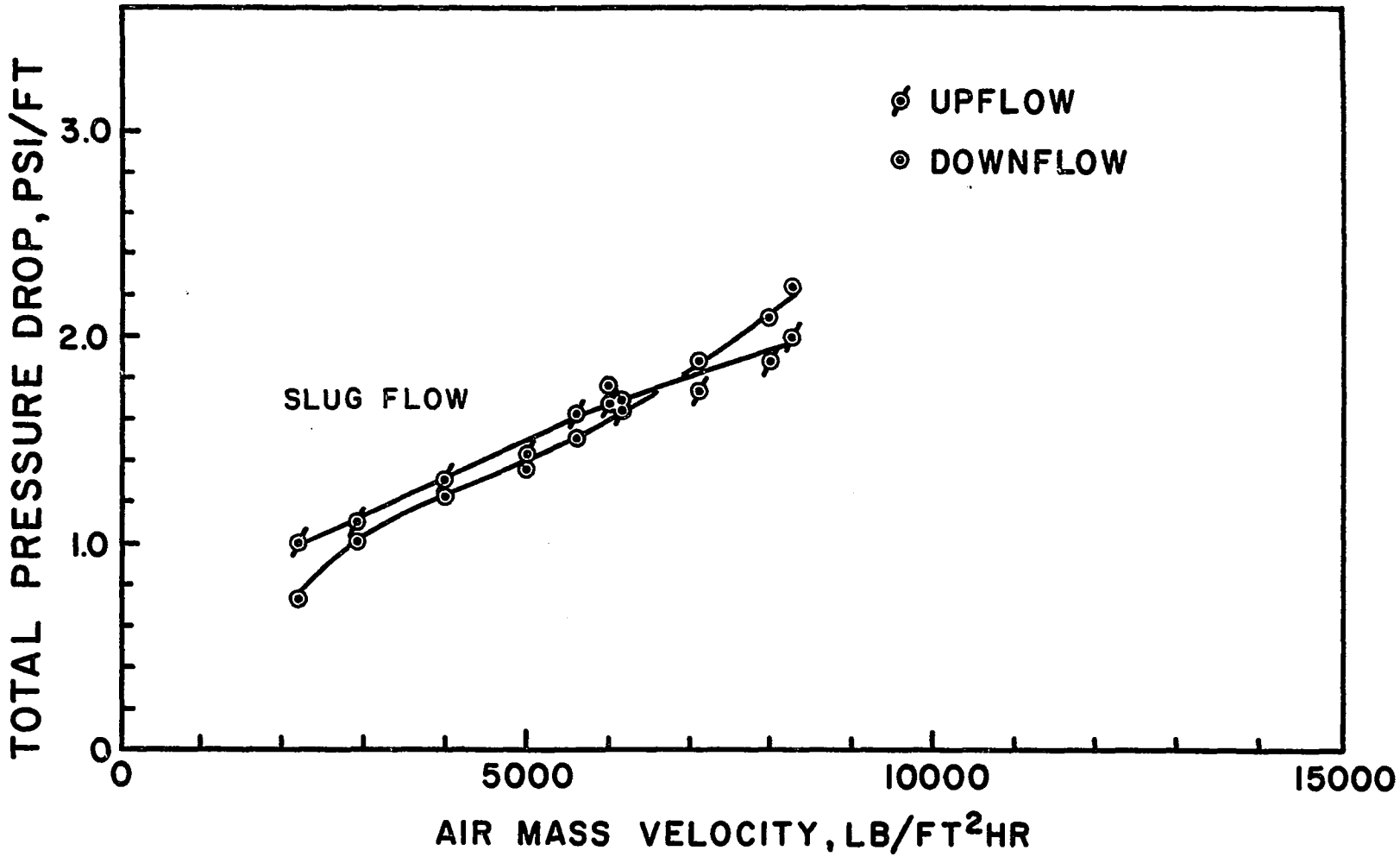

FIGURE 9. TOTAL PRESSURE DROP: 2 INCH DIA. COLUMN
WATER RATE = 56,300 LB/FT²HR

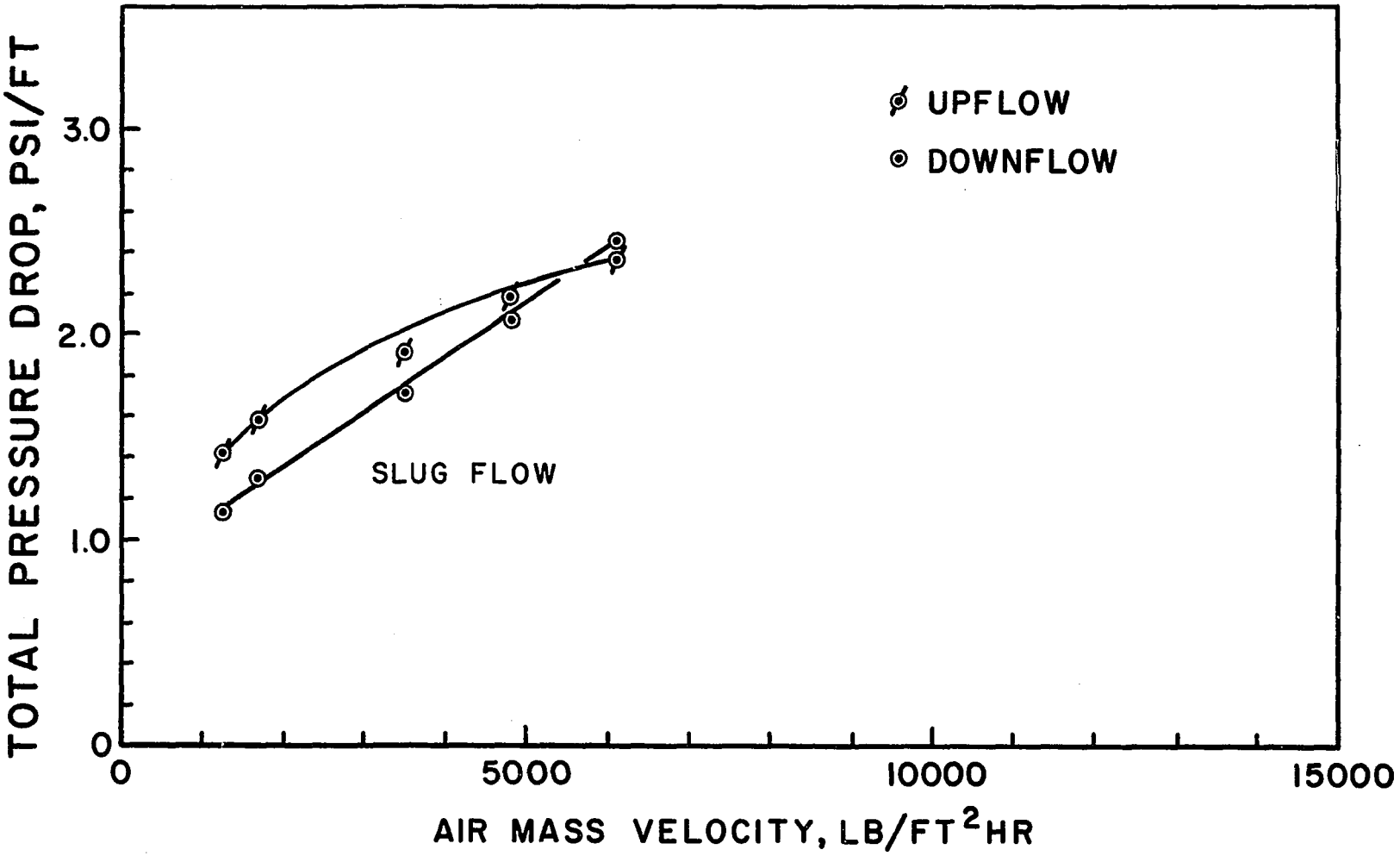

FIGURE 10. TOTAL PRESSURE DROP : 2 INCH DIA. COLUMN
WATER RATE = 112,000 LB/FT²HR

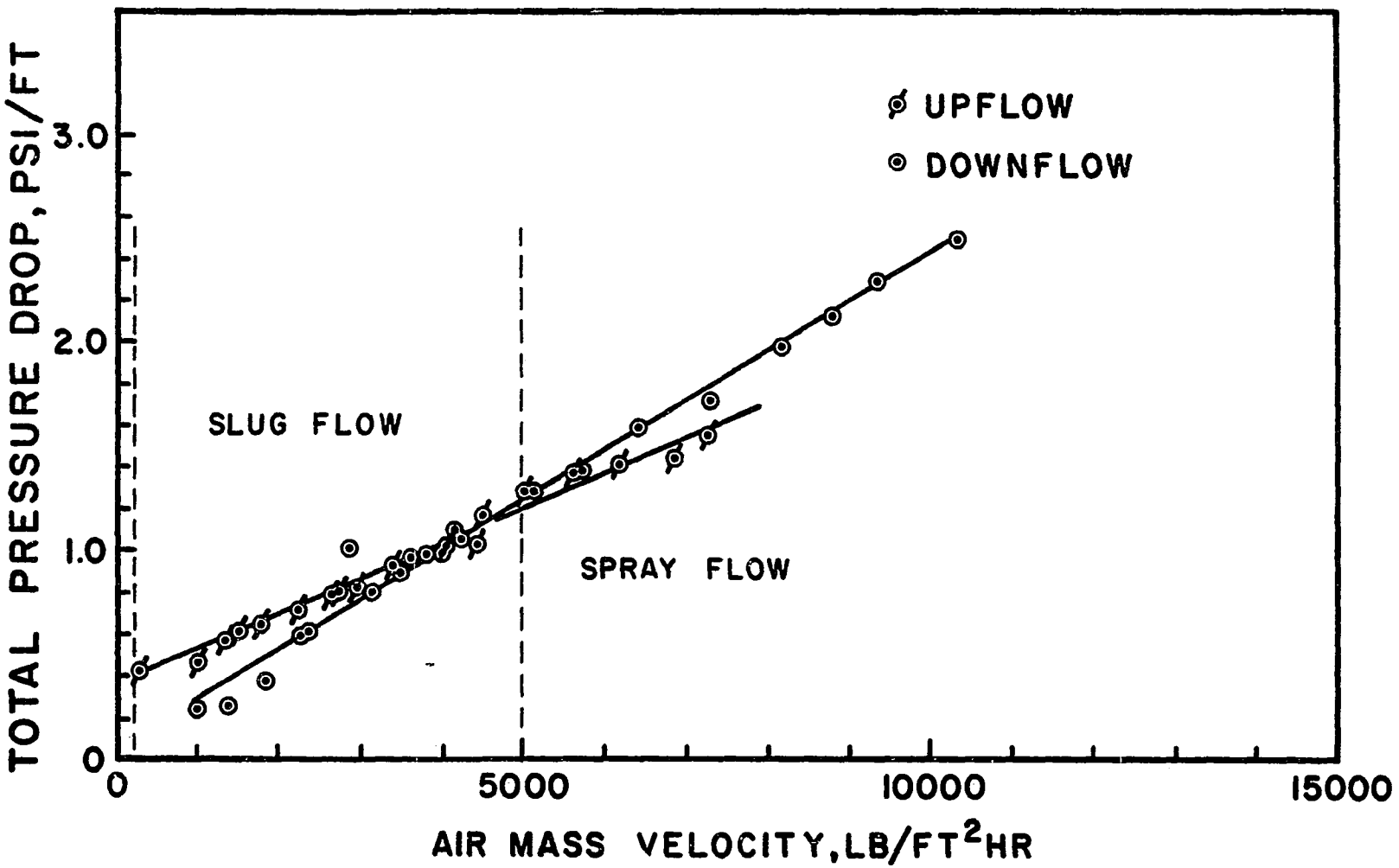

FIGURE II. TOTAL PRESSURE DROP: 4 INCH DIA. COLUMN
WATER RATE = 15,450 LB/FT²HR

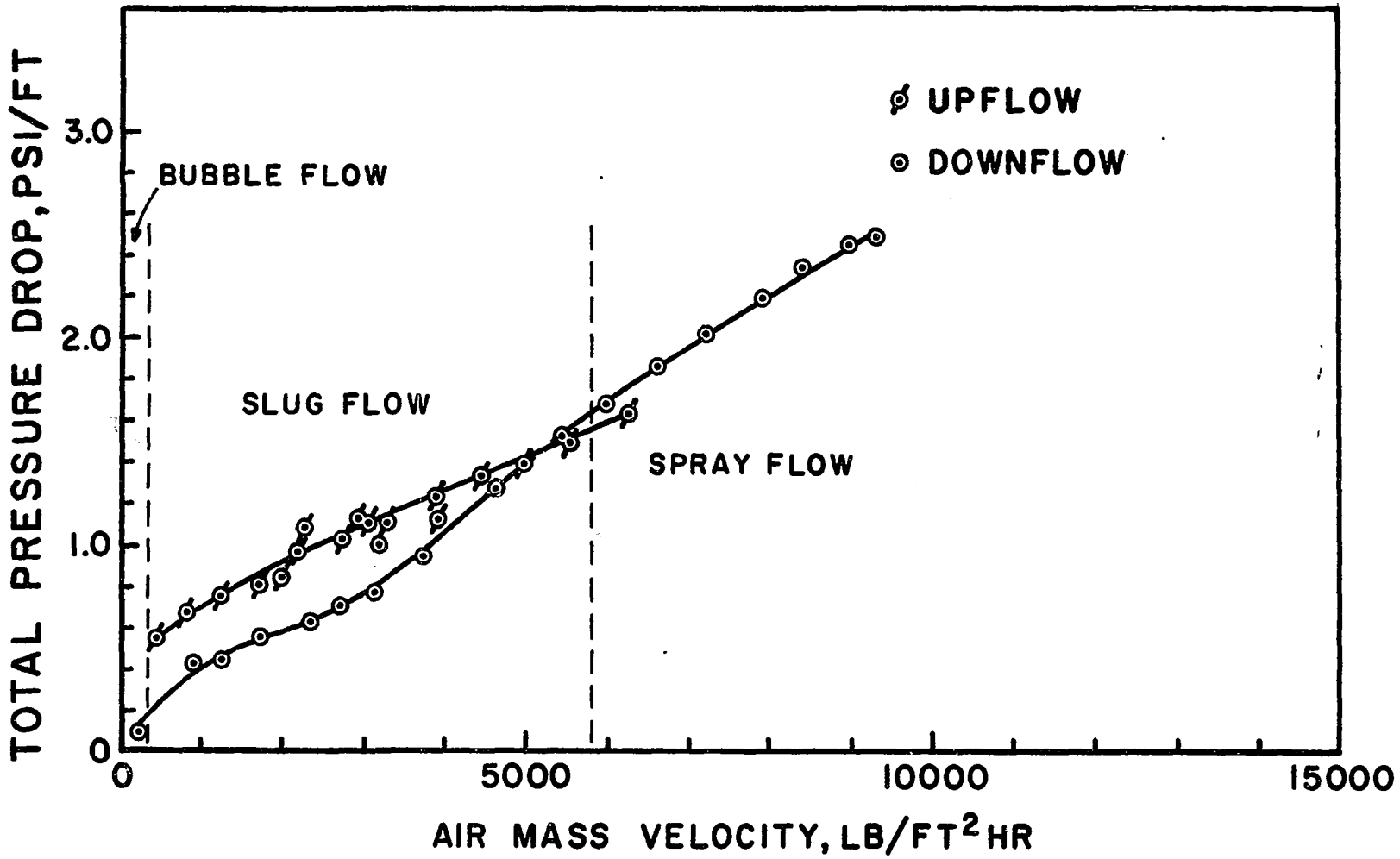

FIGURE 12. TOTAL PRESSURE DROP: 4 INCH DIA. COLUMN
WATER RATE = 29,200 LB/FT²HR

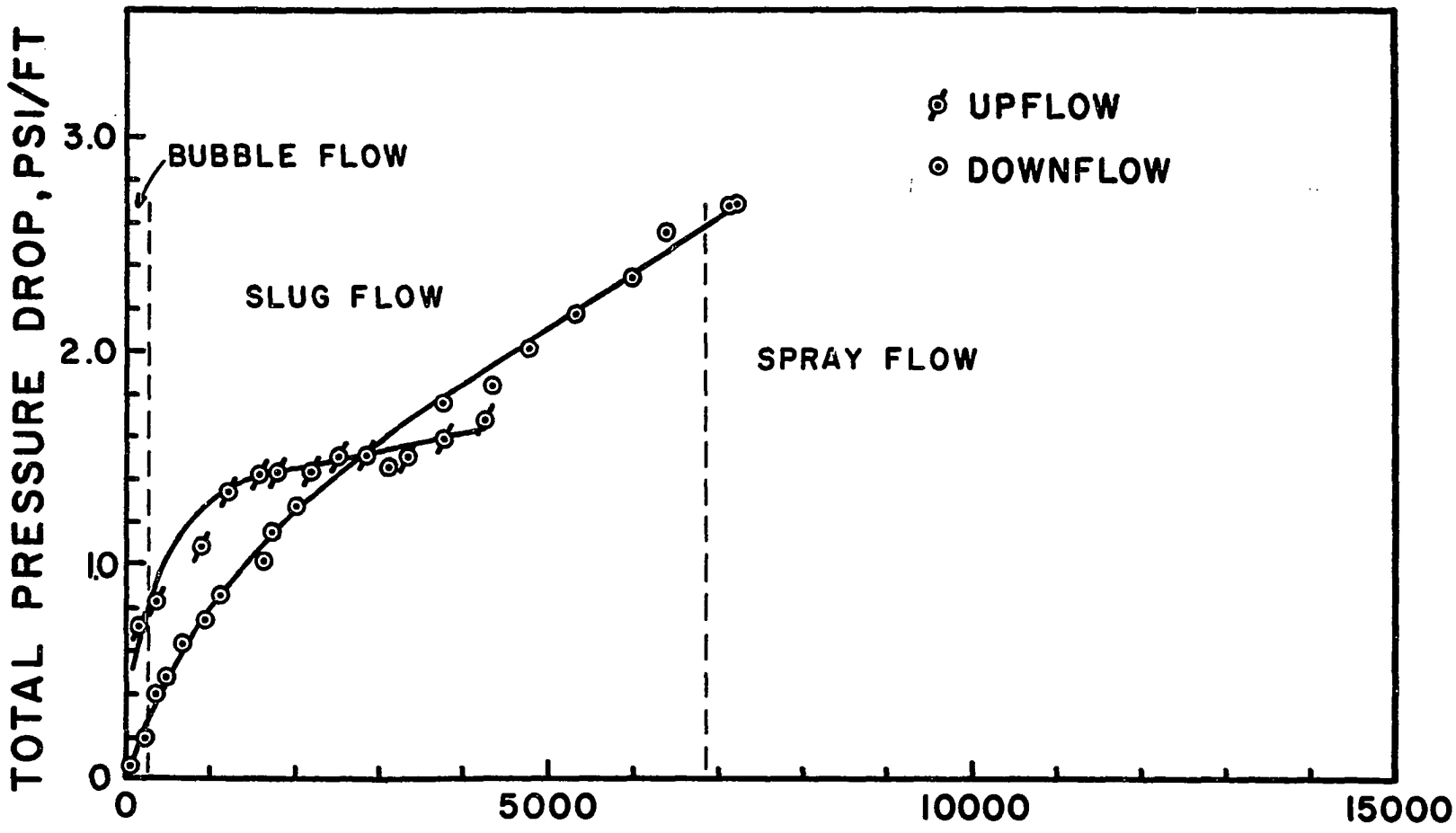

FIGURE 13. TOTAL PRESSURE DROP: 4 INCH DIA. COLUMN
WATER RATE = 58,000 LB/FT²HR

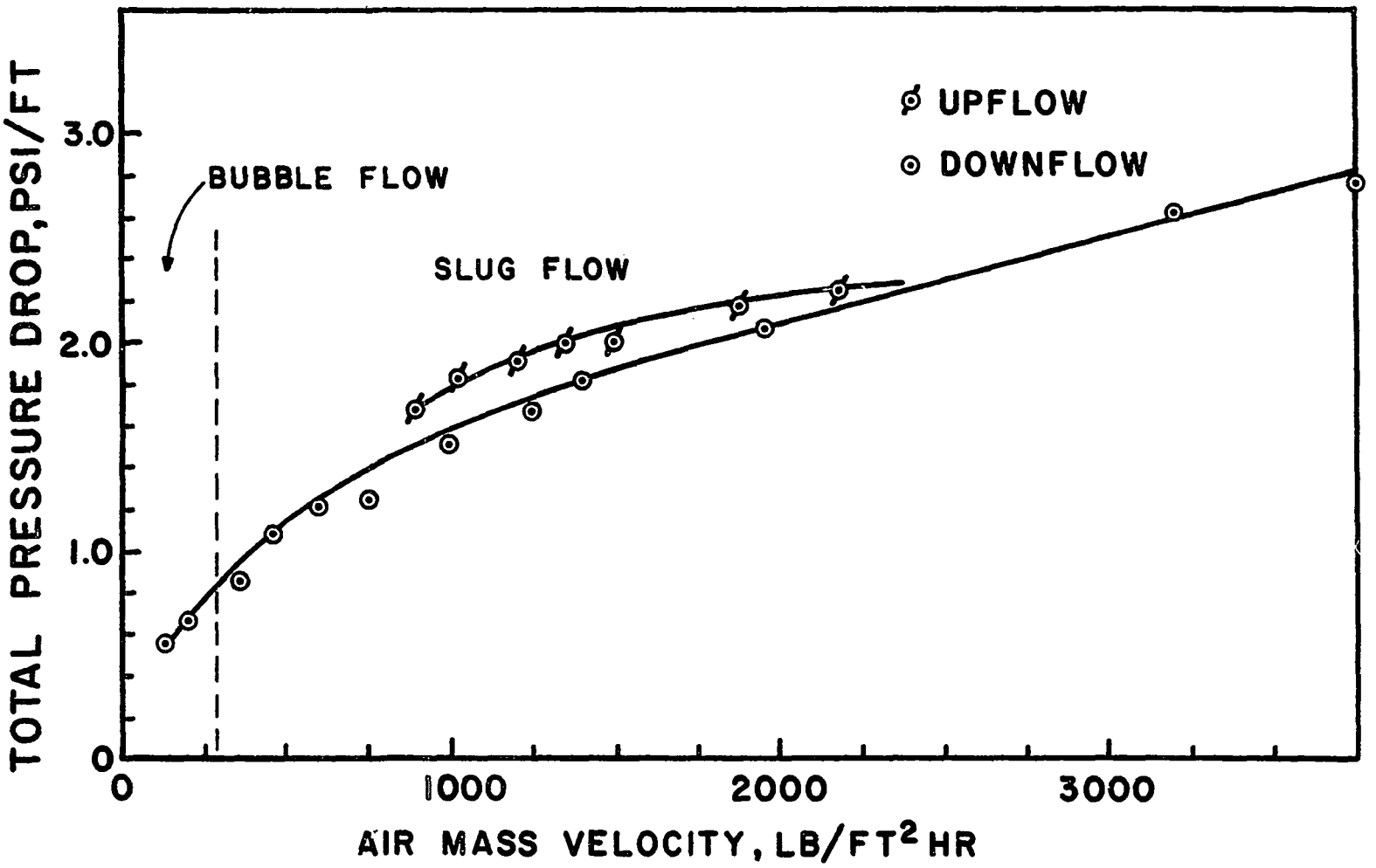

FIGURE 14. TOTAL PRESSURE DROP: 4 INCH DIA. COLUMN
WATER RATE = 114,200 LB/FT²HR

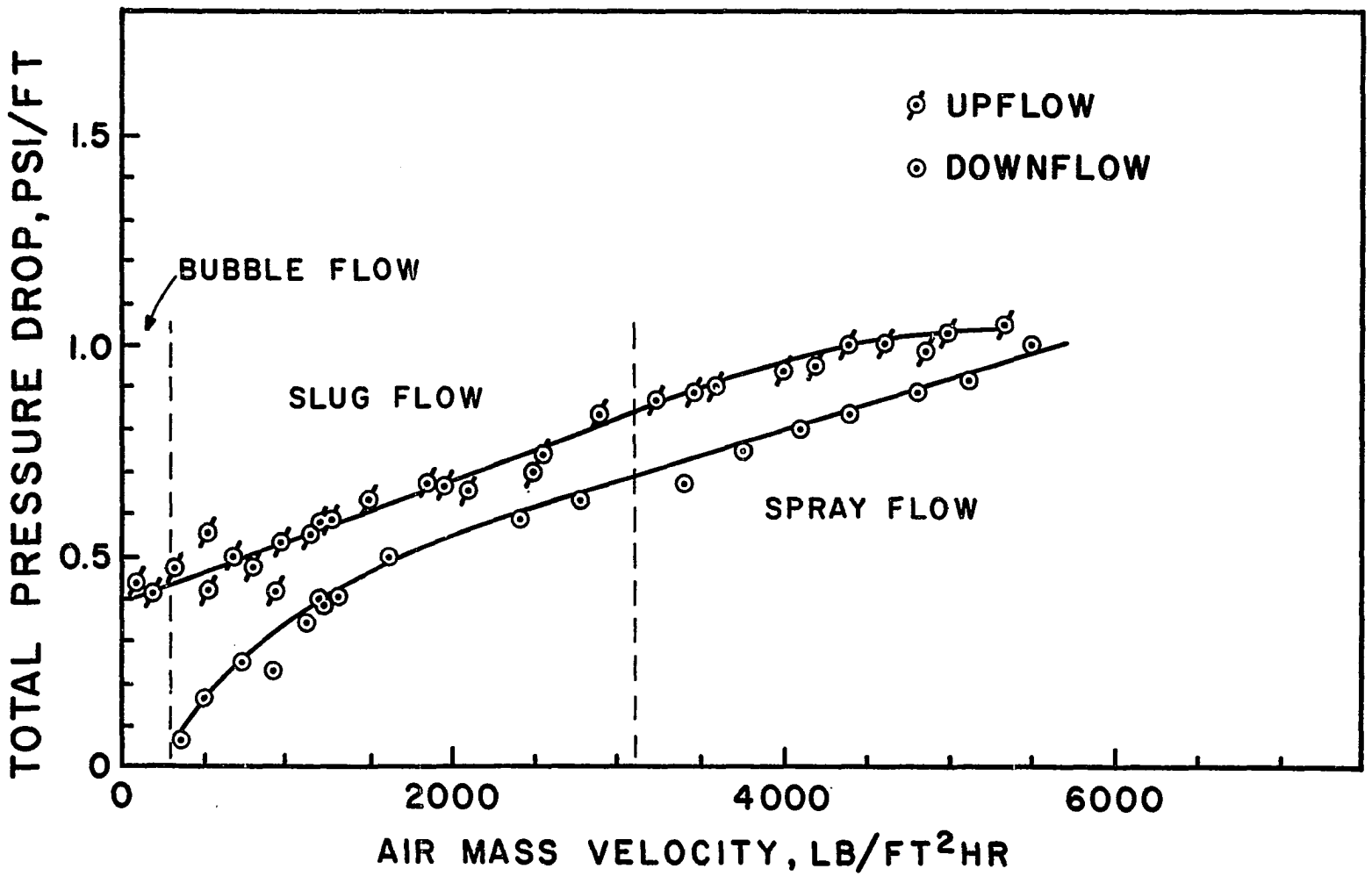

FIGURE 15. TOTAL PRESSURE DROP: 6 INCH DIA. COLUMN
WATER RATE = 16,500 LB/FT² HR

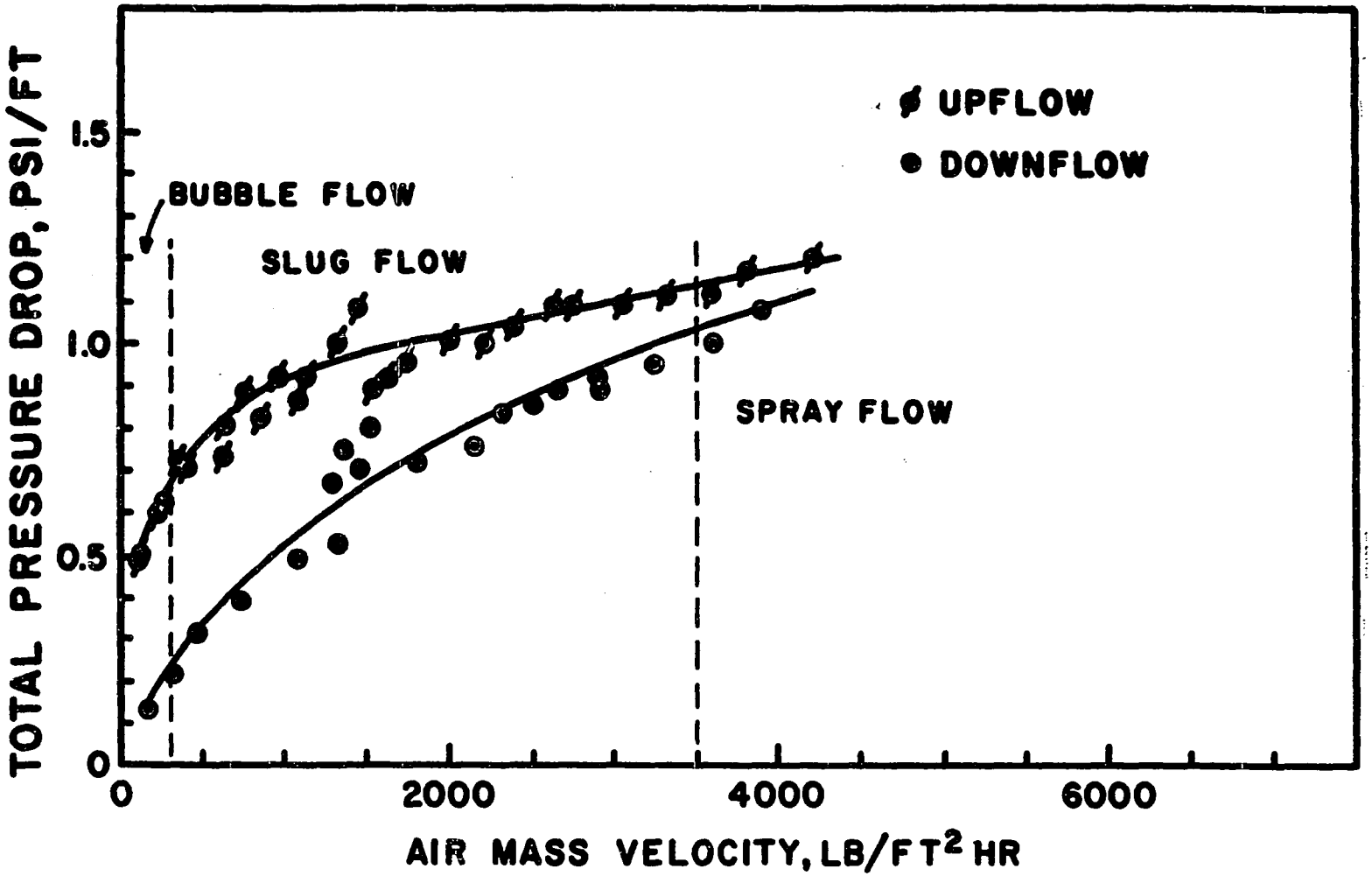

FIGURE 16. TOTAL PRESSURE DROP: 6 INCH DIA. COLUMN
WATER RATE = 33,000 LB/FT² HR

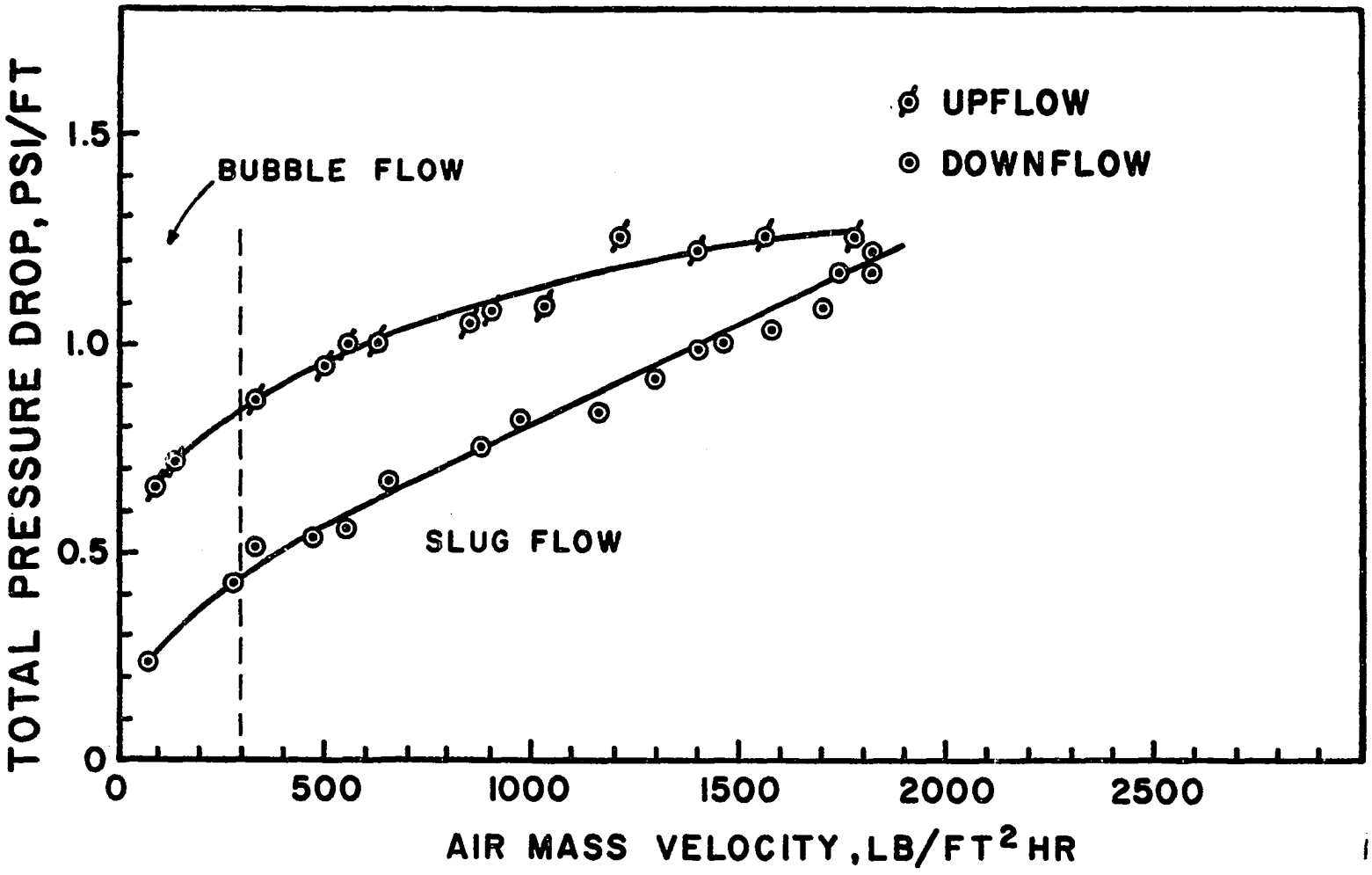

FIGURE 17. TOTAL PRESSURE DROP: 6 INCH DIA. COLUMN
WATER RATE = 65,500 LB/FT²HR

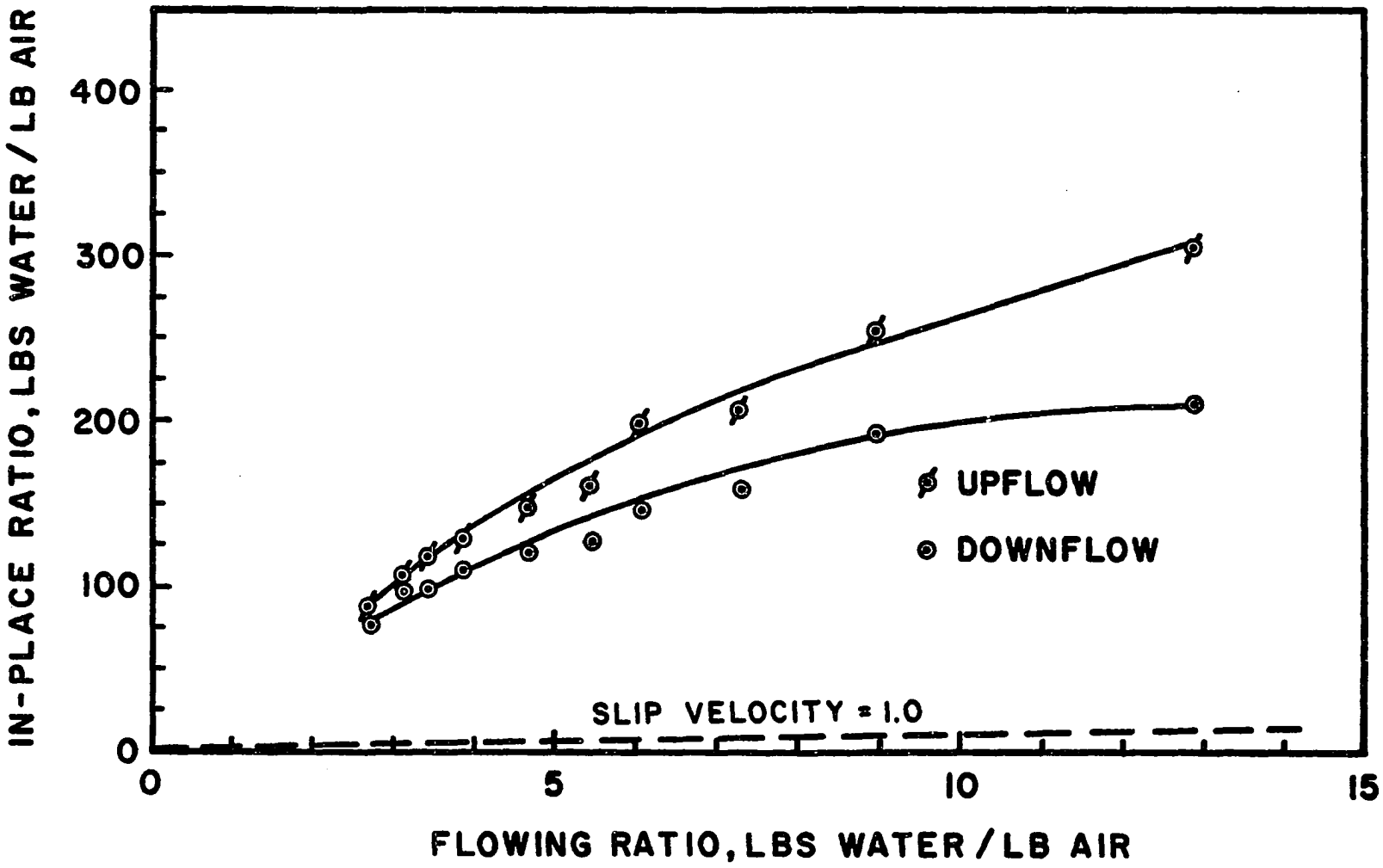

FIGURE 18. LIQUID SATURATION DATA — 2 INCH DIA. COLUMN
WATER RATE = 30,100 LBS / FT^2 HR

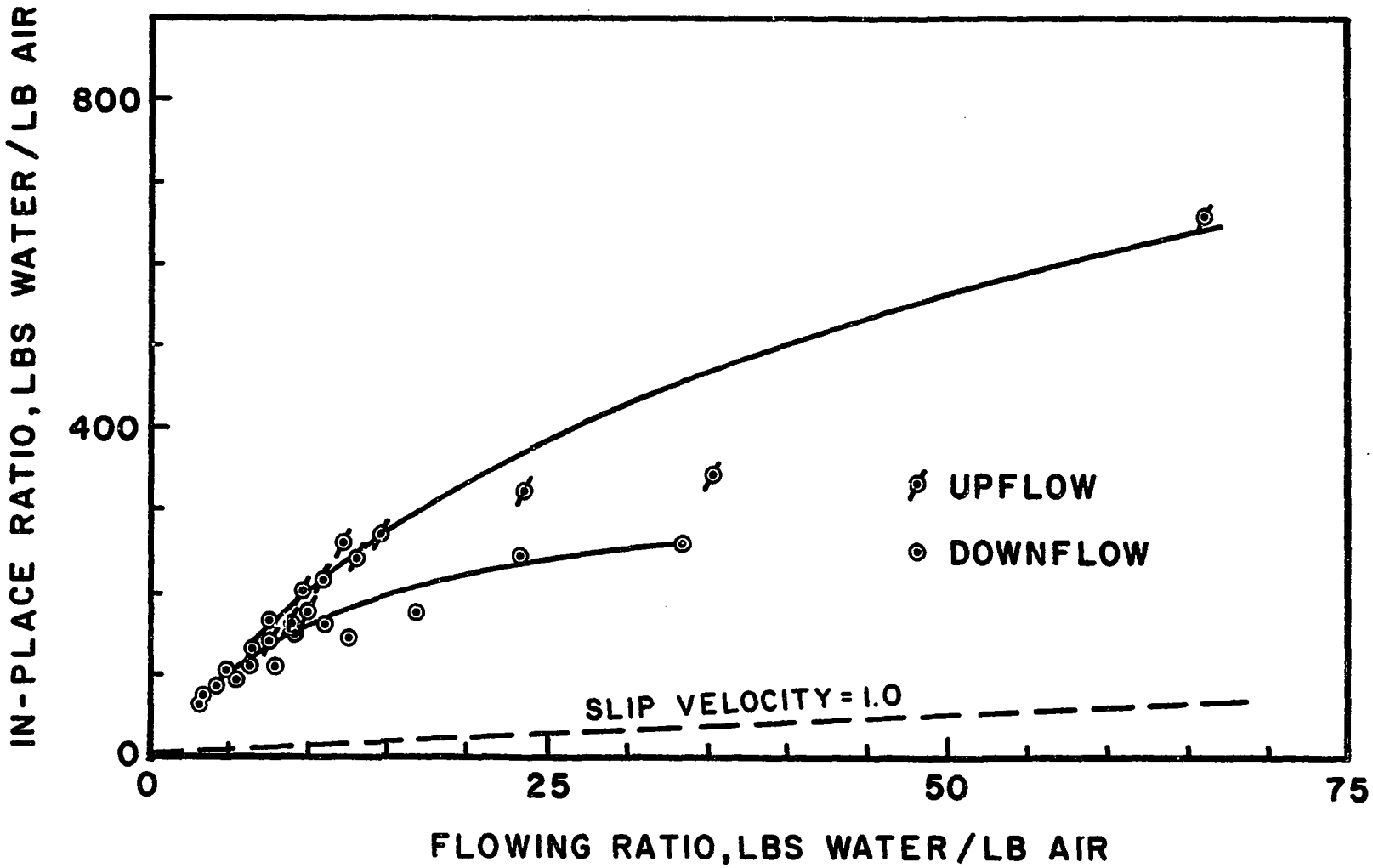

FIGURE 19. LIQUID SATURATION DATA — 4 INCH DIA. COLUMN
WATER RATE = 29,200 LBS/FT^{2}HR

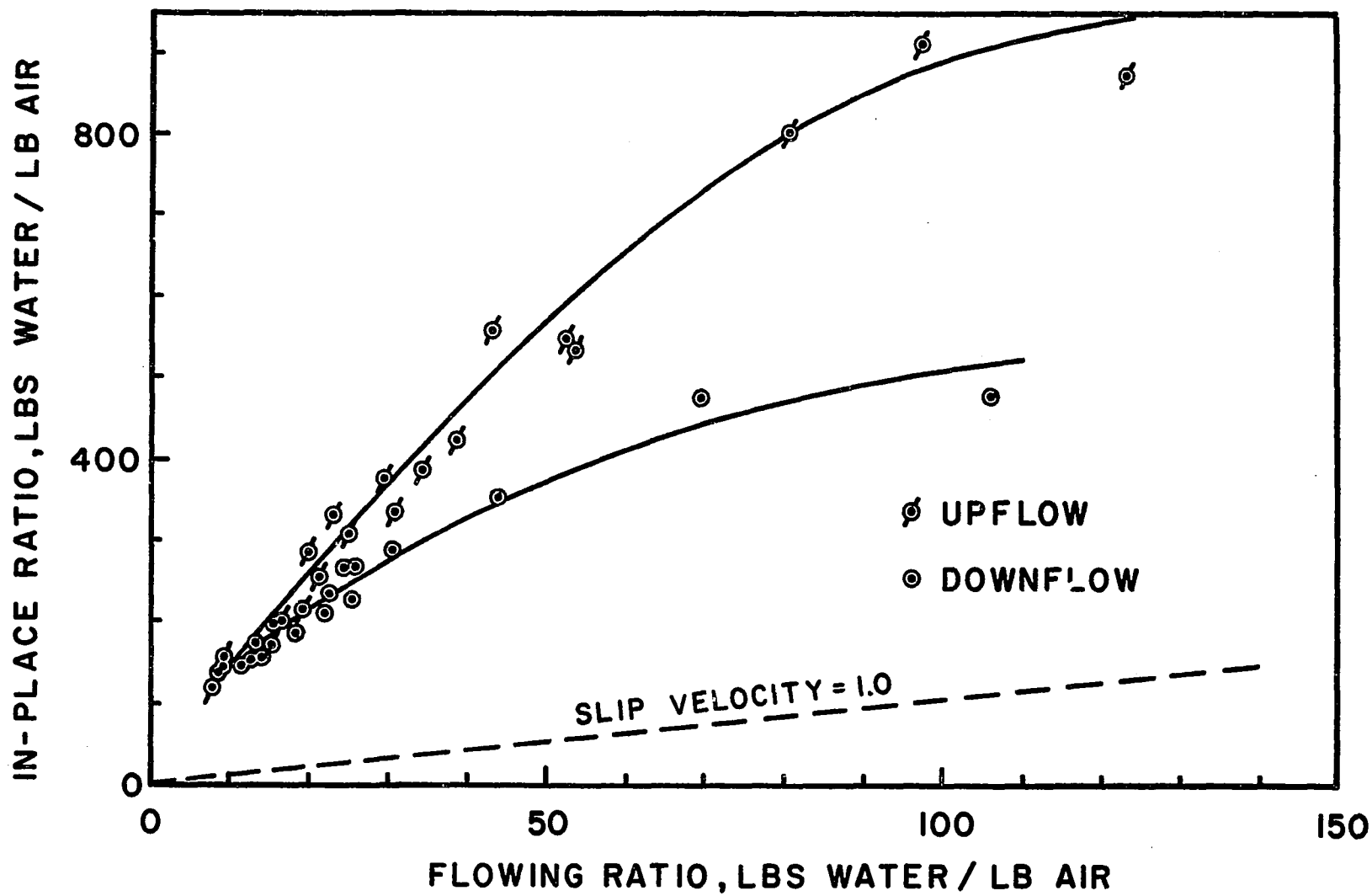

FIGURE 20. LIQUID SATURATION DATA — 6 INCH DIA. COLUMN
WATER RATE = 33,000 LBS/FT^{2}HR

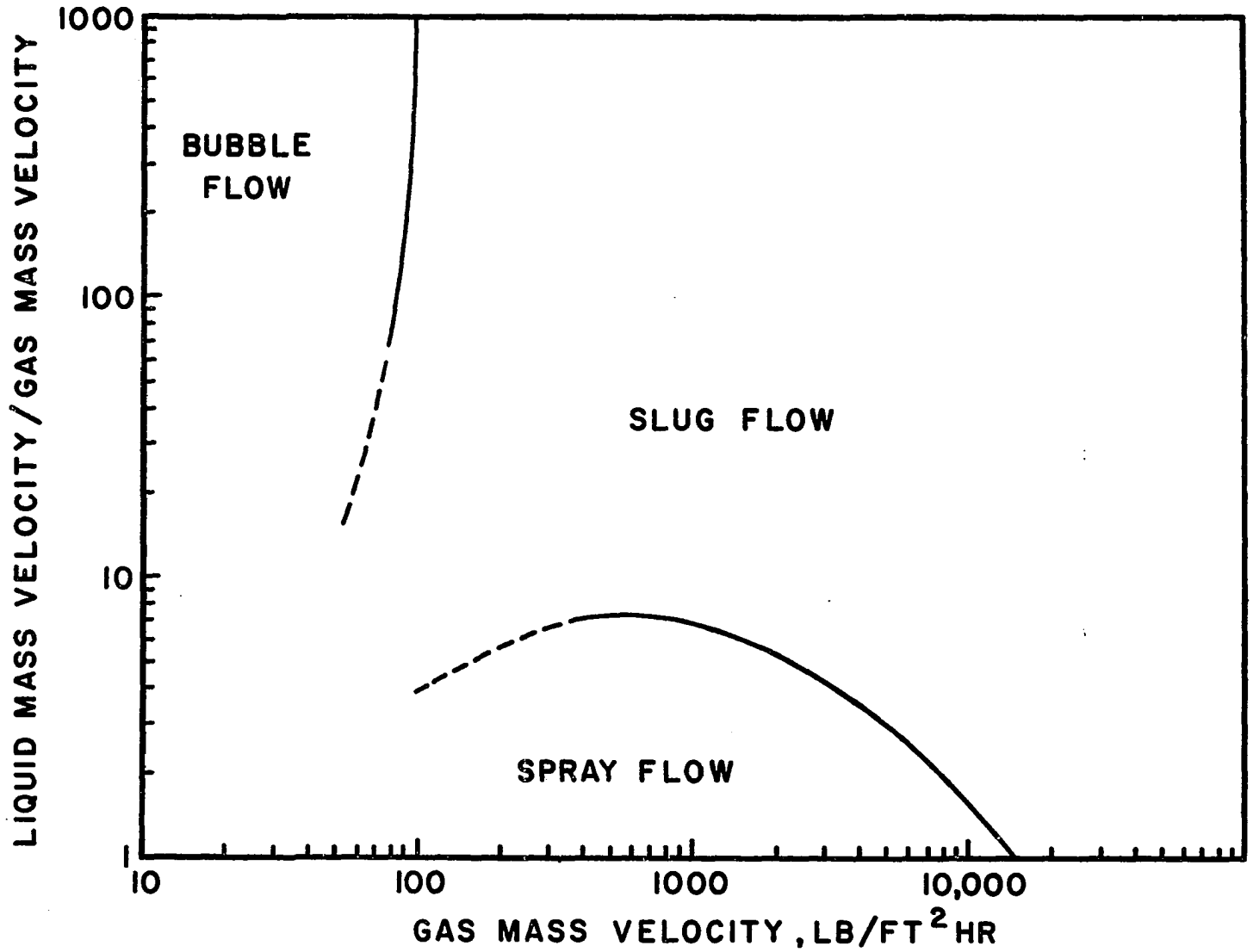

FIGURE 21. FLOW REGIMES—VERTICAL FLOW

CHAPTER VI

CORRELATION OF EXPERIMENTAL DATA

It is the objective of this section to convert and present the experimental data in a more generalized form than that presented in the previous section. To achieve this, the preliminary calculations are described, correlating relationships are established, the calculated data are used to verify these relationships, and the resulting generalized empirical correlations are presented.

Preliminary Calculations

Numerous preliminary calculations were necessary to obtain the required quantities for use in correlation from the raw experimental data. These preliminary calculations included:

(1) Calculation of the weight flow rates of each phase from the recorded meter readings.

(2) Conversion of the weight flow rate of each phase to mass flow rate based on the open cross-sectional area of the packed tube, and subsequent calculation of the flowing ratio of liquid-to-gas, G_L/G_G.

(3) Obtaining the total observed pressure gradient,

$(\Delta P/L)_{total}$, in common units for all experimental determinations from the manometer and/or pressure gage readings.

(4) Conversion of the height of the in-situ liquid interface to a fraction of the void volume filled with liquid, and subsequent determinations of the in-place mass ratio of liquid-to-gas.

(5) Calculation of the pressure drop due to acceleration of the fluids, ΔP_{acc}. The maximum value of ΔP_{acc} was determined to be only 0.5% of the total observed pressure drop which was less than the accuracy of the measurements. This term was thus neglected.

A desk calculator was used for the above preliminary calculations rather than a high-speed electronic computer, because each of the several physical situations of the experimental program would have required separate computer programming, and no saving of time could be envisioned. However, once these calculations were completed and the experimental data from each of the various physical situations were thus reduced to a common basis, the Osage Computer of the University of Oklahoma was utilized almost exclusively for the remainder of the required calculations.

Establishment of the Correlating Relationships

As the basis for establishing the generalized correlations, the final equation derived in the Theoretical

Discussion section will be utilized:

$$-(P_2 - P_1) = \Delta P_{TPf} + (\cos\theta/A)(C_2 \bar{A}_G L + \rho_L \bar{A}_L L + C_3 \bar{A}_G L^2/2) + (W_G/g_c A)(V_{G_2} - V_{G_1}) + (W_L/g_c A)(V_{L_2} - V_{L_1}) \quad (30)$$

Rewriting equation (30) for vertical flow and neglecting ΔP_{acc} as was indicated by the preliminary calculations:

$$-(P_2 - P_1) = \Delta P_{TPf} + (1/A)(C_2 \bar{A}_G L + \rho_L \bar{A}_L L + C_3 \bar{A}_G L^2/2) \quad (32)$$

The use of (32) requires evaluation of the two-phase frictional pressure drop, ΔP_{TPf}, and $\bar{A}_L$ (and thus $\bar{A}_G$). A knowledge of the liquid saturation, R_v, is tantamount to a knowledge of $\bar{A}_L$, and the two-phase frictional pressure drop may be expressed in terms of a two-phase friction factor, f_{TPf}, which is defined below. Thus, correlations of the quantities f_{TPf} and R_v in terms of known system variables for both upward and downward flow are desired, and it is the purpose of this section to establish such correlating relationships for each of these quantities.

The two-phase friction factor to be employed was defined in the manner of a single-phase friction factor:

$$f_{TPf} = \frac{(\Delta P/L)_{fric} D g_c}{2\rho_{Gl} \bar{V}_{Gs}^2} \quad (33)$$

Individual quantities of this defining equation require clarification. The two-phase frictional pressure gradient

is the frictional pressure drop divided by the length of the test section. The diameter, D, is the diameter of a circle having the same area as the open area of the packed tube. Gas density, ρ_{Gl}, is the density at the entering temperature and pressure. The superficial gas velocity, $\overline{V}_{Gs}$, is the velocity which the gas would have if it were flowing alone in the packed bed at the entering density, ρ_{Gl}.

The results of a dimensional analysis of two-phase flow given in Appendix C reveal that the frictional pressure gradient is given by:

$$\left(\frac{\Delta P}{L}\right)_{fric} = \frac{\overline{V}_{Gs}^{2}\,\rho_{Gl}}{Dg_c}\,\varphi\left[\,(N_{Re_L})^{a}(N_{Re_G})^{b}(D_p/D_t)^{c}\,\right] \qquad (34)$$

Rearranging equation (34) and comparing with the definition of the two-phase friction factor given by equation (33):

$$f_{TPf} = \frac{(\Delta P/L)_{fric}\,Dg_c}{2\overline{V}_{Gs}^{2}\,\rho_{Gl}} = \frac{\varphi}{2}\left[(N_{Re_L})^{a}(N_{Re_G})^{b}(D_p/D_t)^{c}\,\right] \qquad (35)$$

or,

$$f_{TPf} = \varphi_1[(N_{Re_L})^{a}(N_{Re_G})^{b}(D_p/D_t)^{c}\,] \qquad (36)$$

for upward flow, and:

$$f_{TPf} = \varphi_2[(N_{Re_L})^{a}(N_{Re_G})^{b}(D_p/D_t)^{c}\,] \qquad (37)$$

for downward flow.

The remaining correlating relationships to be established are those for the liquid saturation, R_v. From a study

of the graphs of in-place ratio versus flowing ratio presented in the previous chapter, the following equations were proposed:

$$R_v = \psi_1 (G_L/G_G)^d \tag{38}$$

$$R_v = \psi_2 (G_L/G_G)^d \tag{39}$$

for upward and downward flow, respectively.

For empirical verification of equations (36), (37), (38), and (39), additional reduced data were required. Using the experimentally determined values of R_v for calculation of $\bar{A}_L$ and $\bar{A}_G$, the two-phase frictional pressure drops were obtained by difference using equation (32). The two-phase friction factors were calculated from equation (33). Reynolds numbers were obtained using the mass flow rates of each respective phase based on the open area of the packed tube as outlined in the preliminary calculations. The ratio of particle diameter to column diameter was then calculated for each of the three columns. These completed the reduced data required for evaluation of equations (36) and (37). No additional reduced data were required for evaluation of equations (38) and (39).

As the first step in the evaluation of equations (36) and (37), it was necessary to determine the values of the exponents a, b, and c. To accomplish this an assumption of the functional form for each of the respective equations was required. It was thus assumed that equations (36) and (37) could be written as:

$$f_{TPf} = (\text{constant})(N_{Re_L})^{a}(N_{Re_G})^{b}(D_p/D_t)^{c} \qquad (40)$$

Taking the logarithm of equation (40) for a constant liquid Reynolds number and for a given diameter ratio gives:

$$\ln f_{TPf} = \text{constant} + b \ln N_{Re_G} \qquad (41)$$

Because the experimental data had been taken at several constant liquid Reynolds numbers in each of the packed beds while varying the gas Reynolds number, evaluation of b was possible with the available reduced data.

Values of $\ln f_{TPf}$ were plotted versus values of $\ln N_{Re_G}$ for each of the eleven available constant liquid Reynolds numbers for upward flow. A least-square fit was obtained for each set of data giving the least-square slope, which is seen from equation (41) to be the value of the exponent b. The average value of these eleven least-square determinations was taken as the value of b for upward flow. These procedures were repeated for downward flow and the average of the eleven least-square determinations of b was calculated. The difference between the average value of b calculated for upward flow and that calculated for downward flow was less than 2%, and an average of these two was thus taken as the final value for b.

To obtain a the logarithm of equation (40) was taken for a constant gas Reynolds number and for a given diameter ratio:

$$\ln f_{TPf} = \text{constant} + a \ln N_{Re_L} \qquad (42)$$

The procedures described above were repeated except that the data for the least-square fit had to be obtained from a cross-plot at constant gas Reynolds numbers. In this instance the difference between the values of the exponent calculated for upflow and downflow was approximately 1 1/2%, and again an average of the two was used.

The logarithm of equation (40) was taken holding both the gas Reynolds number and the liquid Reynolds number constant:

$$\ln f_{TPf} = \text{constant} + c \ln (D_p/D_t) \qquad (43)$$

It was again necessary to obtain the required data from a cross-plot at constant liquid and gas Reynolds numbers. The least-square procedures were repeated for the second time to obtain the value of the exponent c. The deviation between the upflow c and the downflow c was less than 1% and an average of the two was taken.

A final least-square evaluation was made to obtain the exponent d of equations (38) and (39). The calculated values of the exponents are given in Table III. Substitution of the respective values of the exponents into equations (36), (37), (38) and (39) establish the proposed correlating relationships and evaluation of their respective functional form remains.

TABLE III

CALCULATED EXPONENTS

Exponent	Upflow	Downflow	Average
a	0.761	0.773	0.767
b	-1.177	-1.157	-1.167
c	-1.511	-1.525	-1.518
d	0.24	0.24	0.24

Presentation of Correlated Data

As the first step in the presentation of the correlated data, values of

$$1/Z = N_{Re_L}^{0.767} \; N_{Re_G}^{-1.167} \; (D_p/D_t)^{-1.518} \qquad (44)$$

were calculated for each experimental determination. It was noted that the two-phase friction factor was an increasing function of 1/Z for both upward and downward flow. Therefore, in order to produce a correlation with the general appearance of the standard friction factor-Reynolds number plot, the group 1/Z was inverted:

$$Z = \frac{N_{Re_G}^{1.167} \; (D_p/D_t)^{1.518}}{N_{Re_L}^{0.767}} \qquad (45)$$

The final plots of the two-phase friction factor, f_{TPf}, versus the group Z are presented in Figure 22 and Figure 23 for upward and downward flow, respectively. It

was necessary for these to be plotted on logarithmic scales because of the wide range of values covered by each of the variables. The equations of the best fit for these respective data plots were determined using the Osage computer and a curve-fitting program which calculated the least-square fit for any number of parameters and then indicated the degree of polynomial which would provide the minimum variance.

The best fitting curve (minimum variance) for the upward flow data is given by:

$$\ln f_{TPf} = 5.598 - 1.105 \ln Z + 0.0337(\ln Z)^2 + 0.00697(\ln Z)^3 \qquad (46)$$

$$(0.01 \leq Z \leq 100)$$

and this equation is reproduced on Figure 22. Rather than f_{TPf} and Z, it was necessary to use the logarithms of these quantities in equation (46), because the data were presented on a logarithmic rather than a rectangular plot. Slightly more than 90% of the experimental data were within ±25% of the value given by equation (46).

The best fitting curve for the downward flow data is given by:

$$\ln f_{TPf} = 5.41 - 1.065 \ln Z + 0.0332(\ln Z)^2 - 0.00036(\ln Z)^3 + 0.000983(\ln Z)^4 \qquad (47)$$

$$(0.01 \leq Z \leq 100)$$

More than 91% of the experimental data were within ±25% of the value given by equation (47). The curve of equation (47)

is reproduced on Figure 23.

For comparison, values of f_{TPf} and Z were calculated from the downward flow data of Larkins' (62). The best fitting curve for this data is given by:

$$\ln f_{TPf} = 5.426 - 1.117 \ln Z' + 0.0706(\ln Z')^2 \qquad (48)$$

$$(0.01 \leq Z' \leq 100)$$

where Z' differs from Z by a viscosity correction factor which will be discussed in the next chapter. A graphical comparison of equation (46), (47), (48) is presented in Figure 24 and this will also be discussed in the next chapter.

Correlations of the liquid saturation data were obtained using the exponent d reported in Table III in equations (38) and (39). Values of $(G_L/G_G)^{0.24}$ were calculated for each experimental determination, and these were plotted versus their respective liquid saturations. These results are shown graphically in Figures 25 and 26 for upward flow and downward flow, respectively.

The curve-fitting computer program described previously was applied to the data of each of these graphs. The best fitting curve for the upward flow data is given by:

$$R_V = -0.134 + 0.467(G_L/G_G)^{0.24} - 0.237\left[(G_L/G_G)^{0.24}\right]^2 + 0.0737\left[(G_L/G_G)^{0.24}\right]^3 - 0.0075\left[(G_L/G_G)^{0.24}\right]^4 \qquad (49)$$

$$(1.0 \leq (G_L/G_G)^{0.24} \leq 6.0)$$

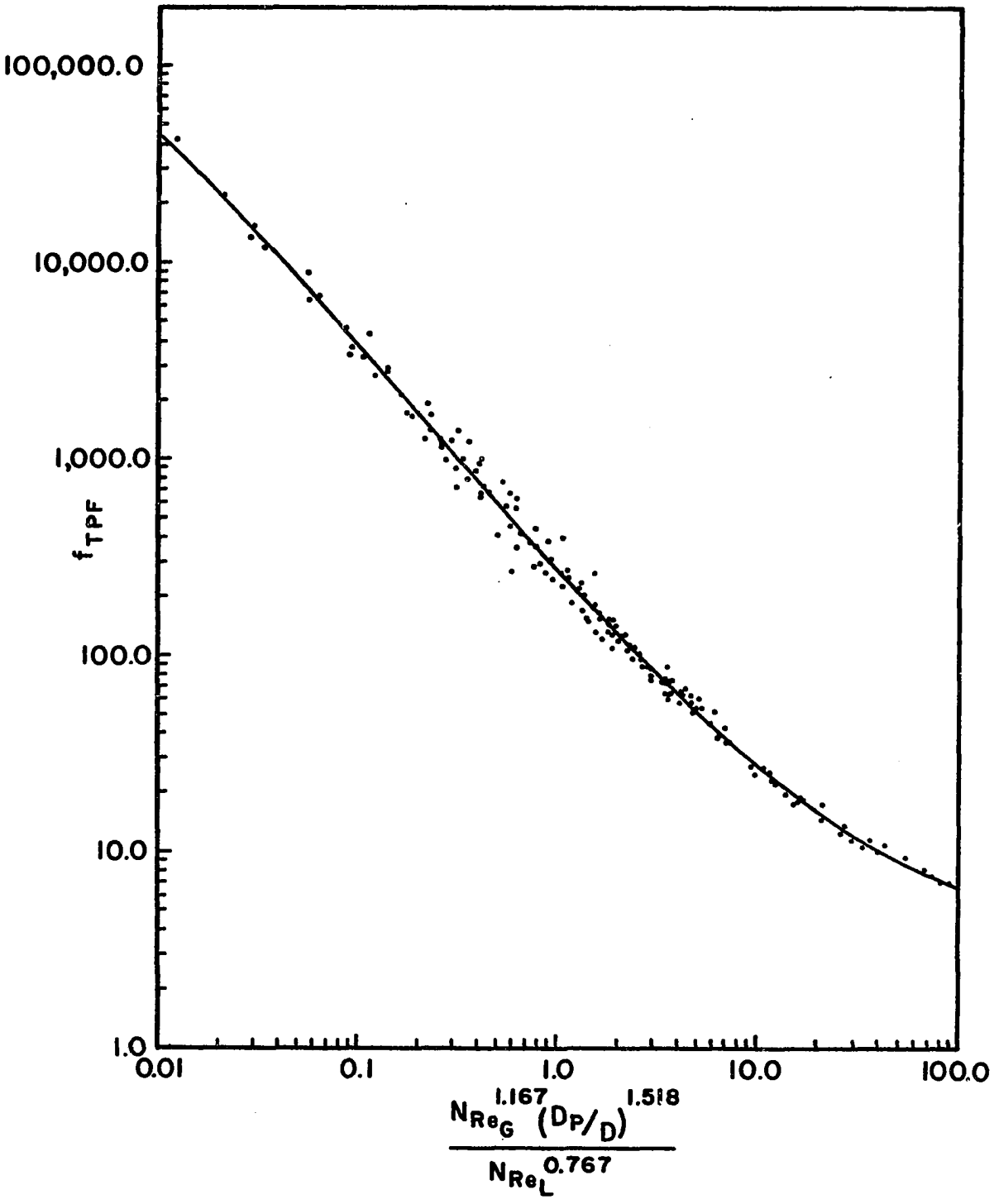

FIGURE 22. FRICTION FACTOR CORRELATION UPWARD FLOW

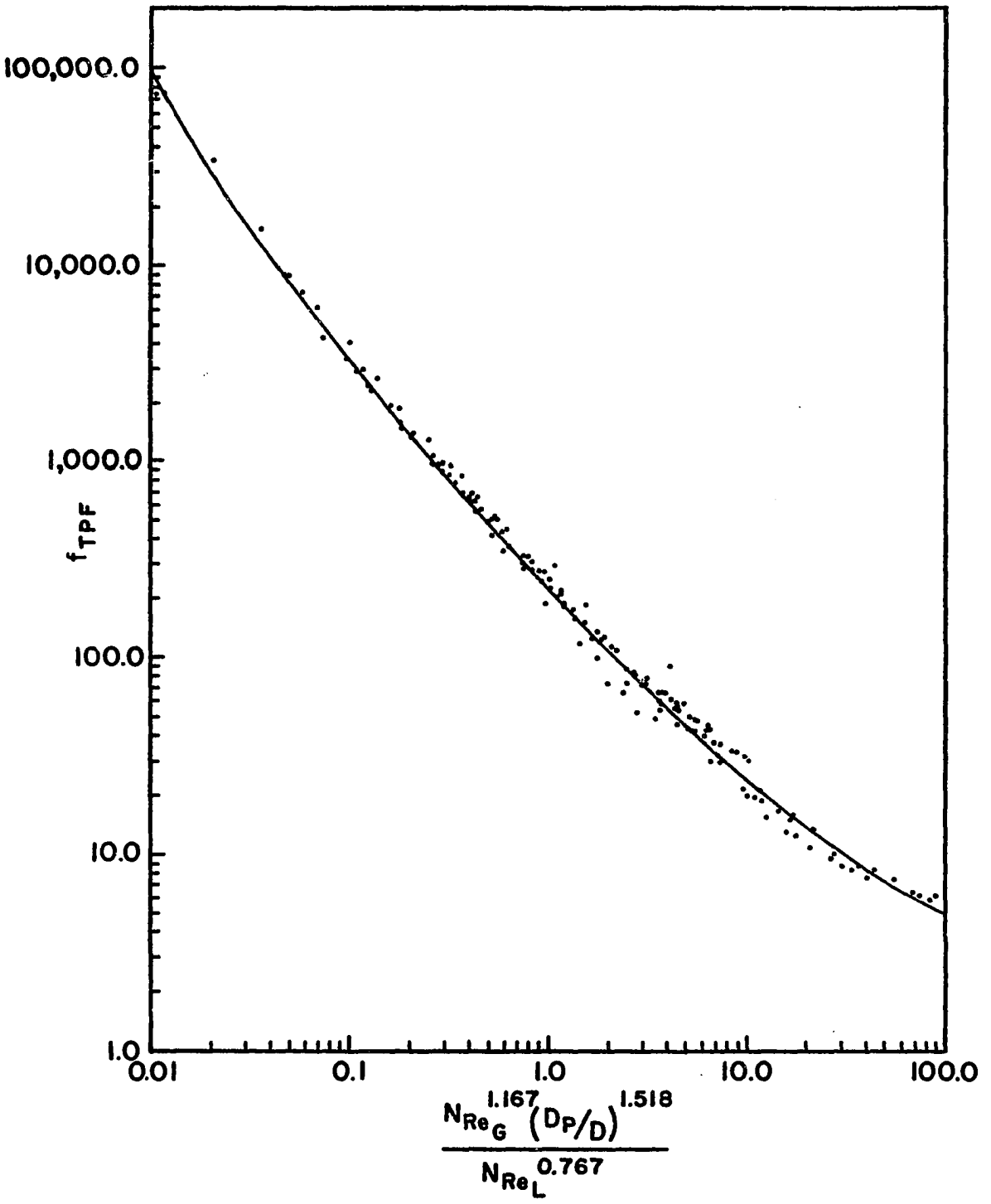

FIGURE 23. FRICTION FACTOR CORRELATION DOWNWARD FLOW

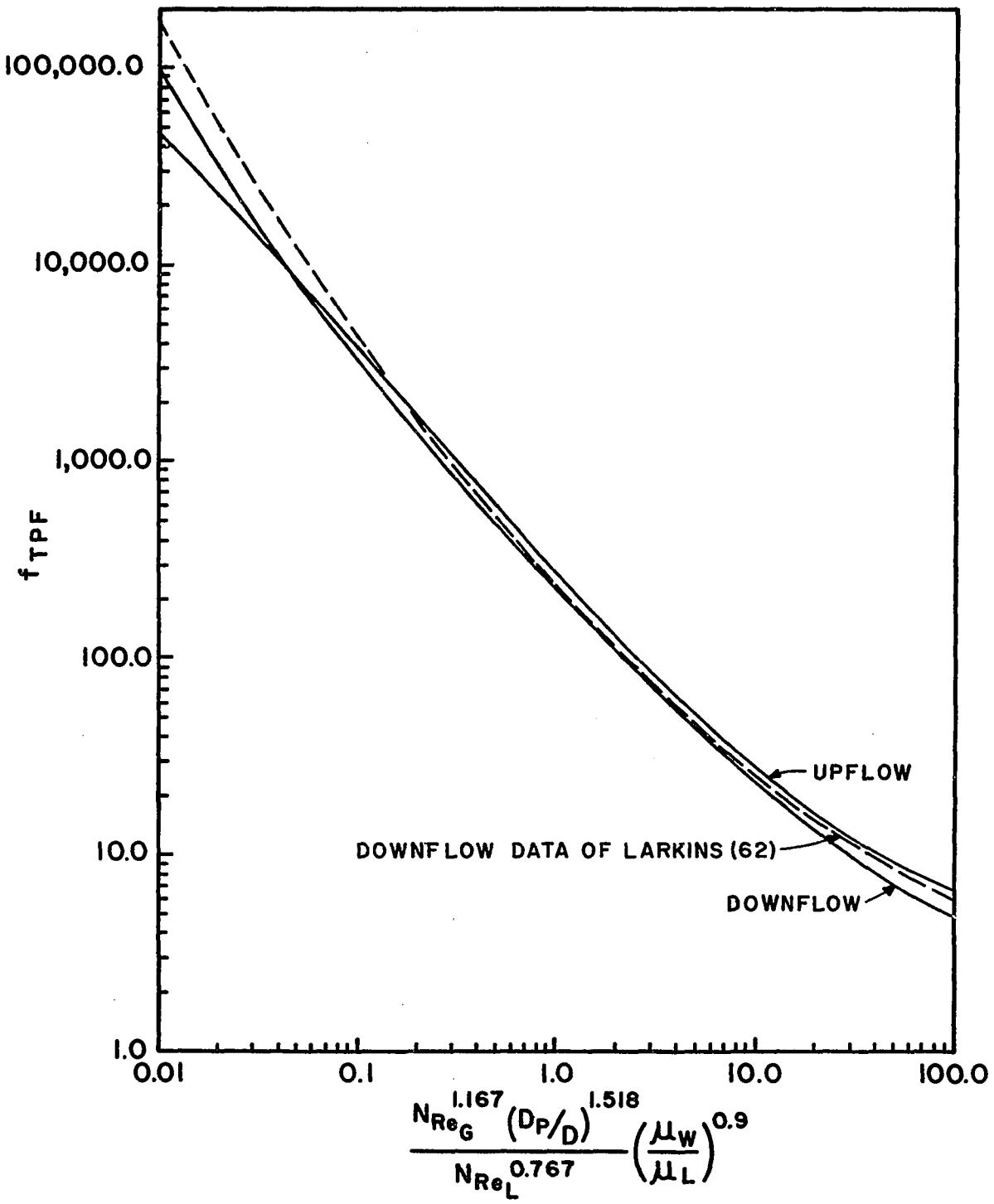

FIGURE 24. COMPARISON OF FRICTION FACTOR CORRELATIONS

However, it was observed that equation (49) was closely approximated by the linear least-square curve:

$$R_V = -0.035 + 0.182(G_L/G_G)^{0.24} \qquad (50)$$

$$(1.0 \leq (G_L/G_G)^{0.24} \leq 6.0)$$

Therefore, because equation (50) is much the easier equation with which to work, it will be utilized as the correlating equation. Although the data were quite scattered, essentially all data points were within ±25% of equation (50). For comparison, both equations (49) and (50) are reproduced on Figure (25).

For the downward flow data the best fitting curve is given by:

$$R_V = -0.215 + 0.445(G_L/G_G)^{0.24} - 0.175\left[(G_L/G_G)^{0.24}\right]^2 + 0.042\left[(G_L/G_G)^{0.24}\right]^3 - 0.0036\left[(G_L/G_G)^{0.24}\right]^4 \qquad (51)$$

$$(1.0 \leq (G_L/G_G)^{0.24} \leq 6.0)$$

which is closely approximated by the linear least-square curve:

$$R_V = -0.017 + 0.132(G_L/G_G)^{0.24} \qquad (52)$$

$$(1.0 \leq (G_L/G_G)^{0.24} \leq 6.0)$$

Approximately 95% of the downflow data were within ±25% of equation (52). As before, both equations are reproduced on Figure 26 with the linear curve to be employed as the

correlating equation.

The correlating method was applied to Larkins' (62) downflow liquid saturation data. The minimum variance curve was a cubic equation, but again the higher order equation was closely approximated by the linear least-square fit of the data:

$$R_V = -0.082 + 0.154(G_L/G_G)^{0.24} \qquad (53)$$

$$(1.0 \leq (G_L/G_G)^{0.24} \leq 6.0)$$

A graphical comparison of equations (50), (52), and (53) is given by Figure 27. However, discussion of equations (49) through (53) and of Figures 25, 26, and 27 is reserved for the next chapter.

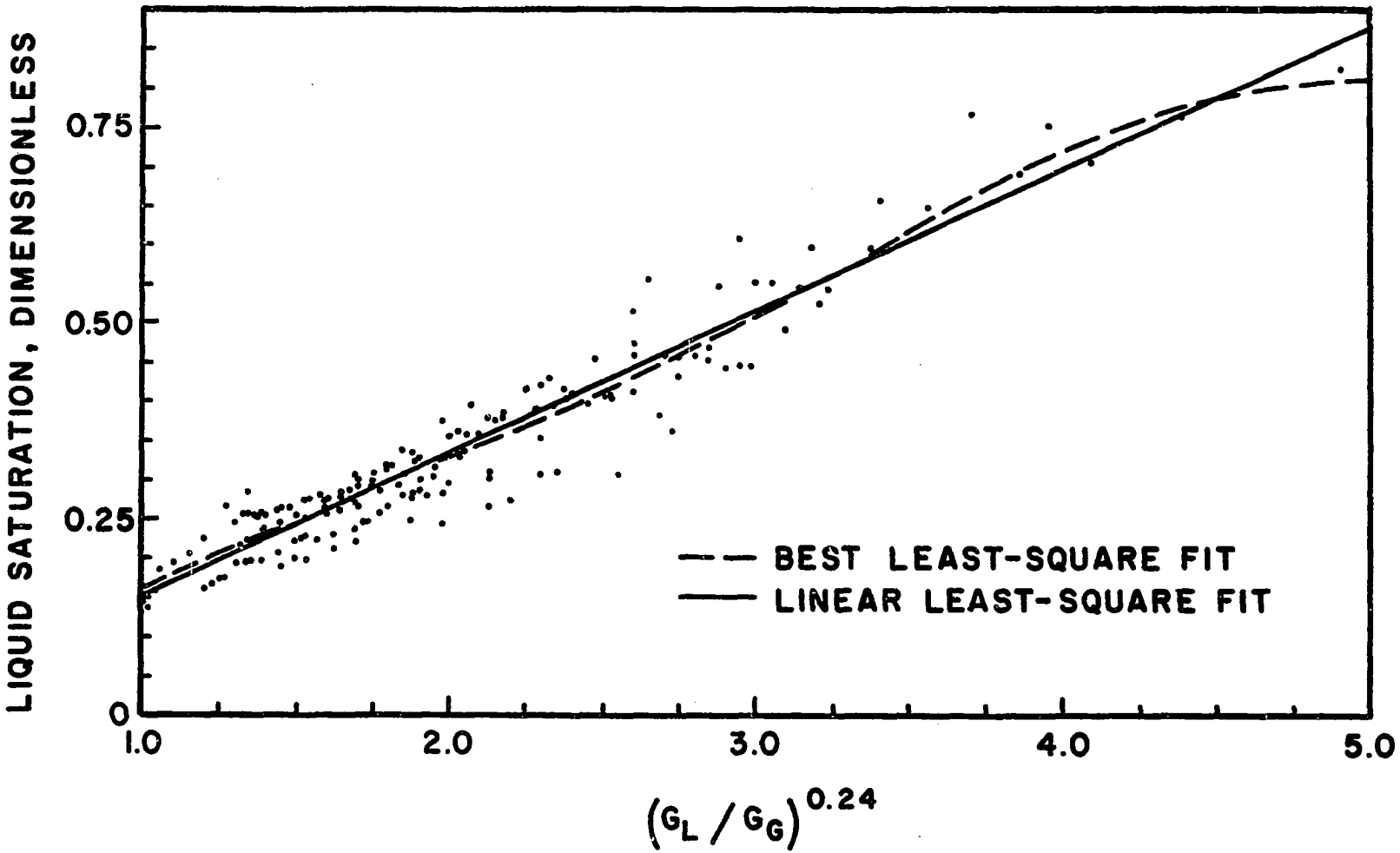

FIGURE 25. CORRELATION OF LIQUID SATURATION DATA — UPWARD FLOW

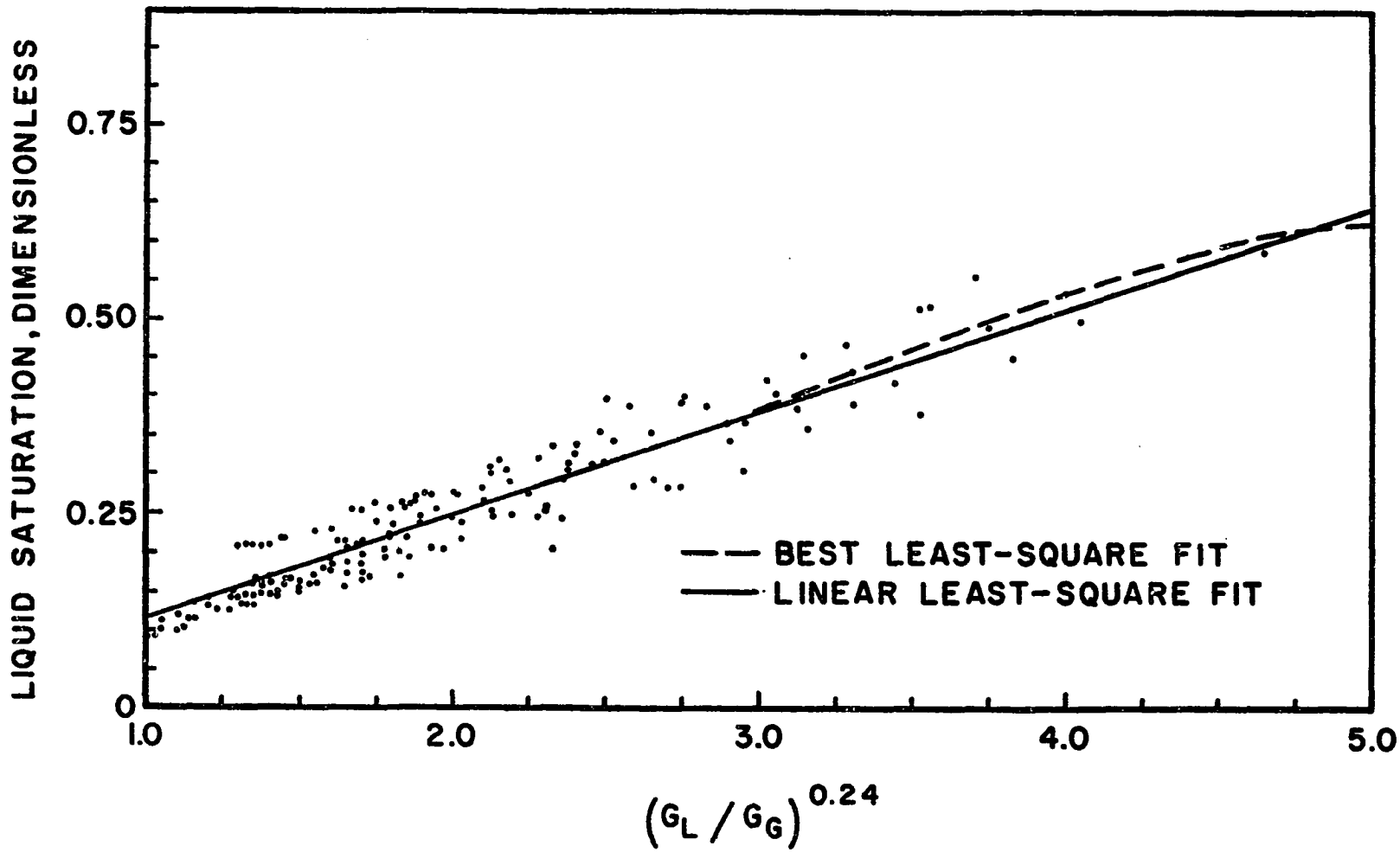

FIGURE 26. CORRELATION OF LIQUID SATURATION DATA — DOWNWARD FLOW

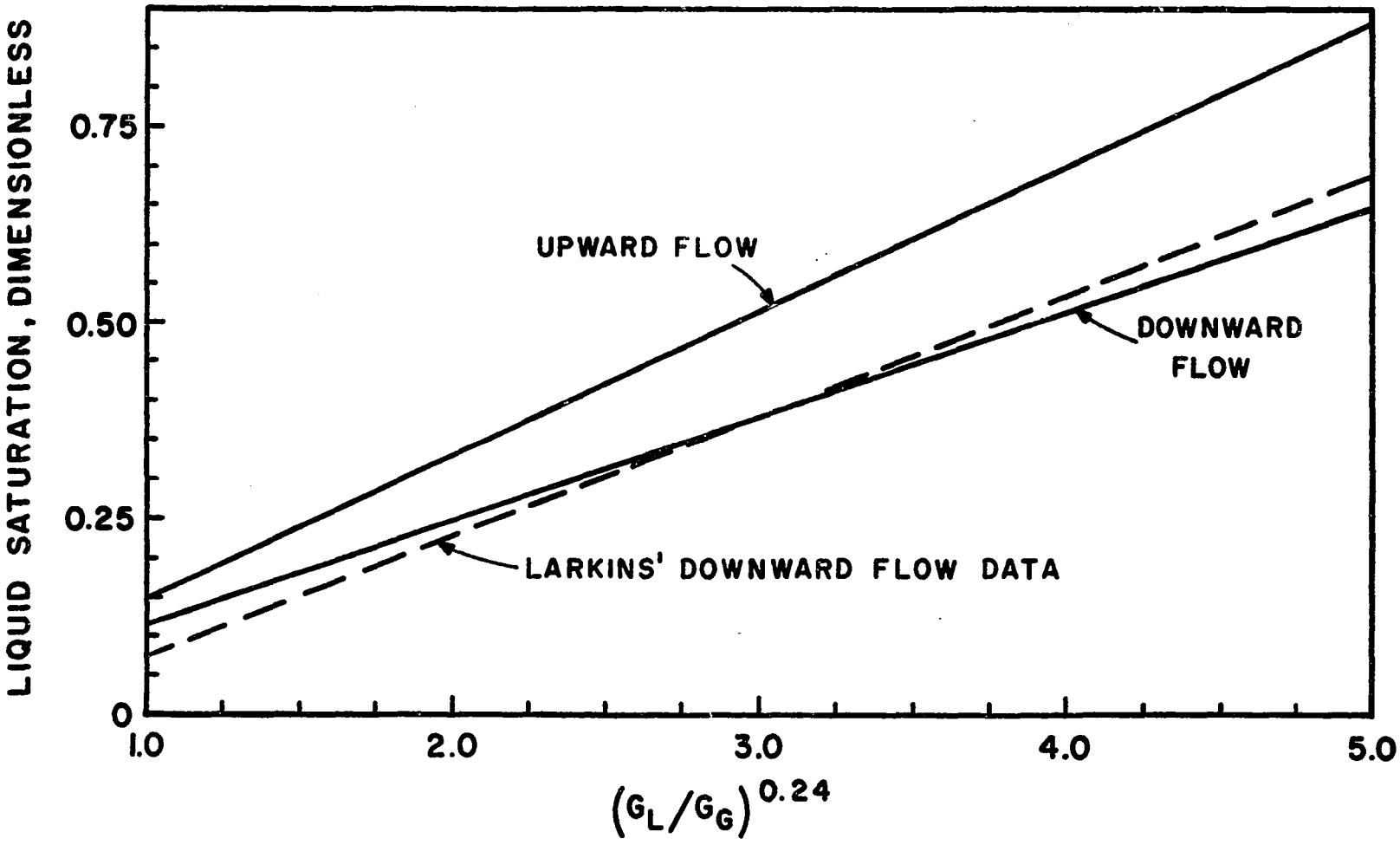

FIGURE 27. COMPARISON OF LIQUID SATURATION CORRELATIONS

CHAPTER VII

DISCUSSION OF RESULTS

The objectives of this investigation were realized with the presentation of the correlated results in the previous chapter. A mathematical model was developed which provided the basis for the prediction of pressure drops for two-phase concurrent flow through packed beds. A complete theoretical solution to the problem was not possible, however, and thus it was necessary to supplement the development with experimental data. These data were obtained and converted to a satisfactory form for use in design calculations. And, finally, the effects of flow orientation are summarized by Figures 24 and 27.

Friction-Factor Correlations

That the two-phase friction factor method of correlation is satisfactory is verified by Figures 22 and 23 for a wide range (10^4) of the correlating variable, Z. As a further check of the validity of these correlations, the end-points of each were checked using single-phase experimental data. It was found that each of the correlations merges into a single-phase gas correlation for higher values of Z.

The value of Z was calculated for single-phase gas

flow for a number of experimental observations by taking the liquid Reynolds number as one. Single-phase Z values calculated in this manner ranged from 155 to 3000, with more than 75% of these calculated points falling within ±25% of the extended curves of Figures 22 and 23. However, this merging of the two-phase curve smoothly into the single-phase curve is to be expected because of the manner in which the two-phase friction factors were defined, that is, in terms of the superficial gas velocity. Because of the large magnitudes of the superficial gas velocity in this region of the curve, both f_{TPf} and Z are strongly influenced by this quantity, and the correlation does not change appreciably in passing from two-phase flow with a very small liquid-to-gas ratio to single-phase gas flow.

Single-phase liquid data could not be fitted to Figures 22 and 23 because of the presence of the superficial gas velocity factor in the defining equation for f_{TPf}. However, it was possible to retain the correlation for gas rates very near zero. The experimental points for Z values between 0.01 and 0.1 are very low gas flows and correspondingly high liquid-to-gas ratios.

To provide a check of these friction factor correlations for a much wider range of experimental conditions than was employed in this investigation, the experimental data of Larkins' (62) were converted to f_{TPf}-Z values for comparison with the data of Figures 22 and 23. This graphical comparison is included as Figure 24.

It is noted that the abscissa of Figure 24 differs from those of Figures 22 and 23 by a viscosity correction term, $(\mu_{water}/\mu_L)^{0.90}$. It was necessary to include this factor in order to correlate the data for liquids of viscosity substantially different from water using the derived correlating method. Successful correlation of Larkins' data, including liquid viscosities of 0.8-19.0 cp, was accomplished using this correction factor.

From Figure 24 it is seen that the two sets of downflow data approximate each other over the central portion of the curve while differences of 20-50% are found near the extremes of the correlations. More scatter was noted in the data of Larkins' than in that of the author. At least a part of this is attributed to the failure to correct his data for the liquid filling the manometer lead lines. From the data which were available, this correction could not be made but in no case did it amount to more than 10%. Also, it is certain that the wider range of experimental conditions employed contributed to this scatter. In addition to the use of near-spherical packing material as was used in this investigation, Larkins utilized 1/8-inch by 1/8-inch solid cylinders and 3/8-inch Raschig rings as packing materials with maximum porosities of 52%.

Concerning the comparison of upward flow and downward flow as given by Figure 24, significant differences between the two are exhibited over portions of the correlation. Quantitatively, the two correlations differ by 30-100% for

the extremes of the correlation and by 15-20% for the intermediate range.

Liquid Saturation Correlations

The liquid saturation correlations given by Figures 25 and 26 for upward flow and downward flow, respectively, exhibit quite a large scatter of the data. This is characteristic of liquid saturation data, however, with large variations having been reported by previous investigators in two-phase flow. Larkins reported maximum errors of 43% for his liquid saturation data in packed beds.

Again, Larkins' downflow data were used as a comparison for the proposed correlation. This graphical comparison is given as Figure 27, which also includes the correlating curve for the upflow data of the author. Maximum deviations between the two downflow correlations of approximately 35% were found for small values of (G_L/G_G) with the difference becoming progressively less for larger values.

Better correlations than those reported were obtained for both upflow and downflow data by combining the abscissa, $(G_L/G_G)^{0.24}$, with a function of the bed porosity. However, it was determined that this correlation was not adequate for porosities divergent from those of this investigation. Therefore, in order to provide the most generalized correlations possible, the porosity function was eliminated from each of the correlations, yielding the correlations of Figure 27. And, since Figure 27 includes data from bed porosities of

34.9-52%, it will be assumed that the proposed liquid saturation correlations are valid for this range of porosity values.

It was noted in the previous chapter that, although fourth power polynomials provided a better fit of the experimental data, linear equations would be utilized to represent the liquid saturation data. Considerable simplification of calculations is attained by this substitution, while no significant loss of accuracy is introduced. One limitation of the correlating equations is that neither passes through the origin although physically each must do so. For this reason, use of equations (50), (52), and (53) below a value of unity for $(G_L/G_G)^{0.24}$ is not recommended.

Scope of the Correlations

The correlations will be examined to ascertain their reliability and their range of applicability. To establish their reliability, 318 individual two-phase data points were used with half of these for upflow and half for downflow. Thus, each individual correlation is the result of approximately 160 data points distributed more or less equally over the range of the correlation. Besides these 318 data points, an additional 204 experimental data points from other sources were utilized as a check of the derived correlations.

To establish the range of applicability of the proposed correlations, the range of the experimental variables will be considered. A wide variation in the flow rate of each phase was utilized with the gas flow rate extending from

45.5 lb/ft^2-hr to 13,780 lb/ft^2-hr and the liquid flow rate having a range of 13,620 - 114,200 lb/ft^2-hr. Only low column operating pressures were utilized with the maximum being near 50 psia and the use of the correlations much beyond this value is not recommended.

Gas viscosity was very nearly constant for the investigation at 0.018 cp. This, however, is not a serious limitation as the viscosities of most gases at moderate temperatures do not vary greatly. All data were obtained with liquid viscosities near 1 cp, and the experimental correlations are based only on these data. It is noted that with the viscosity correction factor, $(\mu_w/\mu_L)^{0.9}$, being utilized, data are correlated in Figure 24 with liquid viscosities ranging up to 19 cp. However, it is suggested that caution be used in application of the Figure 24 correlations to systems having a liquid viscosity widely divergent from 1 cp.

The ratio of the fluid mass flow rates is the basis for the liquid saturation correlations. Using the range of mass flow rates given above, it is seen that the ratio of these varies from 0.99 to 2520. This range is reduced to approximately 1 to 6.5 in terms of the correlating group, $(G_L/G_G)^{0.24}$, and the correlations should be adequate over this interval.

In addition to being a function of the mass flow ratio, the liquid saturation is also a complicated, though not a strong, function of bed porosity. Although the

correlations of this investigation were derived using only bed porosities near 35%, it is believed that they may be used safely up to bed porosities of 50% because of the close agreement with the 52% bed porosity data of Larkins (62).

Use of the Experimental Correlations

With the required experimental correlations now available, their use in design calculations will be discussed. For design purposes it is assumed that the physical properties and dimensions of the bed, the column orientation, the flow rate of each phase, the fluid physical properties, and the delivered pressure of each phase are known. Unknown are the average pressure of the column and the total pressure drop through the bed which is the required quantity.

The frictional pressure drop may be obtained directly. From the known design variables, the value of the correlating group, Z, is calculated, and the two-phase friction factor may be determined from Figure 24 or from equation (46) or equation (47) for upward or downward flow, respectively. The frictional pressure drop is then determined using a rearrangement of equation (33) and the two-phase friction factor.

From this point a trial-and-error solution must be used because, in addition to the total pressure drop, the average operating pressure is an unknown. An operating pressure is assumed and the total pressure drop is determined using equation (32). This procedure is repeated until the average pressure, as determined from the calculated pressure

drop, is sufficiently close to the assumed operating pressure.

Use of equation (32) requires evaluation of $\overline{A}_L$ and $\overline{A}_G$. These are obtained from the derived liquid saturation correlations. A value of $(G_L/G_G)^{0.24}$ is calculated from the known quantities and Figure 27 or from equation (50) or (52), depending upon whether the flow is upward or downward.

Use of equation (32) is not recommended above column operating pressures of 50 psi or for pressure drops greater than 40 psi. Beyond these conditions acceleration of the fluids becomes a significant factor. It then becomes necessary to utilize equation (30) which requires a knowledge of the initial and final velocities in addition to the other known quantities.

CHAPTER VIII

CONCLUSIONS AND RECOMMENDATIONS FOR FUTURE STUDY

The conclusions drawn from this investigation of two-phase concurrent flow in packed beds are:

(1) The momentum exchange mathematical model (equations 14 and 15) may be used as the basis for correlation of experimental data.

(2) Correlation of the liquid saturation data for both upward and downward flow is achieved in terms of a function of the ratio of the mass flow rate of liquid to gas.

(3) Correlation of the frictional pressure loss for both upward and downward flow is achieved in terms of a defined two-phase friction factor and a correlating parameter, Z, which is a function of the liquid Reynolds number, the gas Reynolds number, and the particle-to-column diameter ratio.

(4) A viscosity correction factor is required to extend the friction factor correlation to include liquid viscosities widely divergent from that of water. The reliability of the extended correlation is not determined.

(5) The frictional pressure loss is a function of the column orientation, with the effects becoming significant for either high or low liquid-to-gas flow ratios.

(6) The pressure loss due to acceleration of the fluids is negligible for operating pressures below 50 psig.

(7) The frictional pressure loss is independent of the two-phase flow pattern.

The results of this investigation revealed several points requiring further study:

(1) The variation of liquid saturation with distance through the packed bed is an important item which has not been established. A linear variation was assumed for the present study and this assumption is satisfactory for moderate pressure drops where the acceleration pressure drop is negligible. However, for higher pressure drops the point liquid saturation becomes an important quantity in the determination of the acceleration pressure drop.

(2) In conjunction with (1), investigation of column pressures above 50 psig are needed in order to get into the region where pressure loss due to fluid acceleration is important.

(3) Variation of pressure with distance needs to be established for both low and high pressure operation, although a linear variation can be assumed at low pressures without serious errors.

(4) Determination of the contrast of the effects of liquid viscosity between upward and downward flow is needed for a range of liquid viscosities. The results of this study could also be used to incorporate the viscosity correction factor of Figure 24 into the correlating group.

CHAPTER IX

LITERATURE CITED

(1) Oppenheim, A. K., Sternling, C. V., Sleicher, C. A. Jr., and Stern, R. A., "Fluid Dynamics," Industrial and Engineering Chemistry, 51, p. 437, March, 1959.

(2) Dukler, A. E., Wicks, M., III, and Cleveland, R. G., "Frictional Pressure Drop in Two-Phase Flow," A.I.Ch.E. Journal, 10, p. 38, Jan., 1964.

(3) Dodds, W. S., Stutzman, L. F., Sollami, B. J., and McCarter, R. J., "Concurrent Gas Absorption Mass Transfer," A.I.Ch.E. Journal, 6, p. 197, June, 1960.

(4) Leacock, J. A., and Churchill, S. W., "Mass Transfer Between Isobutanol and Water in Concurrent Flow Through a Packed Column," A.I.Ch.E. Journal, 7, p. 196, 1961.

(5) Larkins, R. P., and White, R. R., and Jeffrey, D. W., "Two-Phase Concurrent Flow in Packed Beds," A.I.Ch.E. Journal, 7, p. 231, 1961.

(6) Weekman, V. W., Jr., and Myers, John E., "Fluid-Flow Characteristics of Concurrent Gas-Liquid Flow in Packed Beds," A.I.Ch.E. Journal, 10, p. 951, Nov., 1964.

(7) Dodds, W. S., Stutzman, L. F., Sollami, B. J., and McCarter, R. J., "Pressure Drop and Liquid Holdup in Concurrent Gas Absorption," A.I.Ch.E. Journal, 6, p. 390, Sept., 1960.

(8) Zeisburg, F. C., "The Resistance of Absorption Tower Packing to Gas Flow," Transactions A.I.Ch.E., 12, Part II, p. 231, 1919.

(9) Blake, F. C., "The Resistance of Packing to Fluid Flow," Transactions A.I.Ch.E., 14, p. 415, 1922.

(10) Burke, S. P., and Plummer, W. B., "Gas Flow Through Packed Columns," Industrial and Engineering Chemistry, 20, p. 1196, Nov., 1928.

(11) Carman, P. C., "Fluid Flow Through Granular Beds," Transactions Inst. of Ch. E. (London), 15, p. 150, 1937.

(12) Morcom, A. R., "Fluid Flow Through Granular Materials," Transactions Inst. of Ch. E. (London), 24, p. 30, 1946.

(13) Ergun, S., and Orning, A. A., "Fluid Flow Through Randomly Packed Columns and Fluidized Beds," Industrial and Engineering Chemistry, 41, p. 1179, June, 1949.

(14) Ergun, S., "Fluid Flow Through Packed Columns," Chemical Engineering Progress, 48, p. 89, Feb., 1952.

(15) Brownell, L. E., and Katz, D. L., "Flow of Fluids Through Porous Media," Chemical Engineering Progress, 43, p. 537, 601, 1947.

(16) Brownell, L. E., Gami, D. C., Miller, R. A., and Nekarvis, W. F., "Pressure Drop Through Porous Media," A.I.Ch.E. Journal, 2, p. 79, Jan., 1956.

(17) Brownell, L. E., Dombrowski, H. S., and Dickey, C. A., "Pressure Drop Through Porous Media," Chemical Engineering Progress, 46, p. 415, 1950.

(18) Furnas, C. C., "Flow of Gases Through Beds of Broken Solids," U. S. Bureau of Mines, Bulletin No. 307, 1929.

(19) Chilton, T. H., and Colburn, A. P., "Pressure Drop in Packed Tubes," Industrial and Engineering Chemistry, 23, p. 913, 1931.

(20) Leva, M., "Pressure Drop Through Packed Tubes," Chemical Engineering Progress, 43, p. 549, 633, 713, 1947.

(21) Leva, M., Weintraub, M., Grummer, M., Pollchik, M., and Storch, H. H., "Fluid Flow Through Packed and Fluidized Systems," U. S. Bureau of Mines Bulletin No. 504, 1951.

(22) Leva, M., "Flow Through Packings and Beds," Chemical Engineering, 64, p. 204, Jan., 1957; p. 263, Feb., 1957;

(23) Martinelli, R. C., Boelter, L. M. K., Taylor, T. H. M., Thomsen, E. G., and Morrin, E. H., "Isothermal Pressure Drop for Two-Phase Two-Component Flow in a Horizontal Pipe," Transactions A.S.M.E., 66, p. 139, Feb., 1944.

(24) Martinelli, R. C., Putnam, J. A., and Lockhart, R. W., "Two-Phase, Two-Component Flow in the Viscous Region," Transactions A.I.Ch.E., 42, p. 681, 1946.

(25) Lockhart, R. W., and Martinelli, R. C., "Proposed Correlation of Data for Isothermal Two-Phase, Two-Component Flow in Pipes," Chemical Engineering Progress, 45, p. 39, Jan., 1949.

(26) Alves, George E., "Cocurrent Liquid-Gas Flow in a Pipe-Line Contactor," Chemical Engineering Progress, 50, p. 449, Sept., 1954.

(27) Huntington, R. L., and White, P. D., "Horizontal Co-Current Two-Phase Flow of Fluids in Pipe Lines," Petroleum Engineer, 27, p. D-40, 1955.

(28) Galegar, W. C., Stovall, W. B., and Huntington, R. L., "More Data on Two-Phase Vertical Flow," Petroleum Refiner, 33, p. 208, Nov, 1954.

(29) Baker, O., "Simultaneous Flow of Oil and Gas," Oil and Gas Journal, 53, p. 185, July 26, 1954.

(30) Brigham, W. E., Holstein, E. D., and Huntington, R. L., "Two-Phase Concurrent Flow of Liquids and Air Through Inclined Pipe," Petroleum Engineer, 29, p. D-39, Nov., 1957.

(31) Chenoweth, J. M., and Martin, M. W., "Turbulent Two-Phase Flow," Petroleum Refiner, 34, p. 151, Oct., 1955.

(32) Chisholm, D., and Laird, A. D. K., "Two-Phase Flow in Rough Tubes," Transactions A.S.M.E., 80, p. 276, 1958.

(33) Bankoff, S. G., "A Variable Density Single-Fluid Model for Two-Phase Flow with Particular Reference to Steam-Water Flow," Transactions A.S.M.E., 82, p. 265, 1960.

(34) Dukler, A. E., Wicks, M., III, and Cleveland, R. G., "Frictional Pressure Drop in Two-Phase Flow; A Comparison of Existing Correlations for Pressure Loss and Hold-up," A.I.Ch.E. Journal, 10, p. 38, Jan., 1964.

(35) Hoogendoorn, C. J., "Gas-Liquid Flow in Horizontal Pipes," Chemical Engineering Progress, 9, p. 205, 1959.

(36) Sobocinski, D. P., and Huntington, R. L., "Concurrent Flow of Air, Gas-Oil, and Water in a Horizontal Pipe," Transactions A.S.M.E., Paper No. 56-A-60, 1957.

(37) Carter, Cecil O., and Huntington, R. L., "Concurrent Two-Phase Upward Flow of Air and Water Through an Open Vertical Tube and Through an Annulus," Canadian Journal of Chemical Engineering, 39, p. 248, Dec., 1961.

(38) Hughmark, G. A., and Pressburg, B. S., "Holdup and Pressure Drop with Gas-Liquid Flow in a Vertical Pipe," A.I.Ch.E. Journal, p. 677, Dec., 1961.

(39) Hughmark, G. A., "Holdup in Gas Liquid Flow," Chemical Engineering Progress, 58, p. 62, April, 1962.

(40) Gouse, S. W., Jr., "Void Fraction Measurement," M.I.T. Dept. of Mechanical Engineering, Report No. DSR 8734-2, April, 1964.

(41) Ros, N. C. J., "Simultaneous Flow of Gas and Liquid as Encountered in Well Tubing," Journal of Petroleum Technology, 13, p. 1037, Oct., 1961.

(42) Griffith, P., and Wallis, G. B., "Two-Phase Slug Flow," Transactions A.S.M.E., 83C, p. 307, Aug., 1961.

(43) Levy, S., "Steam Slip-Theoretical Prediction from Momentum Model," Transactions A.S.M.E., Journal of Heat Transfer, 82, p. 113, May, 1960.

(44) Vohr, John, "The Energy Equation for Two-Phase Flow," A.I.Ch.E. Journal, 8, p. 281, May, 1962.

(45) Lamb, D. E., and White, J. L., "Use of Momentum and Energy Equations in Two-Phase Flow," A.I.Ch.E. Journal, 8, p. 281, May, 1962.

(46) Govier, G. W., Radford, B. A., and Dunn, J. S. C., "The Upwards Vertical Flow of Air-Water Mixtures, Part I," Canadian Journal of Chemical Engineering, 35, p. 58, Aug., 1957.

(47) Govier, G. W., and Short, W. L., "The Upward Vertical Flow of Air-Water Mixtures, Part II," Canadian Journal of Chemical Engineering, 36, p. 195, Oct., 1958.

(48) Brown, R. A. S., Sullivan, G. A., and Govier, G. W., "The Upward Flow of Air-Water Mixtures, Part III," Canadian Journal of Chemical Engineering, 38, p. 62, April, 1960.

(49) Charles, M. E., Govier, G. W., and Hodgson, G. W., "The Horizontal Pipeline Flow of Equal Density Oil-Water Mixtures," Canadian Journal of Chemical Engineering, 39, p. 27, 1965.

(50) Govier, G. W., Sullivan, G. A., and Wood, R. K., "The Upward-Vertical Flow of Oil-Water Mixtures," Canadian Journal of Chemical Engineering, 39, p. 67, April, 1961.

(51) Govier, G. W., and Brown, R. A. S., "High-Speed Photography in the Study of Two-Phase Flow," Canadian Journal of Chemical Engineering, 39, p. 159, Aug., 1961.

(52) Govier, G. W., and Aziz, K., "Horizontal Annular-Mist Flow of Natural Gas-Water Mixtures," Canadian Journal of Chemical Engineering, 40, p. 51, April, 1962.

(53) Govier, G. W., and Omer, M. M., "The Horizontal Pipeline Flow of Air-Water Mixtures," Canadian Journal of Chemical Engineering, 40, p. 93, June, 1962.

(54) Gouse, S. W., Jr., "An Introduction to Two-Phase Gas-Liquid Flow," M.I.T. Engineering Projects Laboratory Report No. DSR 8734-3, June, 1964.

(55) White, A. M., "Pressure Drop and Loading Velocities in Packed Towers," Transactions A.I.Ch.E., 31, p. 390, 1935.

(56) Jesser, B. W., and Elgin, J. C., "Studies of Liquid Hold-up in Packed Towers," Transactions A.I.Ch.E., 39, p. 277, 1943.

(57) Piret, E. L., Mann, C. A., and Wall, T., Jr., "Pressure Drop and Liquid Holdup in a Packed Tower," Industrial and Engineering Chemistry, 32, p. 861, June, 1940.

(58) Rigg, R. G., "Concurrent Flow of Immiscible Liquids in Packed Beds," Ph.D. Thesis, University of Michigan, Ann Arbor, Michigan, May, 1963.

(59) Martinelli, R. C., and Nelson, D. B., "Prediction of Pressure Drop During Forced-Circulation Boiling of Water," Transactions A.S.M.E., 70, p. 695, Aug., 1948.

(60) "Handbook of Chemistry and Physics," Chemical Rubber Publishing Co., Cleveland, Forty-First Ed., 1959.

(61) "International Critical Tables," McGraw-Hill, New York, 1926.

(62) Larkins, R. P., "Two-Phase Cocurrent Flow in Packed Beds," Ph.D. Thesis, University of Michigan, Ann Arbor, Michigan, May, 1959.

CHAPTER X

NOMENCLATURE

A	area
A,B	constants in Furnas' equation
a	area of cross-section of packing
a,b,c,d	exponents of correlating groups
b,c	constants
C	constant in Blausius' equation
C_1	constant (= MW/RT)
C_2	constant (= C_1P_1)
C_3	constant (= C_1k)
D	diameter
$F_{N_{Re}}$	Reynolds number function
F_f	friction factor function
F_T	force due to friction
f	friction factor
f_1	frictional coefficient
G	mass flow rate
g	gravitational acceleration
g_c	gravitational constant
K	permeability
k_1, k_2	constants in Ergun-Orning equation

k	constant
L	length of packed section
L_e	equivalent length
m,n	state-of-flow factor
N_{Re}	Reynolds number
P	pressure
Q	volumetric flow rate
R_v	liquid saturation, fraction of voids filled with liquid
S	total surface area per unit of packed volume
V	linear velocity
W	weight flow rate
X	parameter of Lockhart-Martinelli correlation
y	linear distance through packed bed
Z	correlating parameter
ϵ	porosity
λ	sphericity
μ	viscosity
ρ	density
Φ	parameter of Lockhart-Martinelli correlation
φ	"a function of"
ψ	"a function of"

Subscripts

f	friction
G	gas

L	liquid
p	particle
s	superficial velocity
V	viscous
T	turbulent
t	tube
TP	two-phase
w	water
1	upstream datum point
2	downstream datum point

APPENDICES

APPENDIX A
FLUID PROPERTIES

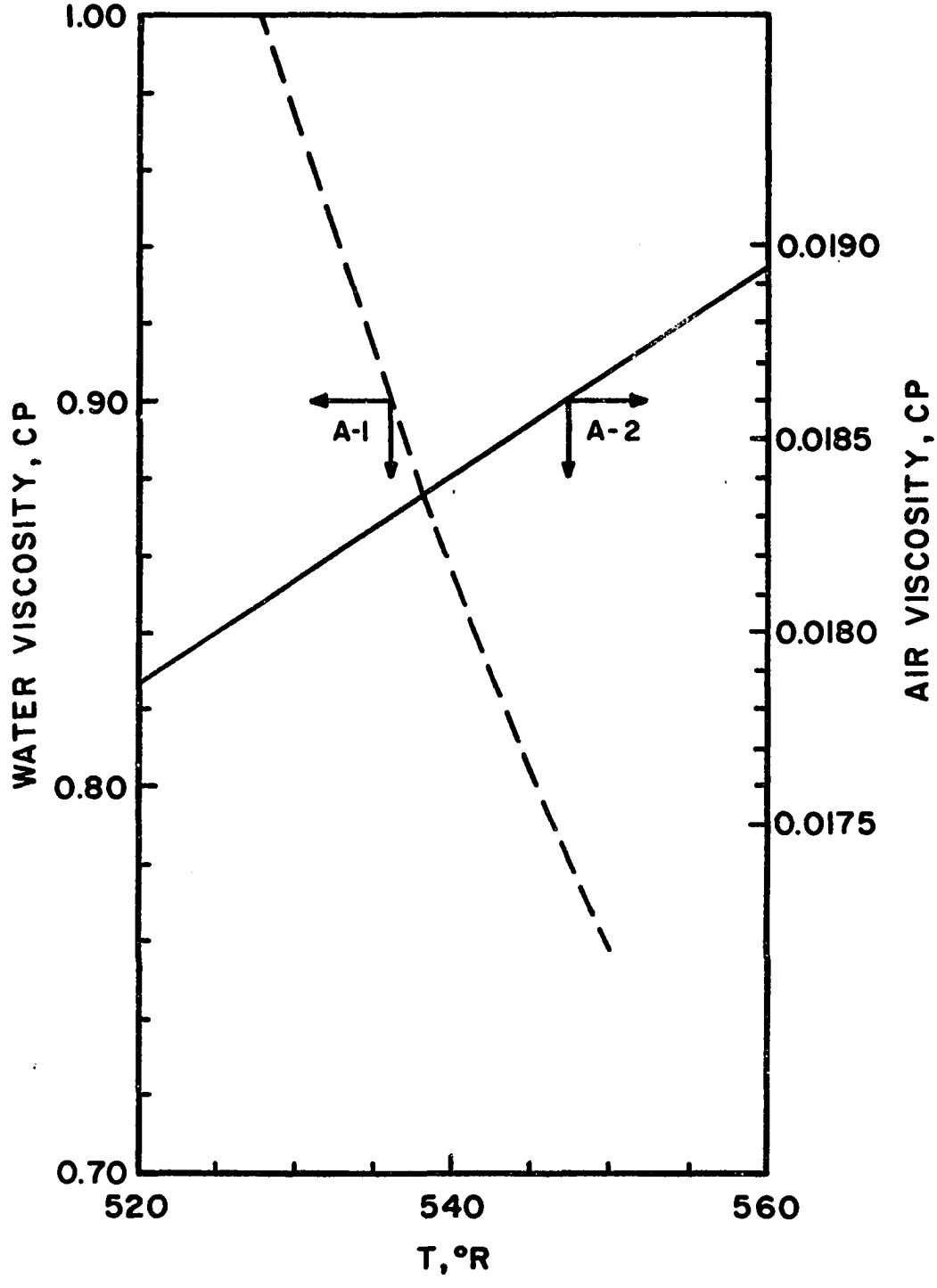

FIGURES A-1 and A-2. FLUID VISCOSITIES

APPENDIX B
ROTAMETER CALIBRATION CURVES

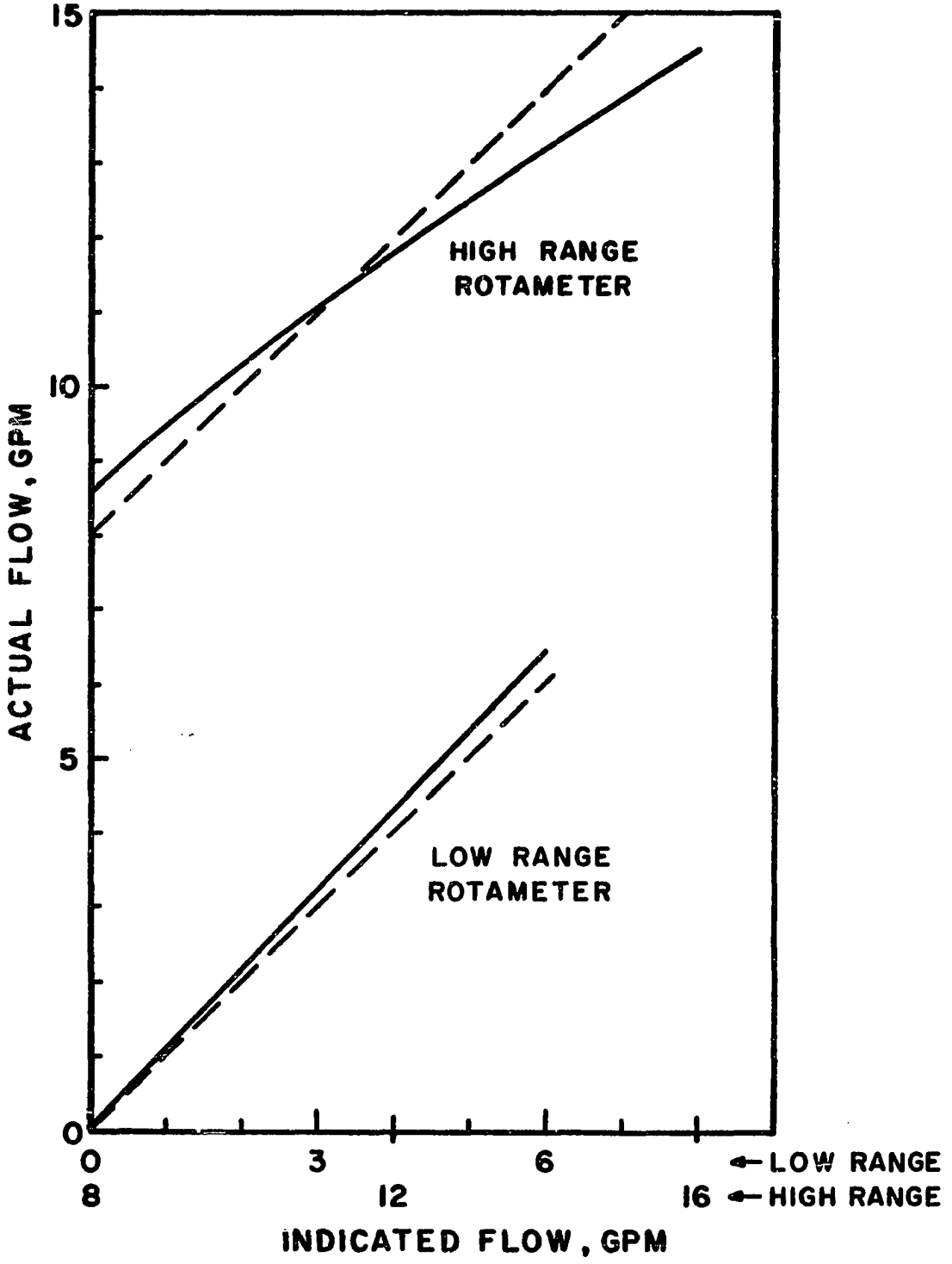

FIGURE B-1. ROTAMETER CALIBRATION CURVES

APPENDIX C

FRICTIONAL PRESSURE GRADIENT

Dimensional Analysis of the Correlating Variables

Assume that the frictional pressure gradient is a function of the following variables:

$$(\Delta P/L)_{fric} = \varphi(V_L, D_p, \rho_L, \mu_L, D, y, g_c, V_G, \rho_G, \mu_G) \qquad (D\text{-}1)$$

and that this function is represented by:

$$(\Delta P/L)_{fric} = V_L^a\, D_p^b\, \rho_L^c\, \mu_L^d\, D^e\, y^f\, g_c^g\, V_G^h\, \rho_G^i\, \mu_G^j \qquad (D\text{-}2)$$

In terms of the dimensions of the respective quantities, (D-2) is written as:

$$F/L^3 = (L/\theta)^a L^b (M/L^3)^c (M/L\theta)^d L^e L^f (LM/F\theta^2)^g (L/\theta)^h (M/L^3)^i (M/L\theta)^j \qquad (D\text{-}3)$$

Equating the exponents of F:

$$1 = -g \qquad (D\text{-}4)$$

Equating the exponents of L:

$$-3 = a + b - 3c - d + e + f + g + h - 3i - j \qquad (D\text{-}5)$$

Equating the exponents of θ:

$$0 = -a - d - 2g - h - j \qquad (D\text{-}6)$$

Equating the exponents of M:

$$0 = c + d + g + i + j \qquad (D\text{-}7)$$

Equations (D-4), (D-5), (D-6), and (D-7) are four equations in ten unknowns and the exponents b, g, h, and i will be solved in terms of the remaining exponents a, c, d, e, f, and j.

$$g = -1 \tag{D-8}$$

$$h = -a - d + 2 - j \tag{D-9}$$

$$i = -c - d + 1 - j \tag{D-10}$$

$$b = -d - 1 - e - j - f \tag{D-11}$$

Substituting (D-8), (D-9), (D-10), and (D-11) into (D-2) and collecting quantities of like exponents:

$$(\Delta P/L)_{fric} = (V_G^2 \rho_G / D_p g_c)(V_L/V_G)^a (\rho_L/\rho_G)^c (\mu_L/D_p V_G \rho_G)^d (D/D_p)^e \cdot (y/D_p)^f (\mu_G/D_p V_G \rho_G)^j \tag{D-12}$$

Assuming that the frictional pressure gradient is independent of the distance through the bed and noting that $G = V\rho$, manipulation of (D-12) leads to:

$$(\Delta P/L)_{fric} = (V_G^2 \rho_G / D g_c)(N_{Re_L})^k (N_{Re_G})^q (D_p/D)^m (G_L/G_G)^n (\rho_L/\rho_G)^p \tag{D-13}$$

It is assumed that the functional form of the Reynolds number grouping, $(N_{Re_L})^k (N_{Re_G})^q$, will account for the density and mass velocity ratios of (D-13). Hence, (D-13) reduces to:

$$(\Delta P/L)_{fric} = (V_G^2 \rho_G / D g_c) \varphi [(N_{Re_L})^a (N_{Re_G})^b (D_p/D)^c] \tag{D-14}$$

APPENDIX D

TABULATED DATA

The complete two-phase experimental data are included in this section. A few explanatory remarks are required concerning the tabulation of the data. Data from the 2-inch diameter column are included as run numbers 1-34, run numbers 35-159 comprise the 4-inch data, and the data from the 6-inch diameter column are presented as run numbers 160-284. It is noted that a given run number includes both upward and downward flow data for the 2-inch column, while data for only one flow direction is included for the 4-inch and 6-inch columns for a given run number. Zeros in either the upward or downward columns of the tabulated data indicate that the flow is in the opposite direction.

In the tabulation of data, a subscript U indicates upward flow, a subscript D indicates downward flow, and the subscripted numbers 1 and 2 indicate the entrance and exit of the test section, respectively. The liquid saturation columns of data, R_v, give the fraction of the packed bed void volume which is filled by the liquid phase. The temperature recorded is the average column temperature in degrees Rankine. The mass flow rates of both air and water are reported in lbs/ft^2-hr based on the open cross-sectional area of the packed column.

Run No.	P_{1U}, Psia	P_{2U}, Psia	R_v, Upflow	Temp, R	P_{1D}, Psia	P_{2D}, Psia	R_v, Downflow	G_{Air}	G_{Water}
1	28.1	21.1	0.3540	538.0	20.6	14.6	0.2360	2920	56300
2	31.1	23.3	0.3240	538.0	22.1	14.8	0.2390	4000	56300
3	33.1	24.6	0.318	538.0	23.1	15.0	0.2260	5000	56300
4	35.1	25.4	0.3060	538.0	24.1	15.1	0.2120	5620	56300
5	37.1	27.1	0.2640	538.0	25.6	15.1	0.2120	6040	56300
6	25.6	19.6	0.3860	540.0	18.9	14.5	0.2490	2175	56300
7	40.1	28.9	0.2540	540.0	27.6	15.0	0.1760	7960	56300
8	42.1	30.1	0.2480	540.0	28.6	15.1	0.1590	8240	56300
9	36.1	26.3	0.2670	540.0	25.1	15.0	0.1850	6150	56300
10	38.3	27.9	0.2580	540.0	26.3	15.0	0.2110	7100	56300
11	22.8	18.5	0.3370	534.0	17.6	14.7	0.2140	2340	30100
12	24.5	19.5	0.3080	534.0	18.6	14.7	0.2100	3360	30100
13	26.1	20.1	0.2720	534.0	19.3	14.8	0.1810	4110	30100
14	27.8	21.3	0.2750	534.0	20.3	14.9	0.1690	4980	30100
15	29.8	22.3	0.2520	534.0	21.0	14.9	0.1610	5500	30100
16	31.1	23.3	0.2420	534.0	22.1	15.0	0.1590	6440	30100
17	34.2	25.4	0.2330	534.0	23.8	15.2	0.1570	7770	30100
18	36.5	26.8	0.2220	539.0	25.0	15.3	0.1450	8770	30100
19	38.3	28.0	0.2180	539.0	26.1	15.5	0.1470	9610	30100
20	41.6	29.8	0.1940	539.0	28.0	15.6	0.1240	11120	30100
21	24.1	19.0	0.2810	539.0	18.6	14.7	0.1600	4040	13620
22	25.8	20.1	0.2630	539.0	19.2	14.7	0.1510	5010	13620
23	28.3	21.6	0.2240	539.0	20.8	14.9	0.1410	6350	13620
24	31.3	23.4	0.2060	539.0	22.3	15.0	0.1370	7440	13620
25	34.4	25.3	0.1950	539.0	24.3	15.2	0.1150	9050	13620
26	37.2	27.1	0.1860	541.0	25.9	15.4	0.1110	10850	13620
27	39.1	28.5	0.1580	541.0	27.1	15.5	0.1000	11800	13620
28	41.5	30.7	0.1370	541.0	28.3	15.7	0.0920	12800	13620
29	43.2	31.3	0.1430	541.0	30.1	15.9	0.0940	13780	13620
30	33.3	23.8	0.4300	541.0	22.8	15.0	0.2830	1688	112000
31	31.3	22.8	0.4420	541.0	21.8	15.0	0.3030	1236	112000
32	38.3	26.8	0.3500	541.0	25.3	15.1	0.2580	3505	112000
33	42.4	29.3	0.3090	541.0	27.8	15.4	0.2460	4800	112000
34	46.5	32.3	0.2920	541.0	30.3	15.7	0.2420	6230	112000
35	0	0	0	536.0	15.84	14.48	0.2560	976	15450
36	0	0	0	536.0	16.4	14.9	0.2200	1352	15450
37	0	0	0	538.0	17.1	14.9	0.2020	1840	15450

Run No.	P_{1U}, Psia	P_{2U}, Psia	R_v, Upflow	Temp, R	P_{1D}, Psia	P_{2D}, Psia	R_v, Downflow	G_{Air}	G_{Water}
38	0	0	0	539.0	17.96	14.41	0.1900	2240	15450
39	0	0	0	539.0	18.08	14.41	0.1832	2365	15450
40	0	0	0	540.0	19.23	14.5	0.1655	3120	15450
41	0	0	0	540.0	19.75	14.41	0.1498	3480	15450
42	0	0	0	542.0	20.25	14.58	0.1610	3660	15450
43	0	0	0	542.0	20.35	14.5	0.1703	3770	15450
44	0	0	0	532.0	20.6	14.8	0.1577	4000	15450
45	0	0	0	535.0	21.0	14.5	0.1590	4150	15450
46	0	0	0	536.0	21.3	15.3	0.1550	2850	15450
47	0	0	0	532.0	21.4	15.1	0.1691	4225	15450
48	0	0	0	534.0	22.9	15.3	0.1438	5160	15450
49	0	0	0	538.0	23.7	15.4	0.1462	5700	15450
50	0	0	0	534.0	24.9	15.4	0.1281	6420	15450
51	0	0	0	534.0	26.0	15.7	0.1343	7280	15450
52	0	0	0	536.0	27.7	15.9	0.1112	8150	15450
53	0	0	0	535.0	28.9	16.2	0.1112	8770	15450
54	0	0	0	536.0	30.1	16.4	0.1047	9360	15450
55	0	0	0	536.0	31.4	16.5	0.1008	10300	15450
56	0	0	0	538.0	14.92	14.42	0.3920	202	29200
57	0	0	0	538.0	16.60	14.17	0.2550	872	29200
58	0	0	0	539.0	16.9	14.3	0.2490	1255	29200
59	0	0	0	539.0	17.5	14.2	0.2010	1743	29200
60	0	0	0	541.0	18.4	14.7	0.1692	2340	29200
61	0	0	0	540.0	19.37	15.2	0.1961	2700	29200
62	0	0	0	540.0	19.37	14.8	0.1707	3130	29200
63	0	0	0	540.0	20.6	14.92	0.1550	3720	29200
64	0	0	0	533.0	20.8	14.8	0.1942	3180	29200
65	0	0	0	534.0	22.0	15.0	0.2125	3910	29200
66	0	0	0	536.0	22.8	15.2	0.1590	4610	29200
67	0	0	0	536.0	24.5	15.3	0.1489	5450	29200
68	0	0	0	535.0	25.6	15.6	0.1640	5980	29200
69	0	0	0	536.0	26.8	15.7	0.1479	6600	29200
70	0	0	0	536.0	28.2	16.1	0.1492	7220	29200
71	0	0	0	535.0	29.3	16.2	0.1513	7910	29200
72	0	0	0	534.0	30.5	16.5	0.1360	8390	29200
73	0	0	0	534.0	31.3	16.6	0.1320	8940	29200
74	0	0	0	534.0	31.6	16.7	0.1333	9300	29200

Run No.	P_{1U}, Psia	P_{2U}, Psia	R_V, Upflow	Temp, R	P_{1D}, Psia	P_{2D}, Psia	R_V, Downflow	G_{Air}	G_{Water}
75	0	0	0	536.0	15.2	14.8	0.5950	46	58000
76	0	0	0	540.0	16.3	15.1	0.4500	220	58000
77	0	0	0	542.0	17.57	15.6	0.4180	340	58000
78	0	0	0	542.0	17.48	14.66	0.3595	476	58000
79	0	0	0	543.0	18.43	14.77	0.3450	680	58000
80	0	0	0	543.0	19.76	15.3	0.2830	936	58000
81	0	0	0	546.0	20.2	15.17	0.2820	1128	58000
82	0	0	0	545.0	20.8	14.77	0.2425	1610	58000
83	0	0	0	545.0	21.7	14.8	0.2055	1742	58000
84	0	0	0	531.0	22.8	15.2	0.2760	2025	58000
85	0	0	0	533.0	24.3	15.6	0.2170	3110	58000
86	0	0	0	533.0	26.3	15.7	0.2075	3745	58000
87	0	0	0	534.0	26.8	15.8	0.1940	4340	58000
88	0	0	0	534.0	27.9	15.9	0.2005	4760	58000
89	0	0	0	534.0	29.3	16.3	0.1990	5360	58000
90	0	0	0	534.0	30.6	16.6	0.1678	5990	58000
91	0	0	0	534.0	32.1	16.8	0.1768	6400	58000
92	0	0	0	534.0	33.3	17.3	0.1722	7160	58000
93	0	0	0	534.0	33.3	17.3	0.1881	7200	58000
94	0	0	0	538.0	18.17	14.87	0.6710	120	114200
95	0	0	0	540.0	19.16	15.20	0.5880	191	114200
96	0	0	0	542.0	20.55	15.47	0.4975	337	114200
97	0	0	0	544.0	21.4	14.98	0.4905	464	114200
98	0	0	0	544.0	22.1	14.87	0.3780	602	114200
99	0	0	0	538.0	22.6	15.1	0.4330	749	114200
100	0	0	0	541.0	24.1	15.1	0.3840	1000	114200
101	0	0	0	543.0	25.1	15.1	0.3685	1245	114200
102	0	0	0	543.0	26.1	15.2	0.3675	1395	114200
103	0	0	0	544.0	28.4	16.0	0.2920	1945	114200
104	0	0	0	546.0	32.1	16.4	0.2940	3190	114200
105	0	0	0	545.0	33.1	16.6	0.2460	3770	114200
106	17.1	14.63	0.5560	535.0	0	0	0	272	15450
107	17.45	14.73	0.3000	537.0	0	0	0	990	15450
108	18.1	14.63	0.2630	539.0	0	0	0	1320	15450
109	18.34	14.63	0.2965	540.0	0	0	0	1500	15450
110	18.59	14.73	0.2310	540.0	0	0	0	1758	15450
111	19.9	15.62	0.2675	540.0	0	0	0	2235	15450

Run No.	P_{1U}, Psia	P_{2U}, Psia	R_v, Upflow	Temp, R	P_{1D}, Psia	P_{2D}, Psia	R_v, Downflow	G_{Air}	G_{Water}
112	20.4	15.72	0.2285	540.0	0	0	0	2620	15450
113	21.3	16.5	0.2245	541.0	0	0	0	2700	15450
114	22.0	17.1	0.2205	541.0	0	0	0	2945	15450
115	23.25	17.7	0.2050	541.0	0	0	0	3400	15450
116	24.9	18.8	0.1961	541.0	0	0	0	4030	15450
117	25.5	19.28	0.1950	540.0	0	0	0	4420	15450
118	29.3	22.3	0.1950	538.0	0	0	0	4500	15450
119	31.8	24.2	0.1910	538.0	0	0	0	5010	15450
120	33.8	25.6	0.1742	538.0	0	0	0	5610	15450
121	35.2	26.8	0.1720	537.0	0	0	0	6180	15450
122	37.5	28.8	0.1680	537.0	0	0	0	6850	15450
123	39.1	29.8	0.1600	538.0	0	0	0	7250	15450
124	17.9	14.64	0.4550	544.0	0	0	0	441	29200
125	18.68	14.73	0.3090	543.0	0	0	0	825	29200
126	19.78	15.33	0.3030	543.0	0	0	0	1248	29200
127	20.5	15.63	0.2810	534.0	0	0	0	1705	29200
128	21.05	16.02	0.2735	530.0	0	0	0	2005	29200
129	22.25	16.42	0.2455	532.0	0	0	0	2180	29200
130	24.05	17.9	0.2580	532.0	0	0	0	2730	29200
131	25.5	18.9	0.2465	533.0	0	0	0	3040	29200
132	26.5	19.86	0.2180	534.0	0	0	0	3290	29200
133	28.0	21.35	0.2100	534.0	0	0	0	3900	29200
134	25.8	19.3	0.2790	540.0	0	0	0	2275	29200
135	28.2	21.5	0.2465	542.0	0	0	0	2960	29200
136	31.5	24.1	0.2295	542.0	0	0	0	3880	29200
137	33.3	25.3	0.2205	541.0	0	0	0	4460	29200
138	34.8	26.5	0.1970	541.0	0	0	0	4970	29200
139	36.8	27.8	0.1975	542.0	0	0	0	5510	29200
140	40.3	30.5	0.1875	541.0	0	0	0	6250	29200
141	19.53	15.38	0.7010	527.0	0	0	0	166	58000
142	20.4	15.44	0.5940	531.0	0	0	0	365	58000
143	25.8	19.3	0.3595	532.0	0	0	0	901	58000
144	27.3	19.3	0.4040	533.0	0	0	0	1233	58000
145	28.8	20.3	0.4160	536.0	0	0	0	1600	58000
146	29.8	21.3	0.3060	536.0	0	0	0	1790	58000
147	31.3	22.8	0.2710	537.0	0	0	0	2190	58000
148	32.3	23.3	0.2650	535.0	0	0	0	2475	58000

Run No.	P_{1U}, Psia	P_{2U}, Psia	R_V, Upflow	Temp, R	P_{1D}, Psia	P_{2D}, Psia	R_V, Downflow	G_{Air}	G_{Water}
149	34.3	25.3	0.3340	536.0	0	0	0	2840	58000
150	35.8	26.8	0.2415	537.0	0	0	0	3340	58000
151	37.3	27.8	0.2740	536.0	0	0	0	3740	58000
152	39.3	29.3	0.2745	536.0	0	0	0	4230	58000
153	32.8	22.8	0.5220	536.0	0	0	0	888	114200
154	34.8	23.8	0.4910	538.0	0	0	0	1025	114200
155	36.8	25.3	0.4440	540.0	0	0	0	1207	114200
156	38.3	26.3	0.4410	541.0	0	0	0	1345	114200
157	38.8	26.8	0.4500	540.0	0	0	0	1502	114200
158	41.3	28.3	0.3780	540.0	0	0	0	1865	114200
159	42.8	29.3	0.3030	540.0	0	0	0	2165	114200
160	0	0	0	538.0	16.47	16.08	0.3970	361	16500
161	0	0	0	540.0	17.13	16.18	0.3365	490	16500
162	0	0	0	541.0	17.72	16.26	0.3090	728	16500
163	0	0	0	542.0	19.7	17.34	0.2640	1210	16500
164	0	0	0	542.0	18.6	17.24	0.2660	910	16500
165	0	0	0	543.0	19.2	17.13	0.2755	1107	16500
166	0	0	0	544.0	20.2	17.82	0.2680	1190	16500
167	0	0	0	544.0	20.35	17.92	0.2590	1310	16500
168	0	0	0	540.0	20.7	17.7	0.2400	1613	16500
169	0	0	0	540.0	23.2	19.7	0.2290	2400	16500
170	0	0	0	541.0	25.0	21.2	0.2280	2765	16500
171	0	0	0	540.0	27.2	23.2	0.2180	3400	16500
172	0	0	0	540.0	28.7	24.2	0.2080	3770	16500
173	0	0	0	540.0	30.0	25.2	0.2080	4090	16500
174	0	0	0	540.0	31.7	26.7	0.2080	4400	16500
175	0	0	0	540.0	33.2	27.9	0.2080	4820	16500
176	0	0	0	540.0	34.5	29.0	0.2080	5120	16500
177	0	0	0	540.0	36.2	30.2	0.2080	5500	16500
178	0	0	0	547.0	17.71	16.96	0.5150	175	33000
179	0	0	0	547.0	18.71	17.43	0.4060	310	33000
180	0	0	0	548.0	20.0	18.12	0.3980	474	33000
181	0	0	0	549.0	21.8	19.4	0.3530	722	33000
182	0	0	0	548.0	23.6	20.7	0.3200	1084	33000
183	0	0	0	549.0	24.6	21.5	0.3070	1315	33000
184	0	0	0	541.0	23.3	19.3	0.2900	1281	33000
185	0	0	0	542.0	24.3	19.8	0.3180	1357	33000

Run No,	P_{1U}, Psia	P_{2U}, Psia	R_v, Upflow	Temp, R	P_{1D}, Psia	P_{2D}, Psia	R_v, Downflow	G_{Air}	G_{Water}
186	0	0	0	543.0	24.8	20.0	0.2845	1511	33000
187	0	0	0	544.0	24.4	20.2	0.3090	1452	33000
188	0	0	0	545.0	26.0	21.7	0.2755	1802	33000
189	0	0	0	545.0	28.2	23.6	0.2730	2140	33000
190	0	0	0	545.0	29.0	24.0	0.2450	2325	33000
191	0	0	0	545.0	29.8	24.7	0.2605	2510	33000
192	0	0	0	545.0	31.0	25.7	0.2620	2660	33000
193	0	0	0	544.0	32.0	26.5	0.2355	2895	33000
194	0	0	0	530.0	30.3	25.3	0.2570	2910	33000
195	0	0	0	530.0	32.5	26.8	0.2620	3270	33000
196	0	0	0	530.0	33.8	27.8	0.2520	3590	33000
197	0	0	0	530.0	35.8	29.3	0.2560	3880	33000
198	0	0	0	546.0	23.5	20.9	0.5560	280	65500
199	0	0	0	547.0	24.5	21.4	0.5160	332	65500
200	0	0	0	548.0	25.2	22.0	0.4660	472	65500
201	0	0	0	550.0	26.45	23.05	0.4540	556	65500
202	0	0	0	552.0	20.4	19.07	0.6460	78	65500
203	0	0	0	545.0	25.8	21.8	0.4210	654	65500
204	0	0	0	546.0	27.8	23.3	0.3860	875	65500
205	0	0	0	546.0	29.2	24.3	0.3960	971	65500
206	0	0	0	547.0	29.8	24.8	0.3560	1161	65500
207	0	0	0	547.0	31.3	25.8	0.3880	1295	65500
208	0	0	0	547.0	32.5	26.6	0.3440	1390	65500
209	0	0	0	547.0	32.8	26.8	0.3190	1462	65500
210	0	0	0	547.0	33.5	27.3	0.3110	1578	65500
211	0	0	0	547.0	34.3	27.8	0.3370	1698	65500
212	0	0	0	547.0	35.8	28.8	0.3140	1815	65500
213	0	0	0	544.0	34.7	27.7	0.3275	1740	65500
214	0	0	0	544.0	35.0	27.7	0.3140	1820	65500
215	17.91	15.3	0.7670	554.0	0	0	0	72	16500
216	17.59	15.11	0.6050	555.0	0	0	0	186	16500
217	18.6	15.8	0.5110	555.0	0	0	0	307	16500
218	19.64	16.3	0.4250	555.0	0	0	0	510	16500
219	19.2	16.7	0.4200	545.0	0	0	0	530	16500
220	19.7	16.7	0.3760	543.0	0	0	0	671	16500
221	19.5	16.7	0.3920	544.0	0	0	0	794	16500
222	19.2	16.7	0.3510	546.0	0	0	0	915	16500

Run No.	P_{1U}, Psia	P_{2U}, Psia	R_v, Upflow	Temp, R	P_{1D}, Psia	P_{2D}, Psia	R_v, Downflow	G_{Air}	G_{Water}
223	19.9	16.7	0.3720	547.0	0	0	0	964	16500
224	20.5	17.2	0.3280	547.0	0	0	0	1141	16500
225	21.2	17.7	0.3080	546.0	0	0	0	1267	16500
226	21.7	18.2	0.3360	543.0	0	0	0	1200	16500
227	22.5	18.7	0.3140	543.0	0	0	0	1472	16500
228	23.7	19.7	0.2900	543.0	0	0	0	1840	16500
229	24.0	20.0	0.2860	544.0	0	0	0	1950	16500
230	24.6	20.7	0.2820	544.0	0	0	0	2095	16500
231	25.7	21.5	0.2720	544.0	0	0	0	2480	16500
232	27.8	23.4	0.2770	529.0	0	0	0	2545	16500
233	28.5	23.5	0.2710	530.0	0	0	0	2870	16500
234	29.5	24.3	0.2630	531.0	0	0	0	3230	16500
235	30.1	24.8	0.2610	530.0	0	0	0	3460	16500
236	30.9	25.5	0.2600	530.0	0	0	0	3590	16500
237	31.8	26.2	0.2560	530.0	0	0	0	4000	16500
238	33.8	28.1	0.2560	530.0	0	0	0	4170	16500
239	35.3	29.3	0.2530	530.0	0	0	0	4390	16500
240	36.8	30.8	0.2530	530.0	0	0	0	4600	16500
241	38.3	32.4	0.2530	530.0	0	0	0	4840	16500
242	40.3	34.1	0.2540	530.0	0	0	0	4990	16500
243	41.8	35.5	0.2440	530.0	0	0	0	5320	16500
244	19.4	16.43	0.7500	539.0	0	0	0	105	33000
245	19.43	16.43	0.6900	540.0	0	0	0	120	33000
246	20.8	17.22	0.6550	542.0	0	0	0	205	33000
247	21.3	17.61	0.5945	544.0	0	0	0	268	33000
248	22.95	18.6	0.5495	545.0	0	0	0	338	33000
249	22.7	18.4	0.5450	546.0	0	0	0	409	33000
250	24.5	19.7	0.4575	546.0	0	0	0	626	33000
251	25.6	20.7	0.4060	547.0	0	0	0	850	33000
252	26.8	21.65	0.3870	546.0	0	0	0	1072	33000
253	22.6	18.2	0.4720	540.0	0	0	0	615	33000
254	23.7	18.4	0.4560	541.0	0	0	0	765	33000
255	24.7	19.2	0.3920	542.0	0	0	0	963	33000
256	25.7	20.2	0.4140	543.0	0	0	0	1120	33000
257	26.7	20.7	0.3770	544.0	0	0	0	1310	33000
258	27.7	21.2	0.3785	544.0	0	0	0	1432	33000
259	29.7	24.4	0.3560	544.0	0	0	0	1533	33000

Run No.	P_{1U}, Psia	P_{2U}, Psia	R_V, Upflow	Temp, R	P_{1D}, Psia	P_{2D}, Psia	R_V, Downflow	G_{Air}	G_{Water}
260	28.2	22.7	0.3570	526.0	0	0	0	1627	33000
261	29.7	24.0	0.3285	527.0	0	0	0	1730	33000
262	31.7	25.7	0.3125	528.0	0	0	0	2005	33000
263	32.7	26.7	0.3005	528.0	0	0	0	2210	33000
264	34.4	28.2	0.2775	528.0	0	0	0	2390	33000
265	35.5	29.0	0.2890	528.0	0	0	0	2635	33000
266	37.7	31.2	0.2820	528.0	0	0	0	3030	33000
267	35.7	29.2	0.3145	528.0	0	0	0	2750	33000
268	39.7	33.0	0.2870	528.0	0	0	0	3310	33000
269	41.3	34.5	0.2970	528.0	0	0	0	3570	33000
270	42.2	35.2	0.2710	528.0	0	0	0	3800	33000
271	45.7	38.5	0.2775	528.0	0	0	0	4200	33000
272	23.95	20.0	0.8200	547.0	0	0	0	87	65500
273	24.95	20.65	0.7610	547.0	0	0	0	140	65500
274	27.35	22.15	0.6460	548.0	0	0	0	330	65500
275	29.3	23.6	0.5420	548.0	0	0	0	500	65500
276	30.25	24.25	0.5445	546.0	0	0	0	554	65500
277	30.75	24.75	0.5500	547.0	0	0	0	626	65500
278	34.45	28.05	0.4590	547.0	0	0	0	900	65500
279	33.5	27.2	0.4645	548.0	0	0	0	856	65500
280	33.7	27.2	0.4540	548.0	0	0	0	1032	65500
281	37.2	29.7	0.4110	548.0	0	0	0	1210	65500
282	38.5	31.2	0.4060	548.0	0	0	0	1395	65500
283	40.7	33.2	0.3945	548.0	0	0	0	1557	65500
284	41.7	34.2	0.4020	548.0	0	0	0	1773	65500

END

Pub. No. 66-5330
Jimmy Lee Turpin
The University of Oklahoma

PREDICTION OF PRESSURE DROP FOR TWO-PHASE TWO-COMPONENT CONCURRENT FLOW IN PACKED BEDS

by

Jim L. Turpin

ERRATA

Page 64:

Equation (34)	$(D_p/D)^c$
Equation (35)	$(D_p/D)^c$
Equation (36)	$(D_p/D)^c$
Equation (37)	$(D_p/D)^c$

Page 66:

Equation (40)	$(D_p/D)^c$

Page 67:

Equation (43)	$(D_p/D)^c$

Page 68:

Equation (44)	$(D_p/D)^{-1.518}$
Equation (45)	$(D_p/D)^{+1.518}$